SOIL SURFACE EVAPORATION STUDIES

ON THE

GLEN/BONHEIM ECOTOPE

NHLONIPHO NHLANHLA NHLABATSI 2010

SOIL SURFACE EVAPORATION STUDIES ON THE GLEN/BONHEIM ECOTOPE

by

NHLONIPHO NHLANHLA NHLABATSI

Thesis submitted in accordance with the requirements of the degree of

Doctor of Philosophy

Department of Soil, Crop and Climate Sciences

Faculty of Natural and Agricultural Sciences

University of the Free State

Bloemfontein

Promoters: Prof. S. Walker and Prof. L.D. van Rensburg

November 2010

CONTENTS

DECLARATION

I declare that the thesis hereby submitted by me for the degree of Doctor of Philosophy at the University of the Free State is my own independent work and has not been previously submitted by me at another University or Faculty. I furthermore cede copyright of the thesis in favour of the University of the Free State.

Nhlonipho Nhlanhla Nhlabatsi Signature: _____

ACKNOWLEDGEMENTS

- Prof. S. Walker and Prof. L.D. van Rensburg for their individual and collective efforts, encouragement, profound guidance, support and advice during the course of the study.

- Professor Malcom Hensley, for his fatherly advice, unreserved, sincere sharing of knowledge during the study and guidance during desorption and weighing lysimeter experiments.

- Department of Science and Technology for the providing funds to undertake part of the study.

- Ms Lorraine Molope, (Corporate Manager Training and Development Employment Eqiuty) of the Agricultural Research Council, who organised the Department of Science and Technology funds for people like me to accomplish this study. May God bless, and protect her from the eels of this world.

- Management, Agricultural Research Council, Institute for Soil, Climate and Water (ARC-ISCW), for allowing me time to undertake the study.

- Mafedile and my children, Sonkhe, Tiphelele, Nothemba and Vusimuzi who have given immeasurable support throughout the duration of the study.

- God for giving me the strength, patience, wisdom and ability to accomplish this work.

LIST OF ABBREVIATIONS AND SYMBOLS

50% R	fifty percent cover by reed mulch
50% S	fifty percent cover by stone mulch
100% R	hundred percent cover by reed mulch
Ab	above the soil surface
AEDP	Adapted evaporative desorption procedure
ARC-ISCW	Agricultural Research Council-Institute for Soil, Climate and Water
a_s	soil albedo
α	significance level at 0.05
Ba	bare soil without cover
Be	below the soil surface
Bo	Bonheim soil
C	capacitance [MHz]
CDF	cumulative distribution function
CEC	cations exchange capacity
C_f	correction factor
Cl	clay
CON	conventional tillage
C_0	specific water capacity
CPC	cylindrical plastic columns
CPS	cylindrical plastic stopper
Cv	coefficient of variation
d	soil hydraulic diffusivity [$mm^2\ d^{-1}$]
D	Wilmott index of agreement
D_d	corrected sum of squares
DUL	drained upper limit
dr	drainage curves
ds	desorption coefficient
ε	permittivity with subscripts (0 = free space; m = mulch; s = soil)
e_a	vapour pressure of air [kPa]
e_s	saturated vapour pressure of air [kPa]
EC	electrical conductivity [$ds\ m^{-1}$]

EDP	evaporative desorption procedure
Es	evaporation rate from the soil surface [mm d^{-1}]
ESP	exchangeable sodium percentage
ERS	electrical resistance sensor
Es(lys)	lysimeter measurement
Es(*k*)	field hydraulic method
Es(*q*)	Darcy equation method
Es(*d*)	soil hydraulic diffusivity method
Es(*ri*)	Ritchie method
Es(*ro*)	Rose method
ETo	FAO-56 Penman-Monteith method
F	geometric factor of ECH_2O-TE probe
FAO	Food and Agriculture Organization
FDR	frequency domain reflectometry
G	soil heat flux [MJ m^{-2} d^{-1}]
h	matric suction [mm or kPa]
H	sensible heat flux [MJ m^{-2} d^{-1}]
ΔH	hydraulic gradient [kPa]
I	irrigation [mm]
τ_l	transmissivity of mulch to longwave radiation
τ_s	transmissivity of mulch to solar radiation
IDM	internal drainage method
ISID	*in situ* internal drainage method
IRWH	infield rainwater harvesting
K_s	soil evaporative coefficient
K-S	Kolmogorov-Smirnov
$K(\theta)$	soil hydraulic conductivity as factor of soil water content [mm d^{-1}]
MAE	mean absolute error
P	rainfall [mm]
PTF	Pedotransfer function
ρb	bulk density [mg mm^{-3}]
ρ_l	reflectivity of mulch to long wave radiation
ρ_s	reflectivity of mulch to solar wave radiation
q	water flux [mm d^{-1}]

θ_v	volumetric soil water content determined [mm mm^{-1}]
θ_5	laboratory calibration soil water content values determined at 5°C [mm mm^{-1}]
θ_{26}	laboratory calibration soil water content values determined at 26°C [mm mm^{-1}]
θ_g	gravimetric soil water content [mm mm^{-1}]
θ_m	volumetric soil water content determined using manufacturer's given equation [mm mm^{-1}]
θ_{le}	lower end soil water content at 1500 kPa [mm mm^{-1}]
θ_{tc}	temperature compensated calibration equation values of soil water content: achieved determined at temperatures between 5 and 26°C [mm mm^{-1}]
R	series resistance [Ohms]
R_{aw}	voltage output of ECH_2O-TE probe [mV]
RMSE	root mean square error
RMSEu	RMSE unsystematic
RMSEs	RMSE systematic
RWP	rainwater productivity
R^2	coefficient of determination
R_a	long wave radiation [W m^{-2}]
R_s	measured global radiation [W m^{-2}]
R_n	net radiant flux [W m^{-2}]
SWRC	soil water release characteristics
SCH	sampling core head
Sd	standard deviation
Si	silt
ΔS	change in soil water content [mm mm^{-1}]
t	time [h]
T	temperature [°C]
T_i	daily maximum temperature for day *i* [°C]
TDR	time domain reflectometry
TG	rate of change of temperature [°C h^{-1}]
U_2	wind speed at 2 m [mm s^{-1}]
V	voltage [V]
VSA	vacuuming and saturation apparatus
V_f	supply voltage of ECH_2O-TE probe [V]
V_i	starting voltage of ECH_2O-TE probe [V]

γ	psychrometric constant [kPa ^{o}C]
λ	soil thermal conductivity [W m^{-2} K^{-1}]
λE	latent heat flux [W m^{-2}]
Δ	slope of vapour pressure curve [kPa ^{o}C]
σ	Stefan-Boltzman constant [5.67 x 10^{-8} W m^{-2} K^{-4}]

ABSTRACT

The biggest challenge in semi-arid areas is finding ways of reducing the major unproductive water loss: evaporation from the soil surface. A large number of subsistence farmers east of Bloemfontein, in and around Thaba'Nchu in the Free State Province of South Africa occupy about 11 000 ha of land. The economic potential of this communal land still needs to be unlocked and the natural resource base is critical for this endeavour. However, the prevalence of clay and duplex soils is a major constrain towards improving food security in this area. Poor soil water regimes resulting from prolific runoff and evaporation losses is one of the reasons especially when conventional tillage is used. It was therefore hypothesized that by quantifying soil surfaces evaporation (Es); characterizing of the soil hydraulic properties and understanding the effect of temperature on mulch type and coverage of the Bonheim (Bo) soil can contribute to the improvement of the infield rainwater harvesting (IRWH) system and fill a gap in knowledge under South African conditions that is in terms of promoting water storage capacity and minimizing Es for better crop yields.

The ECH_2O-TE probes used in this study were calibrated to measure soil water content (θ) and temperature (T). The evaporative desorption procedure (EDP) of Van der Westhuizen (2009) for coir was modified to calibrate probes in undisturbed soils. The probes were evaluated against measured volumetric soil water content (mm mm^{-1}) on their accuracy, precision and repeatability to measure soil water content in the 26^{o}C treatment (Chapter 2). Most of the laboratory derived equations had RMSE close to zero, on average at 0.003 mm mm^{-1} and precision (R^2) ranged between 93 and 99% and accuracies up to 96%. These probes were found to be sensitive to soil temperature changes in the measurement of water content. Under wet to dry soil conditions about 48, 62 and 34% errors were obtained for the A, B and C-horizons, respectively and therefore temperature compensated equations had to be developed in Chapter

3. Temperature compensated equations predicted soil water content measurements with an accuracy, precision and repeatability at 99, 99 and 95%, respectively. Manufacturer's generic equation tended to over predict soil water content measurements and lacked accuracy with errors ±40% and repeatability.

Chapter 4 investigated how mulch type and percentage cover influenced temperature above and below the soil surface. First: results indicated that mulch did not influence air temperature at an elevation of 160 mm above the soil surface. Secondly: percentage coverage affected soil temperature up to 450 mm, and thirdly: the 100% reed mulch cover treatment was recommended for farmers in order to minimise evaporation especially under semi-arid conditions where normally the evaporative demand exceeds supply.

Chapter 5 on the other hand profiled and characterized the hydraulic properties of the Bo soil for the A, B and C-horizons. Soil pores were separated into structural and textural pore classes for each of the horizons that were identified for the three master horizon of the Bonheim soil using a method first used in this study known as the "*in situ* internal drainage" (ISID) method. The drained upper limit (DUL) for each horizon was determined using the ISID method and were found to be associated with micro pore class. The structural pores of the three horizons were found to be associated with low suctions and that they allowed water to flow at rates between 1-20 mm hr^{-1}. The transitional pore class (Meso pores) conducted water at rates between 3-12 mm hr^{-1} and micro pores between 3-10 mm hr^{-1}.

Five methods were used to estimate evaporation (Es) during three Es drying cycles (Chapter 6) and these estimations were compared to a weighing lysimeter [Es(lys)] measurements in order to evaluate their accuracy in the measurement of Es, using Willmot test statistics for paired

values. The field hydraulic method had a good performance with an average D-index value of 0.60 in all the three drying cycles selected and thus estimated Es closer to Es(lys) hence it was recommended for use in estimating Es for Bo soils.

Key words: ECH_2O-TE probe, soil water content, calibration procedure, temperature, soil, mulch, temperature, reed, hydraulic conductivity, drainage, evaporation

CHAPTER 1

INTRODUCTION

1.1 Background and motivation

In South Africa 74% of the total area is used for dryland crop production and forestry, with which 12% is used for dryland crop production and 62% for forestry and rangeland (Bennie *et al*., 1998). The two main climatic factors that play an important role in dryland crop production are rainfall (precipitation) (P) and temperature (T) in semi-arid areas where P is low and erratic and normally characterised by high evaporative demand. The challenge, therefore, for researchers is finding ways to reduce unproductive water losses especially through soil evaporation (Es) and runoff (Rs) from the soil surface, and optimise rainwater productivity (RWP). Bennie and Hensley (2001) concluded that between 50 and 75% of the annul P is lost through Es. According to du Plessis and Mostert (1965), Haylett (1960) and Bennie *et al.* (1998) who independently reported that water loss through R has been found to be between 6 and 30% of annual P on various soils under conventional tillage (CON). CON means the common practice of land preparation of first ploughing with either a mouldboard or disc plough then planting, which is still a general practice in South Africa for crop production. Other unproductive water losses can be through deep drainage especially in sandy soils during periods of high rainfall.

Bennie and Hensley (2001) reported that 80% of the total area in South Africa is semi-arid and that crop production happens where the aridity index varies between 0.2 and 0.5. The total amount of seasonal P is normally low and erratic thus resulting in either short or long seasonal droughts; during which crop water requirements may or may not exceed the water stored in the soil. It must be noted that the amount of rainwater stored at any given time and not used by the plant helps provide the crop with water during deficit periods; thus the more P that can be

stored in the root zone the lesser the chances or risk of crop failure or damage due to water deficit.

To reduce the risk of crop failure and bolster crop production in the marginal areas of the Free State with predominately clay soils, Hensley *et al*. (2000) developed a crop production method called the In-field RainWater Harvesting (IRWH). The technique combines the advantages of water harvesting which is based entirely on a principle of depriving a certain area of its share of rainwater. Which would have been non-productive and diverting its share to another part of the land to make it more useful using the 2 m runoff strips as shown in Figure 1.1. No-till (a practice whereby the soil is only disturbed at planting in the basin of the IRWH) and mulching (a practice of leaving organic or non-organic material on the soil surface to suppress Es) on high drought risk clay and duplex soils. The technique also reduces total R to zero if the basin are maintained and kept at the designed surface capacity.

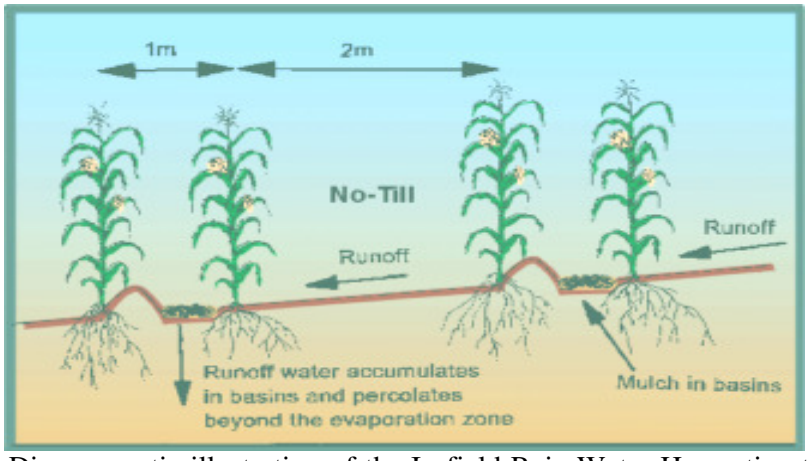

Figure 1.1 Diagrammatic illustration of the In-field Rain Water Harvesting technique (van Rensburg *et al*., 2002)

In the Free State province, the three critical challenges are poverty, food insecurity and unemployment. A large portion (56%) of the population lives in poverty whilst unemployment rate is estimated at 31% (Department of Agriculture-Free State, 2006). Therefore, a large

number of households living on smallholdings are earmarked by the local government to promote crop production from backyard gardens and the crop lands (Backeberg, 2009). The area receives on average between 520-600 mm of P per annum and the cultivated land has been abandoned long ago and is lying fallow around much communal land of Thaba'Nchu. The economic potential of about 14 000 ha of this communal land still needs to be unlocked and could prevent these rural areas from becoming poverty traps. Research in this area that compared the IRWH and CON indicated that there was a 70% probability that yields can increase from 1000 to 1800 kg per ha and 50% probability that yields can increase from 1300 to 2300 kg per ha for maize with rainwater harvesting (Botha, 2006).

The main biophysical hindrance to achieving more than 2000 kg of maize per ha is water lost by Es. Hence, this study investigates the effect different mulching strategies have on temperature of the Bonheim (Bo) soil, which is the main driver for Es to occur from the soil surface (Weiss and Hays, 2005). Soil temperature measurements were collected using ECH_2O-TE probes (Decagon Devices Inc., Pullman, WA) and air temperature measurements were made with HMP-50 probes (Vaisala Inc. Helsinki, Finland). Air and soil temperature varies both in space and time, therefore the determination of energy exchange between the soil and the atmosphere is an important process in the estimation of Es under mulches. Mulching is a technique widely used to conserve soil and moderate its microclimate (Novak *et al*., 2000). The usual purpose of a soil surface treatment has been to influence temperature favorably, to prevent water loss by Es. Traditionally mulch consists of a well aerated, and therefore poorly conducting, surface cover such as straw, leaf litter, stones or gravel. In the last 30 years, the mulching effects of various kinds of natural materials and plastic have been tested in field experiments, especially the effect on soil temperature (Katan, 1979; Maurya and Lal, 1981; Gurnah, 1987; Sui *et al*., 1992; Van Rensburg *et al*., 2002).

An understanding of the Bo soil hydraulic properties and the accurate determination of Es using a weighing lysimeter compared to different methods all seek to improve the IRWH system and unleash its potential to enhance crop production and reduce poverty where it is applicable. Backeberg (2009) wrote that there is 16 million ha of communal land where the IRWH technique can be applied in South Africa. Knowledge of soil hydraulic properties of the Bo soil is very important in the improving the IRWH crop production system. ECH_2O-TE probes were used in the measurement of soil temperature and soil water content. Decagon Devices (2007) reported an accuracy of ± 3% volumetric soil water content for the ECH_2O-TE from their calibration tests. The probe uses capacitance to measure the dielectric permittivity of the soil using an oscillator operating at 70 MHz. Soil hydraulic properties are physical characteristics that describe the soil-water relationship. The most important properties are water retention/release and hydraulic conductivity. The soil water release characteristic (SWRC) describes the relationship between matrix suction (h) and soil water content (θ), with each soil type having a unique or signature characteristic [θ(h)]. On the other hand, hydraulic conductivity (K) describes the ease of water flow in the soil in relation to its θ, hence this relationship is termed [K(θ)] in this study. Knowledge of soil hydraulic properties is a prerequisite for predicting water transport in soils, for example the rate of Es (Fujimaki and Inoue, 2003). Many methods have been developed to measure the hydraulic properties of soils (Bruce and Klute, 1956; Gardner and Miklich, 1962; Hillel *et al.*, 1972), however field measurements of hydraulic properties are difficult, expensive and time consuming. In this study, the internal drainage method (IDM) purported by Hillel *et al.* (1972) was used in the determination of K(θ) relationships for the whole profile of the Bo soil at Glen (Bloemfontein).

Lastly, knowing the evaporative capacity and how it can be reduced for the Bo soil is of paramount importance in improving the IRWH system in the areas where it is or can be

applied. The understanding of the evaporative capacity for the Bo soil was achieved by importing soil from the field in Glen to the University of the Free State, Bloemfontein campus research site weighing lysimeter to estimate Es using soil based and empirical methods and then comparing the results from these methods with weighing lysimeter Es measurements. This was done in order to extrapolate Es data from the lysimeter measurements to field conditions, especially using the relationship between hydraulic conductivity (K) and soil water content (θ).

1.2 Objectives of the study

The main objective of the study was to estimate soil surface evaporation from the Bo soil. This objective was achieved through overarching objectives in five independent studies outlined below. Each study was carried out with its own set of specific objectives.

Study 1 (Chapter 2) titled **"Laboratory calibration of the ECH$_2$O-TE probes for measuring water content".** The specific objectives of this study were to:

(i) adapt the evaporative desorption procedure of Van der Westhuizen (2009) to calibrate ECH$_2$O-TE probes in a soil, using the Bonheim (swelling clay) as the test soil, and

(ii) compare the laboratory obtained calibration equations with that provided by the manufacturer.

Study 2 (Chapter 3) titled "**The effect of soil temperature on the ECH$_2$O-TE probes performance in measuring soil water content".** The purpose of this study was to evaluate the influence of soil temperature on water content measurements made with ECH$_2$O-TE probes installed in a swelling clay soil.

Study 3 (Chapter 4) titled "**Influence of mulch types and coverage on temperature regimes in a clay soil under semi-arid conditions".** The specific objectives of this study were to:

(i) evaluate the effect of percentage cover and type of mulch on the diurnal temperature profile of both the soil and air temperatures; and to

(ii) determine the changes in temperature gradient with soil depth during day-night cycles.

Study 4 (Chapter 5) titled "**Characterization of the hydraulic properties of a Bonheim soil".** The specific objectives of this study were to:

(i) describe the pedological features of the Bonheim; and to

(ii) characterise the hydraulic properties [$\theta(h)$ and $K(\theta)$ relationships] of the Bonheim soil.

Study 5 (Chapter 6) titled **"Determination of evaporation from the melanic horizon using a weighing lysimeter".** The objective of this study was to evaluate six evaporation estimation methods against lysimeter measurements of Es namely: Field hydraulic conductivity, Darcy's equation, Soil hydraulic diffusivity, Ritchie, Rose and FAO-56 Penman-Monteith methods.

1.3 Layout of thesis

This thesis consists of six chapters. Chapter one deals with the motivation and objectives of the study. Individual chapters (2, 3, 4, 5 and 6) contain an abstract, introduction including a review of literature, detailed materials and methods, and results and discussion with pertinent information to the experiments conducted to achieve study objectives. The site and soil selected for the study are generic for all content chapters; therefore a detailed soil description is given in the first content chapter (Chapter 2). Lastly, Chapter 7 (General discussion) which includes the summary and recommendations.

CHAPTER 2

LABORATORY CALIBRATION OF ECH_2O-TE PROBES FOR MEASURING WATER CONTENT

Abstract

Capacitance probes play an integral part in the measure of soil water. However, in South Africa their acceptance over other well established instruments lies squarely on their accuracy, applicability, affordability and the ease at which they can be calibrated to give accurate results. The objective of this study was to adapt a desorption evaporative procedure (EDP) of Van der Westhuizen (2009) to calibrate ECH_2O-TE probes in the laboratory using undisturbed samples from master horizons associated with a swelling clay (Bonheim). The laboratory derived and manufacturer's equations were compared with measured volumetric soil water content. A soil sampling procedure using a modified hydraulic jack (Model: SS-Jacko-Hyd-08-12) to acquire undisturbed horizontal soil samples in a 200 mm long by 105 mm diameter perforated cylindrical plastic columns. During the EDP process the change in mass of columns were recorded hourly during drying. Soil water in the core samples were allowed to evaporate (after saturation) whilst hung on calibrated load cells and volumetric soil water content were calculated from gravimetric water content. Most laboratory derived equations had RMSE values close to zero, on average at 0.003 mm mm^{-1} and precision ranged between 93 and 99% characterized by high accuracy levels between 93 and 96%. All manufacturer's equations had low accuracy levels, the highest level was at 69% and these equations over predicted soil water content for the A, B and C soil horizons by 45, 39 and 42%, respectively. The K-S statistics revealed that each ECH_2O-TE probe was unique for the probes calibrated and they were significantly different at $\alpha = 0.05$; hence each probe must be individually calibrated for clayey soils prior to use for the measurement of soil water content.

Key words: ECH_2O-TE soil water probe, soil water content, calibration procedure, temperature, clay soils

2.1 Introduction

Modern capacitance based soil water probes are widely used in various sectors. In South Africa, they are mainly used to monitor soil water status as part of the weather services for advisory purposes (Mokhele, 2010); in water catchments for the study of hydrology of soils (le Roux, 2010); in the study of evaporation from coir, clay and sandy soils (Chimungu, 2009; van Westhuizen 2009). These types of probes are very popular in recent times in irrigation scheduling services (van Rensburg, 2010). However, the sector that lacks behind is dryland agriculture, where water is the most limiting factor. One of the reasons given for the lack of application in dryland crop production is the uncertainty of the performance of these probes in a wide range of conditions associated with soil types. Despite the affordability of the probes, questions on the performance of these probes with respect to sensitivity, consistency, durability and accuracy are frequently asked by farmers and researchers.

Answers to this question are not always readily available, because for example general equations are provided by the manufacturers for soils that are not ideal for South African soils. For example, Decagon Devices (2007) reported an accuracy of ± 3% volumetric soil water content for soils with bulk electrical conductivities (EC) between 3 to 14 dS/m for the ECH_2O-TE which was used in this study to measure soil water content. They calibrated the coated probes for soil water content in small samples of soil in a beaker at known bulk densities and provided generic calibration equations for mineral soils (sand, sandy loam, silt loam and clay), potting soils and rock wool as follows:

Mineral soils: $\theta = 1.087 * 10^{-3} * Raw - 0.629$ (2.1)

Potting soil: $\theta = 1.04 * 10^{-3} * Raw - 0.50$ (2.2)

Rock wool media: $\theta = 5.15 * 10^{-7} * Raw + 1.41 * 10^{-4} * Raw - 0.160$ (2.3)

where θ is volumetric water content of the medium (mm mm^{-1}) and *Raw* is the output voltage of the probe. Morgan *et al*. (1999) concluded that manufacturer's equations may over or under estimate the θ when used in different medium types and customers are encouraged by the manufacturers to perform medium specific calibrations. This is especially critical in growth mediums with high proportions of bound free water, especially at low water contents (Hilhorst *et al*., 2001; Seyfried and Murdock, 2001; Fares and Polyakov, 2006).

Most calibration methods use disturbed samples and are normally calibrated in beaker size samples under very artificial conditions that bring doubt to their applicability in the field. A more accurate calibration procedure was described by Lane and Mackenzie (2001), and entailed the insertion of a TDR sensor in a cylindrical plastic core, which was slowly wetted from below to reach saturation. After approximately two weeks, the un-perforated core assemblige suspended on load cells and allowed to dry through evaporation; whilst making continuous measurements until no detectable change in mass was observed. This aforementioned procedure was completed roughly after 33-44 days. However, the evaporative desorption procedure (EDP) of van Westhuizen (2009) for the calibration of EC-10 and EC-20 probes in coir in the laboratory was adopted in this study. The EDP method took ten days to complete the process and hence it was modified for the calibration of ECH_2O-TE probes in soils. It provided valuable alternative laboratory determined equations for a swelling clay soil. Hence, this study seeks to: (i) adapt the evaporative desorption procedure of Van der Westhuizen (2009) to calibrate ECH_2O-TE probes in a soil, using the Bonheim (swelling clay) as the test soil, and (ii) to compare the laboratory obtained calibration equations with that provided by the manufacturer.

2.2 Material and methods

2.2.1 Site location and description of soil

The soil samples were taken in a soil profile pit (Figure 2.1) at the Glen Agricultural Research Station (28º57´ S, 26º20´ E), near Bloemfontein, in the Free State Province of South Africa. Because the soil is used in all the studies presented in this study, a detailed soil classification is given in this section.

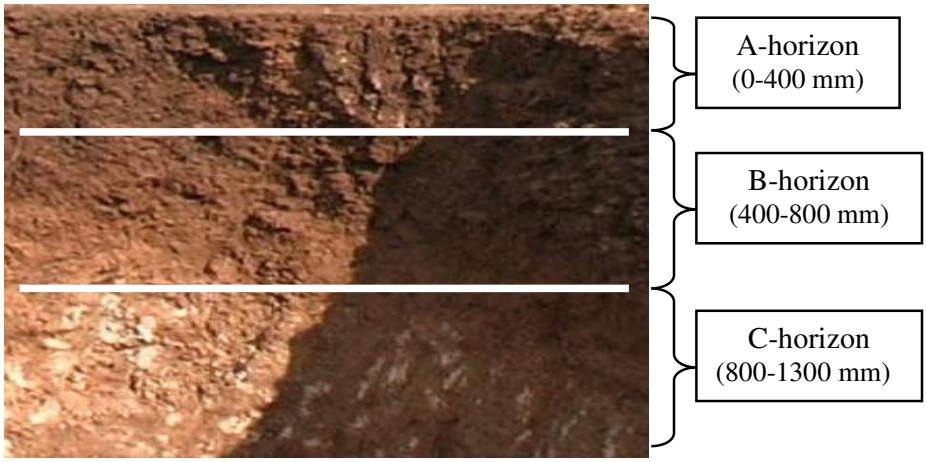

Figure 2.1 Bonheim soil at Glen (Bloemfontein) (Photo by: N. Nhlabatsi)

The soil is classified as a Bonheim (Bo) form belonging to the Onrus family (Soil Classification Working Group, 1991) or a vertic phaeozem according to the classification system of the World Reference Group for Soil Resources (1998). Some of the profile attributes and relevant soil properties are summarized in Tables 2.1 and 2.2. Accordingly, the A and B-horizons are all brown in color and have a high clay content (40 - 45%), with a high proportion of smectite clay minerals resulting in strongly developed structure and a high CEC (24-26 $cmol_c\ kg^{-1}$ soil). The threshold plasticity index (P*i)* value for a diagnostic vertic horizon is 32 or more in the South African soil classification system (Soil Classification Working Group, 1991). The P*i* value for the B-horizon is 33, indicating that this is a strongly expanding clay. The B-horizon overlying a $CaCO_3$ enriched sandstone saprolite at a depth of 800 mm. The parent material is a mixture of dolerite and sandstone colluvium, with dolerite dominating. The

calcareous underlying saprolite is sufficiently weathered to a depth of at least 1200 mm and offers no significant impedance to root development to that depth. The melanic layer (A-horizon) has high P*i* values of 21, thus promoting self-mulching. The exchangeable Na content in the profile is fortunately low (ESP <5%) and therefore cannot be blamed for exacerbating the swell-shrink properties (Appendix 1), but the relatively high exchangeable Mg content in both A and B-horizons between 11-12 $cmol_c\ kg^{-1}$ soil and more than 50% of the exchangeable cations may be a factor that has contributed to the high P*i* value (Hensley *et al*., 2000).

Table 2.1 Profile description of the Bonheim soil form at Glen (Hensley *et al*., 2000)

Map / photo	2826CD Glen	Soil Form	Bonheim
Latitude and Longitude	-28°55´13´´ / 26°21´12´´	Soil Family	Onrus
Land type No	Ea39c	Surface rockiness	None
Climate zone	45S	Surface stoniness	None
Altitude	1330 m	Occurrence of flooding	None
Terrain unit	Upper Foot slope (4)	Wind erosion	None
Slope	1%	Water erosion	Sheet slight, partially stabilized
Slope shape	Straight	Vegetation / Land use	Agronomic cash crops
Aspect	West	Water table	0 mm
Micro relief	None	Described by	M. Hensley and P.P. van Staden
Parent material solum	Origin binary, local colluvium, mainly dolerite; solid rock	Weathering of underlying material	Moderate physical and chemical
Underlying material	Sandstone (feldspatic)	Alteration of underlying material	Calcified

Horizon	Depth (mm)	Description	Diagnostic horizons
A	0-400	Dry soil; color: dry: dark brown 7.5YR3/2; moist color: dark brown 7.5YR3/2; disturbed; clay; moderate coarse, angular blocky; very hard; few normal fine pores; fine cracks; many clay cutans; very few fine pedotubules; water absorption: 1 second(s); few roots; gradual smooth transition.	Melanic
B1	400-550	Dry soil; color: dry: dark brown 7.5YR3/4, moist color: dark brown 7.5YR3/4; undisturbed; clay; strong coarse angular blocky; very hard; few normal fine pores; fine cracks; many slickensides; many clay cutans; very few fine pedotubules; water absorption: 10 second(s); few roots; gradual smooth transition.	Pedocutanic
B2	550-800	Moist soil; color dry: brown to dark brown 7.5YR4/4, moist color: dark brown 7.5YR3/4; undisturbed; clay loam; common medium distinct black illuvial humus mottles; common medium distinct oxidized iron oxide mottles; moderate medium sub-angular blocky; friable; few normal fine pores; non-hardened free lime, slight effervescence; few clay cutans; very few fine bio-casts; water absorption: 8 second(s); few roots; gradual smooth transition	Pedocutanic
C	800-1300	Moist soil; undisturbed; clay loam; many coarse distinct white lime mottles; many medium distinct crumb porous peds, many colored geogenic mottles; non-hardened free lime, strong effervescence; few roots; transition not observed.	Saprolite

Table 2.2 Selected physical and chemical properties of the Bo soil used for the calibration of ECH_2O-TE probes (Hensley *et al*., 2000)

	Melanic (A-horizon)	Pedocutanic (B-horizon)	Saprolite (C-horizon)
	0 – 400 (mm)	400 – 800 (mm)	800 – 1300 (mm)
	Physical properties		
Coarse sand (2 – 0.5 mm)	0.1	0.45	1.3
Medium sand (0.5 – 0.25 mm)	1.7	1.85	2.1
Fine sand (0.25 – 0.106 mm)	23.1	22.25	20.4
Very fine sand (0.106 – 0.05 mm)	19.5	19.7	17.1
Coarse silt (0.05 – 0.02 mm)	5.1	7.05	5.7
Fine silt (0.02 – 0.002 mm)	4.4	5.8	14.3
Clay (> 0.002 mm)	43.5	41.3	37.7
Texture	Clay	Clay	Clay-loam
Bulk density (g cm^{-3})	1.48	1.33	1.47
Plasticity Index	21	33	28
	Chemical properties		
Carbon (%)	0.57		
Resistance (ohms)	340	280	240
pH (H_2O)	7.56	8.25	8.49
pH (KCl)	6.11	7.06	7.21
	Exchangeable/extractable cations ($cmol_c$ kg^{-1} soil)		
Sodium	0.56	1.05	1.19
Potassium	0.65	0.59	0.58
Calcium	8.33	7.98	13.77
Magnesium	12.22	11.74	8.86
S value	21.76	21.35	24.4
CEC	24.30	23.58	26.21
*ESP (%)	2.5	4.9	4.9
Exch. Mg (%)	56	55	36

*exchangeable sodium percentage

2.2.2 Calibration of ECH_2O-TE probes

2.2.2.1 Laboratory calibration procedure of Van der Westhuizen (2009)

Van der Westhuizen (2009) developed a laboratory evaporative desorption procedure (EDP) for calibrating EC-10 and EC-20 probes in coir for measuring water content. The procedure is based on packing a known mass of coir in a perforated cylindrical plastic column (CPC) with dimensions of 500 mm (length) by 105 mm (diameter). The probes were inserted from the ends using a guide and then saturated by placing it in a container with water for 24 hours. The CPC were then hung on a frame installed in a climate controlled cabinet set at a temperature of 26^{o}C. The water in the coir was then allowed to evaporate over a period of 10 days. During the EDP process the weight of the drying CPC columns with probes were recorded hourly using hanging load cells. From this data gravimetric water content was calculated and converted to volumetric water content (θ_v).

2.2.2.2 Adapted calibration procedure for soils

The equipment needed to carry-out the adapted evaporation desorption procedure (AEDP) comprised of: a perforated CPC (Figure 2.2); a vacuum chamber to saturate samples; load cells (Figure 2.2); data logger for monitoring water loss; a controlled climate chamber for controlling temperature and lastly, a modified hydraulic jack to take undisturbed soil samples. Since, the EDP of van der Westhuizen (2009) was solely developed for coir, the procedure had to be modified for soils, which entails the sampling of horizontal *in situ* cores from the field in such a way that the soil remains undisturbed during transportation, oven-drying, saturation, and desorption processes. Therefore, a soil sampling procedure had to be developed in this study to be able to take undisturbed soil samples from the field.

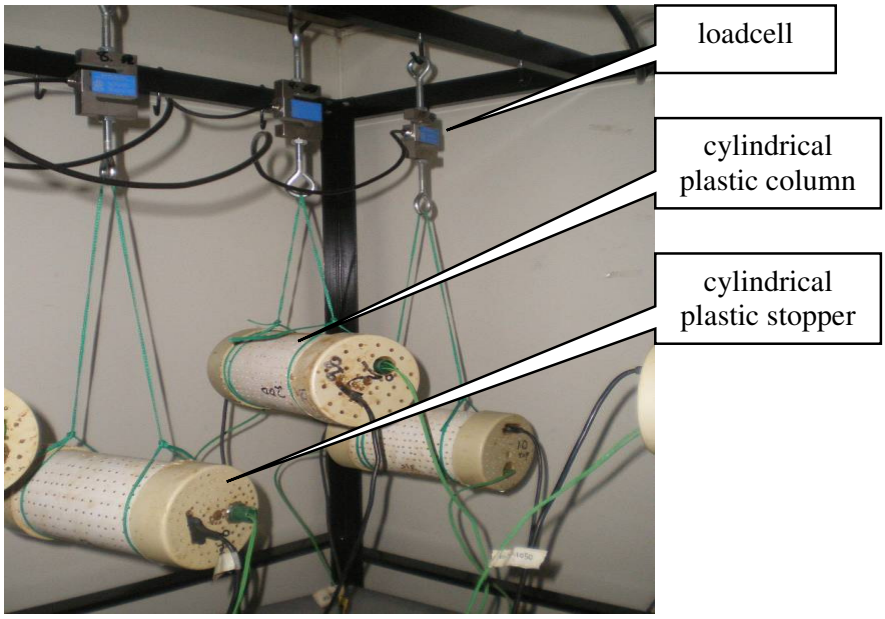

Figure 2.2 Cutting edge, sampling core head and perforated cylindrical plastic columns (105 mm diameter and 200 mm length) hanging from load cells in a constant air temperature cabinet

A hydraulic jack (Model: SS-Jacko-Hyd-08-12) normally used in the automotive industry for tensioning or de-tensioning car body parts was modified making it possible to take undisturbed core with dimensions of 200 mm length and diameter 105 mm; hence termed modified hydraulic jack (MHJ). The MHJ consists of the following parts: hydraulic pump, hydraulic extension arms, steel core head (SCH), and steel plates (Figure 2.3). Soil samples were taken by pushing the core head, which housed the perforated CPC into the face of the profile pit, during the operation the jack was horizontally anchored against the face of the profile pit, pivoted against metal plates as shown in Figure 2.3.

Figure 2.3 The modified hydraulic jack positioned in a profile pit of the melanic A-horizon to take undisturbed soil cores (105 mm diameter and 200 mm length).

For the study, core samples were taken at three diagnostic horizons (A, B and C) with three replications at each horizon when the soil was moderately moist. Each of the samples was sealed at both ends using cylindrical plastic stoppers (CPS) that had 3 mm holes at a density of 1.5 holes cm^{-2} (Figure 2.2) and and then transferred from the field to the laboratory where the samples were prepared to be de-aired and saturated.

The apparatus for de-airing and saturation is diagrammatically presented in Figure 2.4. Accordingly, the apparatus consists of two large chambers with dimensions 550 mm long and diameter of 400 mm. Both chambers were equipped with vacuum tight lids connected to the vacuum pump using pipes fitted with valves to control air flow. One of the chambers (chamber one) was used for de-airing the distilled water and the other chamber (chamber two) for de-airing the soil samples. A suction of 70 kPa was applied for about 48 hours, ensuring that the water and soil samples were de-aired.

Saturation of the samples was obtained by opening the water valve on the water pipe that connects the two chambers near their bottoms. The water chamber (chamber one) was placed on an elevated platform with respect to the soil sample chamber (chamber two) thus ensuring that there was gravitational flow between the chambers. Before opening the water outlet valve the suction should be reduced to 0 kPa (atmospheric pressure) for 24 hours to stabilize.

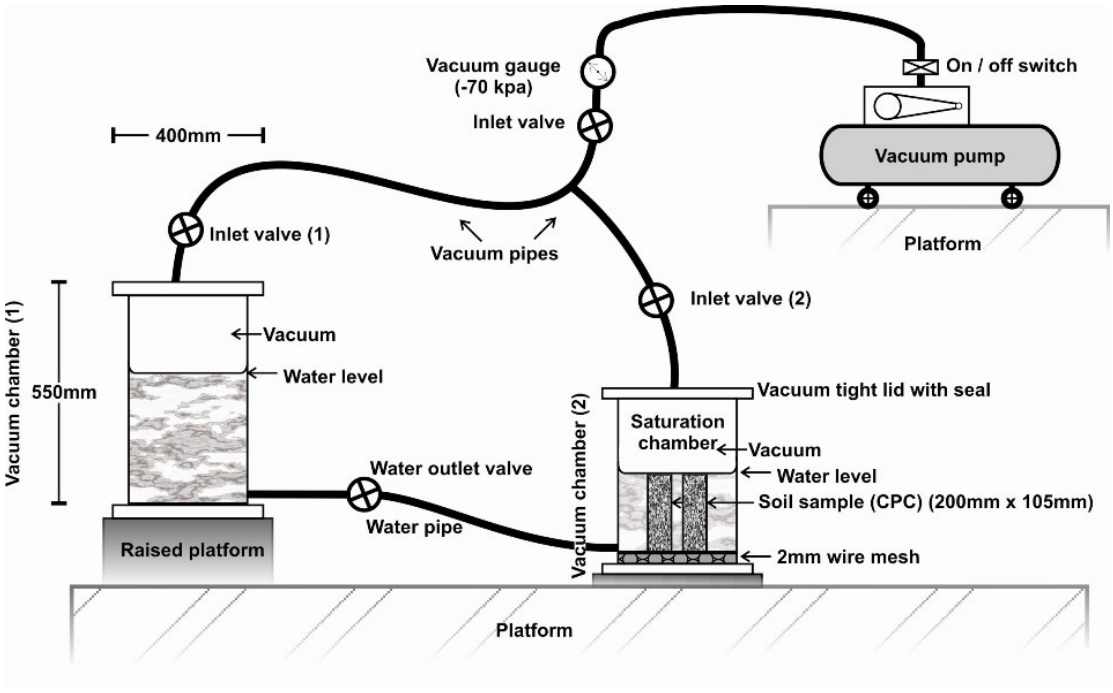

Figure 2.4 Diagrammatic illustrating the vacuum and saturation chamber apparatus setup

After the samples were completely saturated they were taken out of their chamber. To cater for the swelling property (Appendix 1) of the Bonheim soil of about 9 and 13% for the A and B-horizons, a clearance of 1 mm was allowed when the cylindrical plastic stoppers (CPS) were fitted onto the soil columns. Thereafter, the probes were firmly inserted into the soil cores, and ensured that maximum contact between the probe and the soil was established. The amount of soil that was removed was placed in a beaker of known mass, weighed and oven dried for 24 hours at 105^{o}C to determine how much of the soil was removed from each column. Each CPC was labelled and hung on calibrated load cells (Figure 2.2) and half-hourly continuous weight

loss (gravimetric) measurements were recorded for a 20 day drying or desorption cycle at a constant air temperature of 26^{o}C. Gravimetric soil water content was converted to volumetric soil water content using bulk density obtained from the core method. Three samples were taken from each master horizon.

The load cells were calibrated using known standard weights hung (adding and removing the weights) on the load cell whilst recording the change in load cell output voltage (mV) with a CR1000 data logger every two minutes. The response of the load cell voltage output versus weight was plotted and regressed. All the equations obtained had an accuracy of not less than R^2 of 0.99.

2.2.3 Statistical analysis

To evaluate the accuracy of the laboratory calibration equations for the ECH_2O-TE probes a Willmott procedure was used (Willmott, 1981 and 1982; Willmott *et al.*, 1985). Willmott and Wicks (1980) proposed and used the "index of agreement" (D) as a descriptive measure which is used to make cross-comparisons between measured and predicted values in terms of accuracy of predictions. Because a model ought to "explain" most of the major trends or patterns present in observations, it is important to know how much of the root mean square error (RMSE) is "systematic" (RMSEs) and what portion of the error is "unsystematic" (RMSEu). For a "good" model, the systematic difference should approach zero while the unsystematic should be almost equal to the RMSE. Willmott (1982) also recommended that the coefficient of determination or precision (R^2) and mean absolute error (MAE) be used as inferable statistics. Fox (1981) concluded that regardless of whether or not the accuracy or potential accuracy is evaluated, it was made clear in his findings that no single index mentioned above can solely adequately describe model performance and, therefore researchers should report an array of complimentary measures. Therefore, to test the degree to which the ECH_2O-

TE probes were statistically different from each other in the measurement of θ, the Kolmogorov-Smirnov (K-S) two sample test was also applied (Steel *et al*., 1997; Langyintuo *et al*., 2002). When using the K-S test statistics, two distributions are said to be significantly different if the maximum vertical deviation between them exceeds the critical value at the specified significance level (α). In other words, the hypothesis that the probes are similar (H_o) is tested, using the K-S test.

2.3 Results and discussion

2.3.1 Laboratory calibration of soil water probes

2.3.1.1 Soil water content response during desorption

Figure 2.3 shows the change in volumetric soil water content with time during the desorption procedure as a result of soil water lost through evaporation from the columns with soil from the A-horizon (four probes), B-horizon (four probes) and C-horizon (three probes). For clarity, Figure 2.3 shows only two data lines instead of four in the A-horizon due to the fact that probe (#1 and #2) and (#3 and #4) were installed in the same column therefore had the same values of soil water contents and the same for probe #17 and #18 in the B-horizon. The results in Table 2.3 indicated that variation between soil columns water contents was moderate in the wet range (11%) after five hours (10^{th} reading) during desorption and none in the dry range (900^{th} reading) for the A-horizon. The opposite was observed in the B-horizon instead the coefficient of variation increased from 24% (wet range) to 87% (dry range) maybe due to differences in the rate of evaporation from soil columns. In the C-horizon, there was little variation in soil water content between columns with the highest value at 6% and a moderate value was obtained in the dry range (18%). Table 2.3 also indicates that between the three master horizons that there was general increase in variation from wet to dry.

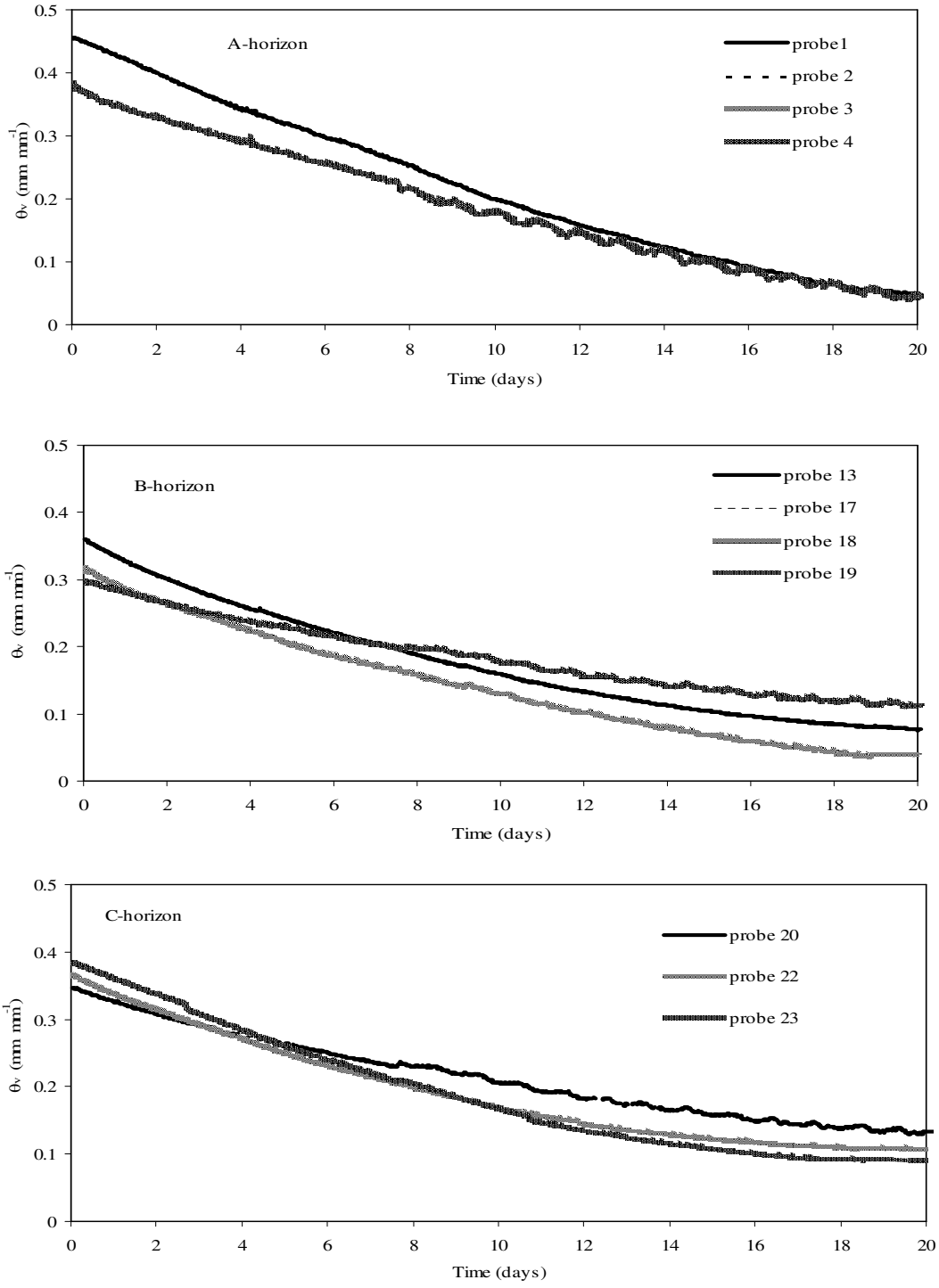

Figure 2.5 Half-hourly volumetric water content (mm mm^{-1}) of the soil columns during a desorption cycle of 20 days for the A-horizon (four probes), B-horizon (four probes) and C-horizon (three probes)

Table 2.3 Mean and coefficient of variation (%) results of measured soil water content (mm mm^{-1}) taken at specified time intervals, during desorption results for the A-horizon (four probes), B-horizon (four probes) and C-horizon (three probes)

Diagnostic horizon	Record number during desorption (1 reading = 0.5h)									
	10	100	200	300	400	500	600	700	800	900
A-horizon: Mean (mm mm^{-1})	0.411	0.318	0.273	0.252	0.203	0.176	0.135	0.098	0.068	0.049
Cv (%)	11.0	1.8	7.4	0.7	1.4	8.5	2.1	3.5	16.3	0.0
B-horizon: Mean (mm mm^{-1})	0.366	0.317	0.273	0.234	0.204	0.173	0.146	0.123	0.102	0.088
Cv (%)	23.9	26.8	30.0	34.8	41.3	47.5	53.7	62.5	71.5	87.2
C-horizon: Mean (mm mm^{-1})	0.361	0.317	0.268	0.231	0.203	0.172	0.144	0.129	0.117	0.112
Cv (%)	5.1	5.3	3.8	2.2	6.2	10.4	12.7	15.4	18.9	18.9
Overall: Mean (mm mm^{-1})	0.379	0.317	0.271	0.239	0.203	0.174	0.142	0.117	0.096	0.083
Cv (%)	13.3	11.3	13.7	12.6	16.3	22.1	22.8	27.1	35.6	35.4

2.3.1.2 Probe output response during desorption

Figure 2.6 shows the response in probe output (mV) as the soil looses weight (water) through evaporation during desorption procedure for the ECH_2O-TE probes (Appendix 2) inserted in the A, B and C-horizons. Results in Table 2.4 suggest that the variations amongst probes within soil horizons are low; between 4 and 6% in the A, between 3-8% in the B and between 1-5% in the C-horizon. From Figure 2.6 it can be concluded that the difference between the lowest and highest readings at a particular time in the A-horizon is about 150 mV in the beginning of the drying cycle (wet range) and 80 mV at the end of the drying cycle (dry range); in the B-horizon about 100 mV (wet) and 120 mV (dry); and in the C-horizon about 100 mV (wet) and 10 mV (dry). However, the integration of the volumetric soil water content and probe output was the only way to establish whether the probes were unique in their response.

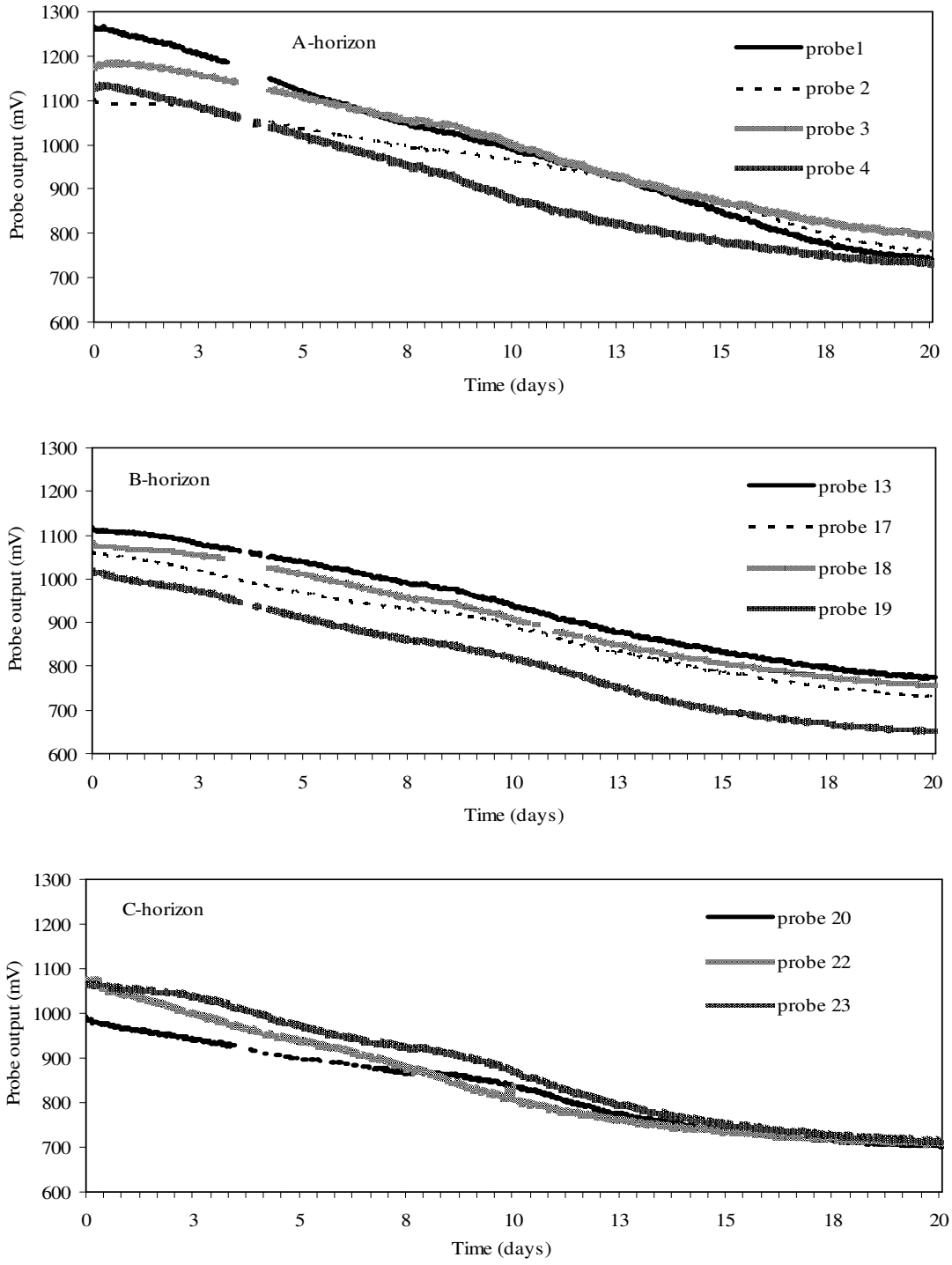

Figure 2.6 Hourly probe output (mV) of the ECH_2O-TE soil water probes during a desorption cycle of 20 days for the A-horizon (four probes), B-horizon (four probes) and C-horizon (three probes)

Table 2.4 Mean and coefficient of variation (%) results of measured soil water content (mm mm^{-1}) taken at specified time intervals, during desorption results for the A-horizon (four probes), B-horizon (four probes) and C-horizon (three probes)

Diagnostic horizon	Record number during desorption (1 reading =0.5h)									
	10	100	200	300	400	500	600	700	800	900
A-horizon: Mean (mm mm^{-1})	1169	1140	1091	1048	1002	947	900	856	805	770
Cv (%)	6.2	5.7	4.9	5.3	5.9	5.6	6.0	5.1	4.1	4.1
B-horizon: Mean (mm mm^{-1})	1062	1039	996	956	924	871	826	787	757	735
Cv (%)	3.8	4.5	5.4	6.0	6.0	7.0	6.6	7.4	7.5	7.7
C-horizon: Mean (mm mm^{-1})	1038	1004	952	913	876	825	778	748	725	714
Cv (%)	4.7	4.8	4.3	3.3	3.7	3.3	2.3	1.3	1.2	0.9
Overall: Mean (mm mm^{-1})	1090	1061	1013	972	934	881	835	797	762	740
Cv (%)	4.9	5.0	4.9	4.9	5.2	5.3	5.0	4.6	4.3	4.2

2.3.1.3 Laboratory determined calibration equations

The volumetric soil water content (θ_v in mm mm^{-1}) values obtained during the drying cycle were plotted against the corresponding millivolt (mV) output measured by the probes for the different horizons to obtain laboratory soil water content (θ_{26} in mm mm^{-1}) equations. Polynomial, exponential or linear functions were fitted for each probe and the statistical results were summarized in Table 2.5. Good correlations were generally obtained, with an average precision of more than 95% and with accuracies to 0.001 mm mm^{-1} for the three diagnostic soil horizons. The probes in the dry range had soil water content values at 0.05; 0.12 and 0.13 mm mm^{-1}, and at saturation had values at 0.40; 0.37 and 0.35 mm mm^{-1} for A; B and C-horizons, respectively. However, there was some variation between these probes in their response as shown in Table 2.3. For example probe #19 in the B-horizon (Figure 2.7) had slightly higher voltage output values than probes #13, #17 and #18 for the duration of the drying cycle. It must be noted that no one type of curve provided the best fit for the 11 probes. The K-S test results

for the comparison of pairs of probes in measurement of soil water content are presented in Table 2.6. The results clearly indicate that individual ECH_2O-TE probes were highly significantly different from each other at $\alpha \leq 0.05$; except for probes (#1-#2) in the A-horizon that were found not to be significantly different at $\alpha \leq 0.05$. The K-S results also revealed that each probe was unique and it was merely by chance that any two probes can yield similar soil water calibration curves for example probe pair's #1-#2 mentioned above.

Table 2.5 Linear, exponential or fourth degree polynomial equations that describe laboratory soil water content (θ_{26} in mm mm^{-1}) determined from the relationship between actual soil water content and probe output (x in mV) for all the ECH_2O-TE probes used for the calibration (n = 968)

Diagnostic horizon	Probe No:	Linear, exponential or fourth degree polynomial equations	R^2
A-horizon	1	$\theta_{26} = 0.001x - 0.7081$	0.984
	2	$\theta_{26} = 2 \times 10^{-21} x^{6.7485}$	0.995
	3	$\theta_{26} = 8 \times 10^{-4}x - 0.5763$	0.982
	4	$\theta_{26} = 8 \times 10^{-4}x - 0.4969$	0.994
B-horizon	13	$\theta_{26} = 4 \times 10^{-13}x^{3.9117}$	0.995
	17	$\theta_{26} = 8 \times 10^{-18}x^{5.493}$	0.991
	18	$\theta_{26} = 1 \times 10^{-17}x^{5.4044}$	0.982
	19	$\theta_{26} = 1 \times 10^{-7}x^{2.0033}$	0.994
C-horizon	20	$\theta_{26} = 4 \times 10^{-9}x^{2.6635}$	0.978
	22	$\theta_{26} = 4 \times 10^{-10}x^{2.9827}$	0.994
	23	$\theta_{26} = 6 \times 10^{-12}x^{3.5725}$	0.998

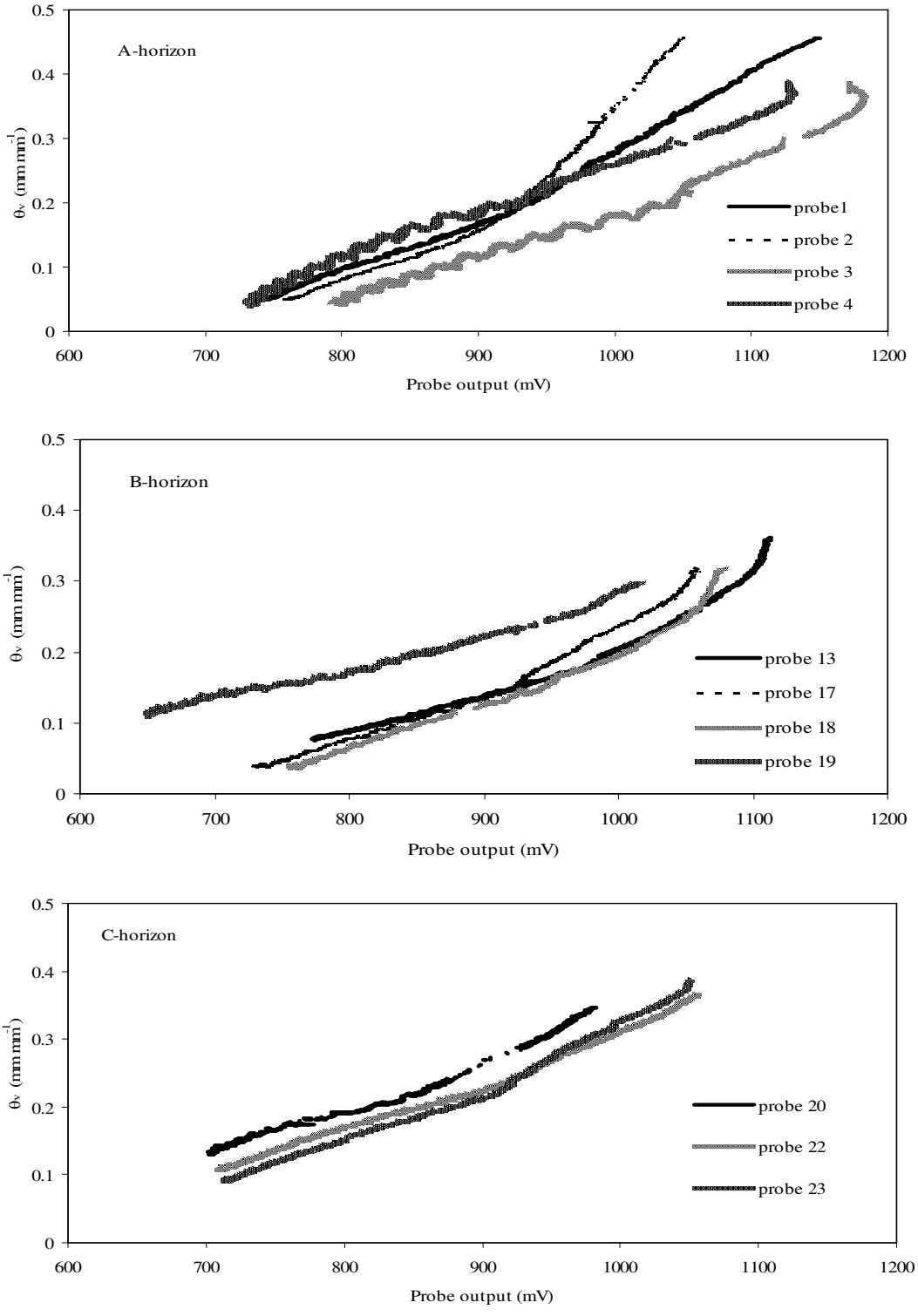

Figure 2.7 Relationship between probe output (mV) and volumetric soil water content for the ECH_2O-TE probes measured at 26^oC

2.3.2 Evaluation of calibration models

An independent data set was used for the evaluation of the manufacturers and laboratory equations. Graphical results showing a comparison of volumetric soil water content values determined using manufacturer's and laboratory equations are presented in Figure 2.8. The manufacturer's equations tended to over predicted soil water content by more than 40%, except for probe #20 in the C-horizon. For example, probe #4 had a low precision (D index) at 0.33, low accuracy (RMSE) of 0.282 mm mm^{-1} compared to the 0.026 mm mm^{-1} obtained from laboratory equation in the A-horizon (Figure 2.8). When laboratory derived equations values were compared with measured values, the precision (R^2) and accuracy (D-index) were high on average at 0.98 and 0.92, respectively for most of the probes. For example, six of the probes (#1; #3; #17; #18; #22 and #23) had soil water content values falling within the 10% accuracy lines and the remaining five probes outside the lines. The RMSEu was very close to the RMSE for all the probes in the A-horizon when using laboratory equations; which meant that the laboratory calibrations were very accurate with the lowest MAE of 0.007 mm mm^{-1} (Table 2.7). For example probe #1 had similar RMSEu and RMSE values of 0.108 mm mm^{-1} and RMSEs approaching zero, at 0.010 mm mm^{-1} and precision of 99%. Probe #19 and #20 (Figure 2.8) were the only probes where the manufacturer's equations estimated soil water content with accuracies of 0.013 and 0.042 mm mm^{-1}. For probe #19, the precision indices (R^2 and D-index) were high at 0.96 and 0.95 derived from comparing measured versus manufacturer's soil volumetric soil water content values. For probe #20, a precision of 98% was observed when using both manufacturer's and laboratory equations. Similar accuracy levels were reported by Kizito *et al.* (2008) for the ECH_2O-TE probe. Cobos (2009) and Czarnomski *et al.* (2005) wrote after testing their probes that soil - specific calibration of the ECH_2O-TE probe achieves accuracies of ±2% similar to that of TDR probe at a fraction of the price. Hence, they concluded that the resolution (0.1-100%), precision (±2%), repeatability, and probe to probe

agreement of the ECH_2O-TE probe were excellent at ±5% accuracy with the generic factory calibration. Furthermore, they wrote that soil specific calibration of one probe can be applied to all other probes of the same type in that particular soil. In contrast what is evident from the results from this study was that each ECH_2O-TE probe has its own precision levels maybe due to the minor differences in the component parts that make up the probe and therefore need to be calibrated individually for the specific soil medium where it is going to be used before any meaningful statistical inferences can be made. The results obtained in this study had precisions generally better than 95% and with probe to probe repeatability at 0.93% in the measurement of volumetric soil water content.

Table 2.6 K-S test results comparing the predicted soil water content pairs from the A, B and C-horizons for eleven ECH_2O-TE probes

Diagnostic horizon	Pairs of probes	D-statistics	Significance level (α)
A-horizon	1 – 2	0.0788^{ns}	0.0190
	1 – 3	0.3323*	0.0000
	1 – 4	0.2237*	0.0000
	2 – 3	0.3324*	0.0000
	2 – 4	0.1862*	0.0000
	3 – 4	0.1476*	0.0000
B-horizon	13 – 17	0.2310*	0.0000
	13 – 18	0.2331*	0.0000
	13 – 19	0.5291*	0.0000
	17 – 18	0.0817*	0.0050
	17 – 19	0.6443*	0.0000
	18 – 19	0.6754*	0.0000
C-horizon	20 – 22	0.5424*	0.0000
	20 – 23	0.4512*	0.0000
	22 – 23	0.2095*	0.0000

* Significantly different at α = 0.01; ^{ns} not significantly different at α =0.01

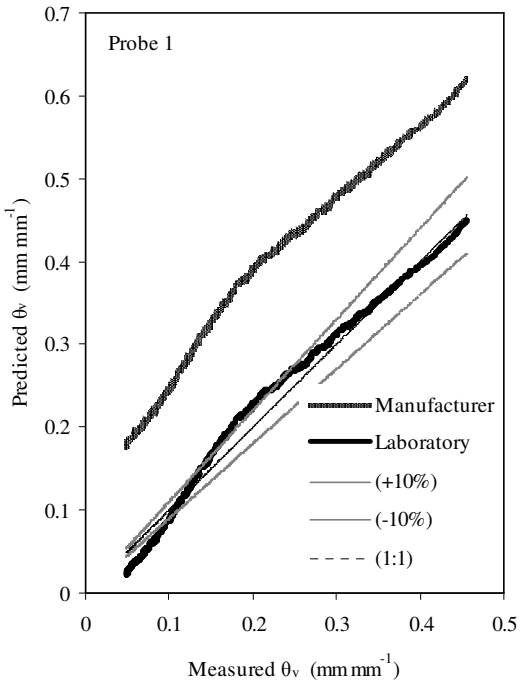
Probe 1
Predicted θv (mm mm-1)
Measured θv (mm mm-1)
Manufacturer
Laboratory
(+10%)
(-10%)
(1:1)
0
0.1
0.2
0.3
0.4
0.5
0.6
0.7

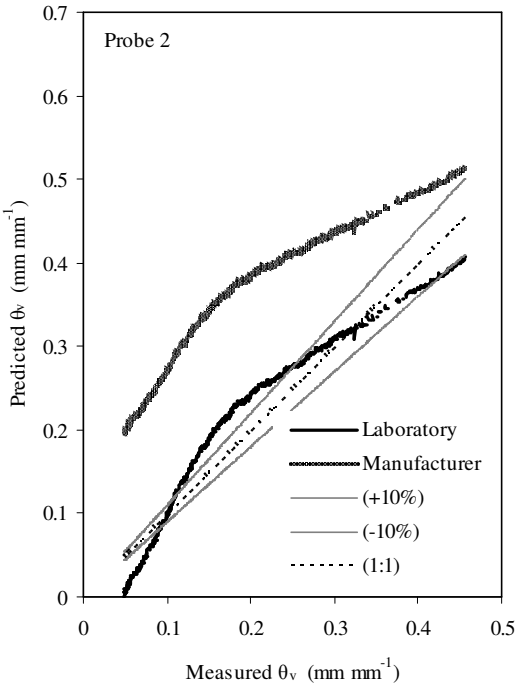
Probe 2
Predicted θv (mm mm-1)
Measured θv (mm mm-1)
Laboratory
Manufacturer
(+10%)
(-10%)
(1:1)
0
0.1
0.2
0.3
0.4
0.5
0.6
0.7

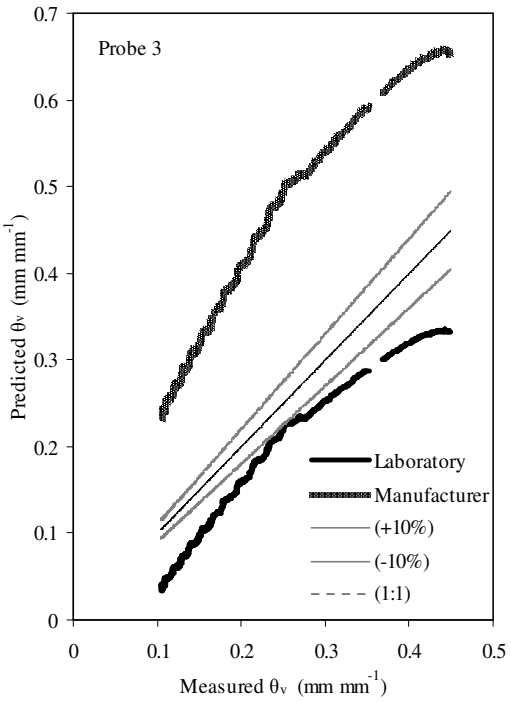
Probe 3
Predicted θv (mm mm-1)
Measured θv (mm mm-1)
Laboratory
Manufacturer
(+10%)
(-10%)
(1:1)
0
0.1
0.2
0.3
0.4
0.5
0.6
0.7

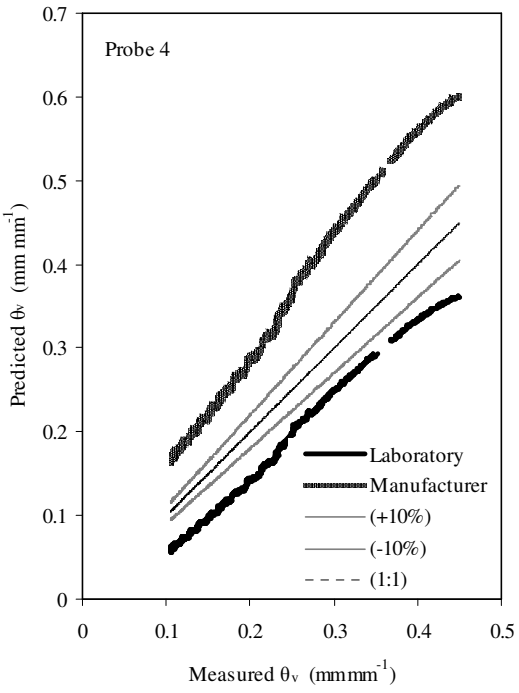
Probe 4
Predicted θv (mm mm-1)
Measured θv (mm mm-1)
Laboratory
Manufacturer
(+10%)
(-10%)
(1:1)
0
0.1
0.2
0.3
0.4
0.5
0.6
0.7

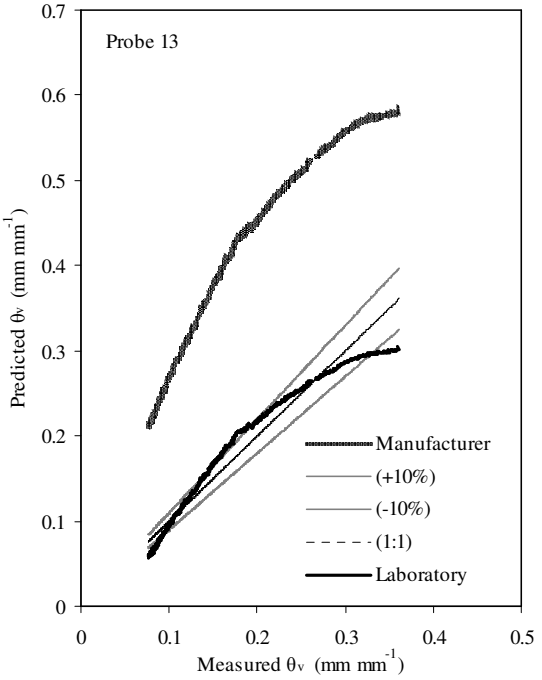
Probe 13
Predicted θv (mm mm-1)
Measured θv (mm mm-1)
Manufacturer
(+10%)
(-10%)
(1:1)
Laboratory

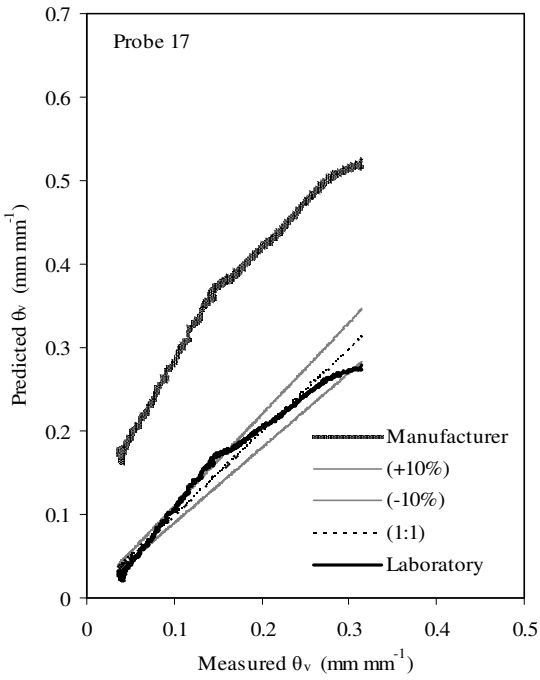
Probe 17
Predicted θv (mm mm-1)
Measured θv (mm mm-1)
Manufacturer
(+10%)
(-10%)
(1:1)
Laboratory

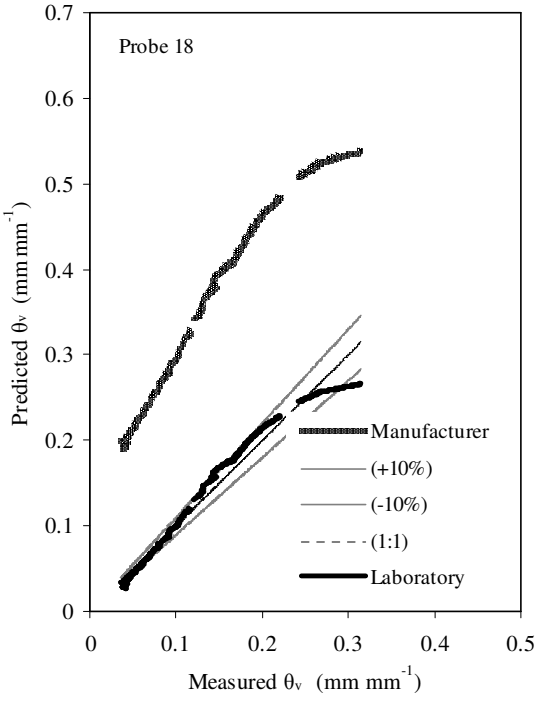
Probe 18
Predicted θv (mm mm-1)
Measured θv (mm mm-1)
Manufacturer
(+10%)
(-10%)
(1:1)
Laboratory

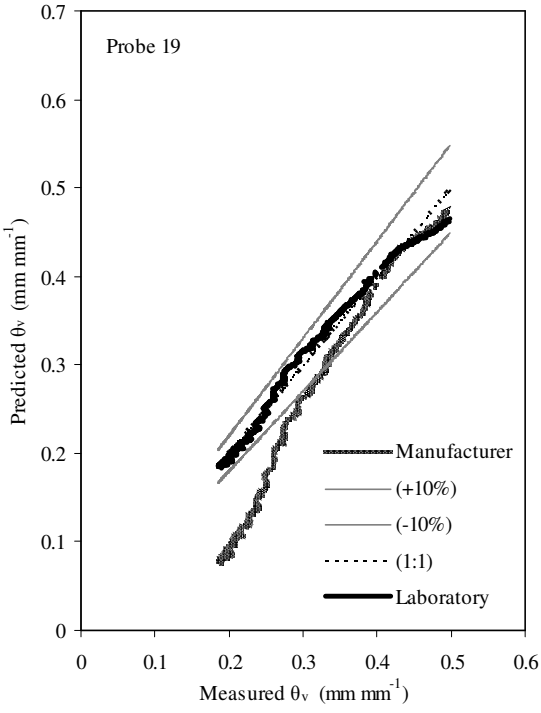
Probe 19
Predicted θv (mm mm-1)
Measured θv (mm mm-1)
Manufacturer
(+10%)
(-10%)
(1:1)
Laboratory

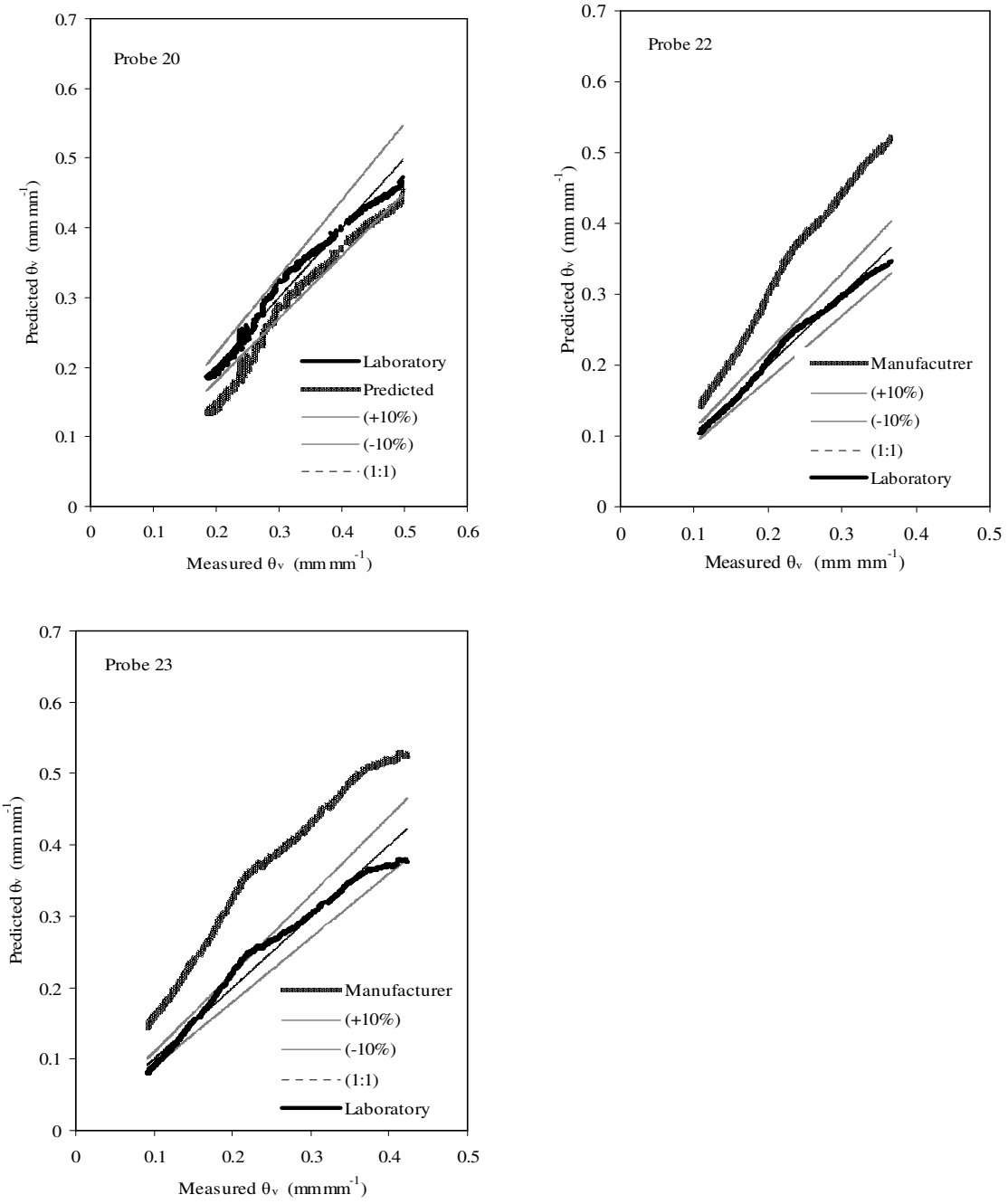

Figure 2.8 Relationships between measured volumetric water content and predicted volumetric soil water content using the manufacturer's and proposed laboratory calibration equation volumetric soil water content (mm mm^{-1}) measurements for the eleven probes calibrated at 26^{o}C (average n per probe = 442).

Table 2.7 Quantitative measures comparing measured volumetric soil water content versus predicted volumetric soil water content using laboratory and manufacturer's calibration equations*

		A-horizon				B-horizon				C-horizon		
Probe Number		1	2	3	4	13	17	18	19	20	22	23
Measured θ_v versus Predicted θ_{26}	RMSE	0.108	0.068	0.071	0.026	0.021	0.013	0.020	0.014	0.016	0.009	0.021
	RMSEs	0.010	0.010	0.029	0.017	0.021	0.013	0.019	0.014	0.016	0.009	0.021
	RMSEu	0.108	0.067	0.065	0.019	0.005	0.003	0.005	0.005	0.004	0.002	0.004
	MAE	0.038	0.038	0.044	0.018	0.017	0.010	0.016	0.010	0.012	0.007	0.016
	R^2	0.990	0.929	0.968	0.974	0.970	0.988	0.953	0.964	0.980	0.989	0.921
	D-index	0.899	0.928	0.682	0.920	0.928	0.962	0.914	0.951	0.931	0.958	0.758
Measured θ_v versus manufacturer's θ_v	RMSE	0.180	0.194	0.188	0.282	0.254	0.219	0.253	0.013	0.042	0.148	0.128
	RMSEs	0.127	0.154	0.189	0.283	0.254	0.219	0.253	0.012	0.042	0.148	0.128
	RMSEu	0.129	0.118			0.008	0.004	0.010	0.005	0.003	0.003	0.005
	MAE	0.151	0.180	0.187	0.282	0.254	0.219	0.253	0.011	0.041	0.148	0.127
	R^2	0.936	0.990	0.987	0.979	0.973	0.991	0.951	0.964	0.978	0.989	0.921
	D-index	0.687	0.743	0.504	0.336	0.302	0.302	0.288	0.952	0.633	0.263	0.281

*The terms *d* and r^2 are dimensionless, while the remaining terms have the unit's mm mm^{-1}

2.4 Conclusions

The evaporation desorption procedure (EDP) of van der Westhuizen (2009) was successfully adapted to calibrate ECH_2O-TE probes in soil. Two very important sub-procedures were developed and applied; firstly the adaptation of a standard hydraulic jack for pushing a core sampler with a cylindrical plastic column (105 mm diameter by 200 mm length) horizontally into the profile. Secondly, developing a large vacuum apparatus for saturating the de-aired soil columns in distilled water and thereafter hung the columns on calibrated load cells in a controlled climate cabinet to dry in accordance with the EDP procedure. The EDP enables scientists to calibrate capacitance probes (probe length 95 mm) in soils within a month. It was concluded that there was 6% variation in probe output attributed to temperature sensitivity of the probes and that laboratory derived equations had high precision between 93 and 98%; with accuracy levels between 68 and 96%. On the other hand, manufacturers had low accuracy levels which ranged from 28 to 69%. This section of the study concluded that each ECH_2O-TE probe was unique and must be calibrated first for a specific medium rather than using manufacturer given equations blindly, especially when used in scientific experiments to get accurate measurements of volumetric soil water content. Therefore, it can be concluded that the ECH_2O-TE probe can be deployed in reactive clay soils thereby reducing research costs.

CHAPTER 3

THE EFFECT OF SOIL TEMPERATURE ON THE ECH_2O-TE PROBES PERFORMANCE IN MEASURING SOIL WATER CONTENT

Abstract

This study evaluated the effect of temperature on soil water content (θ) measurements made with ECH_2O-TE probes in the laboratory employing an adapted evaporative desorption procedure (AEDP) and using two different soil temperature treatments (5 and 26°C) in a swelling clay soil (Bonheim) to determine their accuracy, precision and repeatability. Undisturbed soil cores in 200 mm long perforated cylindrical plastic pipe (diameter 105 mm) were used to calibrate the ECH_2O-TE probes. Laboratory calibrated soil water content equations were developed for each of the probes for each of the treatments and had precision (R^2) ranging between 0.90 and 0.99. Temperature compensated equations were determined through multiple regression analysis for each probe. Temperature and voltage output (as independent variables) and measured soil water content (dependent variable) were regressed to yield a probe specific 'temperature compensated' equation (θ_{tc}). The soil water content measurements obtained using these compensated equations were found to be accurate (D-index) to within ±1% and precision varied between 0.93 and 0.99 during desorption. Kolmogorov-Smirnov (K-S) comparison results revealed that soil water content measurements between pairs of probes were significantly different at $\alpha = 0.05$. It was concluded that temperature compensated equations yielded better predictions. Therefore based on the results it is advisable that each probe must be calibrated at more than one temperature to derive a probe specific equation. The manufacturer's equation (θ_m) provided by Decagon Devices tended to over predict soil water content for the swelling clay (Bonheim).

Key words: soil water content, calibration, soil temperature, ECH_2O-TE probe

3.1 Introduction

Chapter 2 of this study revealed that the ECH_2O-TE probes (Decagon Devices Inc., Pullman, WA), if calibrated properly for soils at a constant soil temperature of 26^oC could yield soil water calibration equations with accuracies that varied between 0.95 and 0.99 and repeatability levels that range from 0.93 to 0.99. From a theoretical point of view water potential (being a chemical potential of water) is dependent on temperature, so one expects temperature to influence how these instruments measure soil water content (Pepin *et al*., 1995; Seyfried and Murdock, 2001; Wraith and Or, 2001; Czarnomski *et al*., 2005; Bogena *et al*., 2007; Saito *et al*., 2008; Kizito *et al*., 2008). Kizito *et al.* (2008) concluded that the use of a single calibration curve in a specific soil medium for different ECH_2O-TE probes does not always truly evaluate the temperature effect. The method of calibration that they used may not be the ideal in simulating natural field conditions especially in the top 150 mm of soil profile where there are daily temperature fluctuations. Furthermore, they stated that the measurement frequency is one of the primary factors that affect the sensitivity of capacitance probes to soil variables such as soil texture, electrical conductivity and temperature.

Kizito *et al.* (2008) concluded that among all the techniques developed to measure soil water content, electromagnetic methods have received the most attention. Most instruments use capacitance and frequency domain reflectometry (FRD) techniques that offer an alternative to time domain reflectometry (TDR) because of their low costs, among other advantages such as allowing continuous monitoring, data logging capabilities, repeatability, and applicability to a wide range of soil types (Nalder and Lapid, 1996; Mohamed *et al*., 1997; Seyfried and Murdock, 2001 and 2004). However, the accuracy and precision of these instruments vary, and the calibration of these instruments may change with soil type, electrical conductivity, and temperature (Czarnomski *et al*., 2005; Bogena *et al*., 2007). Therefore calibration for these effects is essential for accurate determination of soil water content. ECH_2O-TE probes have a

measurement frequency of 70 MHz. Campbell (1990) determined that a measurement frequency of 50 MHz was required to obtain stable real soil dielectric permittivity values. However, Kelleners *et al.* (2005) concluded that measurement frequencies must be equal or above 500 MHz for stable dielectric permittivity values, whereas Chen and Or (2006) concluded that the measurement frequency should be greater than 100 MHz to minimize Maxwell-Wagner polarization. The general conclusion from all the studies was that high measurement frequencies are required for accurate measurement of soil water content, while minimizing sensitivity to changes in soil electrical conductivity and temperature.

Cobos and Campbell (2007) had concluded that correction for temperature sensitivity for ECH_2O probes was meant primarily for users who have sensors placed in the top 150 mm of the soil profile under a bare surface, or whose sensors otherwise undergo strong temperature cycling. None of the above mentioned researchers calibrated these probes in conditions similar to the field in swelling clay and therefore this created a gap in knowledge that needed to be filled to scientifically calibrate these probes in a Bonheim soil. The aim of this study was to evaluate the influence of soil temperature on soil water content measurements made with ECH_2O-TE probes installed in a swelling clay soil.

3.2 Material and methods

3.2.1 Measurement of soil water content

Site and soil description for this study are detailed in Chapter 2, Section 2.2.1 and the instrument used for the measurement of soil water content is the ECH_2O-TE probe. The ECH_2O-TE probe uses a capacitance technique. By rapidly charging and discharging a positive and ground electrode (capacitor) in the soil, an electromagnetic field at 70 MHz is generated whose charge time (t) is related to the capacitance (C) of the soil by the equation (Bogena *et al*., 2007; Kizito *et al*., 2008):

$$t = RC\ln\left[\frac{V - V_f}{V_i - V_f}\right] \quad (3.1)$$

where R is the series resistance, V is voltage at time t, V_i is the starting voltage, and V_f is the applied or supply voltage. Furthermore, for a capacitor with a geometric factor of F, the capacitance is related to the dielectric permittivity (ε) of the soil between the capacitor electrodes by:

$$C = \varepsilon_o \varepsilon F \quad (3.2)$$

where ε_o is the permittivity of the free space. Thus the ε of the soil can be determined by measuring the change time (t) of the sensor buried in the soil. Consequently, as water has a dielectric permittivity that is much greater than soil minerals or air, the charge time t in the soil of equation (3.1) can be correlated with soil water content. A thermistor installed in contact with the sensor body measures soil temperature, while the gold traces on the surface of the sensor form a four-pole array to measure electrical conductivity.

The manufacturer's generic probe calibration equation (Decagon Devices, 2007) for clay soils was given as:

Mineral soils: $\theta_m = 1.087 * 10^{-3} * R_{aw} - 0.629 \quad (3.3)$

where θ_m is volumetric soil water content (mm mm^{-1}) of the probe and R_{aw} is the output voltage of the probe (mV).

3.2.2 Procedure for laboratory calibration

The ECH$_2$O-TE probe soil water calibration procedure described in Chapter 2, Section 2.2.2.2 was used as basis for determining the influence of soil temperature on the voltage output of the probes. After the completion of the adapted evaporation desorption procedure (AEDP) which was carried out at a constant soil temperature of 26^{o}C (near room temperature), the samples were re-saturated and desorbed using the EDP method of van der Westhuizen (2009). However, the aim was to obtain observations at 5^{o}C; but the desorption process was too slow making the method impractical. Therefore, a decision was made to increase the temperature to 26^{o}C for 12

hours to enhance evaporation from the soil columns and then switched back to 5°C. This procedure was followed until evaporation was negligible after 44 days. Only the data associated with stable soil core temperatures of 5°C were used for the analysis. Soil temperatures were obtained from the probes temperature readings.

3.2.3 Procedure for testing the effect of soil temperature

Three ECH_2O-TE probes (#1, #13 and #23) were randomly selected one from each of the master horizons and the temperature effect was calculated as the difference in soil water content per layer based to the water content at 26°C multiplied by 100 to get percentage difference from very wet to dry conditions during the desorption procedure. The reason why the probes were calibrated between 5 and 26°C was that the climate cabinet could only reach these amplitudes in temperature.

3.2.4 Procedure for testing temperature compensated and manufacturers equations

First: Temperature compensated calibration equations (θ_{tc}) were developed by multiple regressions of measured soil water content values (dependent variable) with two independent variables namely: probe output (x in mV) and temperature (T in °C) for ECH_2O-TE probes. Secondly: For testing the compensated and manufacturers equations an independent data set was used. The data was obtained from the 5°C desorption measurements, where the temperature oscillated between ≥ 5 and 26°C.

3.2.5 Statistical analysis

The accuracy of the derived calibration equations was determined by using the Willmott procedure and to test the degree to which the individual ECH_2O-TE probes were statistically different from each other in the measurement of soil water content at different temperatures, the Kolmogorov-Smirnov (K-S) two sample tests were applied as described in Chapter 2 (Section 2.2.3).

3.3 Results and discussion

3.3.1 Effect of temperature on soil water content measurements

Three probes, one from each horizon, were randomly selected to illustrate the influence of soil temperature on water content measurements (Table 3.1 and Figure 3.2). Table 3.1 shows clearly that temperature influenced soil water content measurements most in the dry range during desorption. For example, probe #1: 790 mV during the 5 and 26°C treatments, the soil water contents were 0.135 and 0.091 mm mm^{-1}, respectively; relative to the reference water content (26°C) it represented an error of 48.4% with respect to the depth of the horizon. Under very wet conditions, the error was 10% compared to 46.5% under wet conditions. This result indicated that temperature influenced ECH_2O-TE probes more under drier conditions compared to very wet conditions as this trend was observed in all three selected probes (Table 3.1). It is important to observe that in between dry and wet ranges the percentage error within a horizon was almost similar for instance about 34% for probe #23.

Table 3.1 Temperature effect on probe output (mV) for three randomly selected probes used to measure soil water content in the master horizons during desorption

Diagnostic horizon	Probe	(mV)	Soil water content level	(mm mm^{-1})		(mm/horizon)		% water difference*
				5°C	26°C	5°C	26°C	
A-horizon (0 – 400)	1	790	Dry	0.135	0.091	54.0	36.4	48.4
		958	Wet	0.337	0.230	134.8	92.0	46.5
		1105	Very wet	0.451	0.410	180.4	164.0	10.0
B-horizon (400 – 800)	13	800	Dry	0.137	0.087	54	34.8	57.5
		980	Wet	0.267	0.164	106.8	65.6	62.8
		1058	Very wet	0.354	0.257	141.6	102.8	37.7
C-horizon (800 – 1300)	23	721	Dry	0.132	0.098	66.0	49.0	34.7
		900	Wet	0.286	0.213	143.0	106.5	34.3
		1024	Very wet	0.362	0.347	181.0	173.5	4.3

*Percentage difference was calculated based on water content per horizon at 26°C

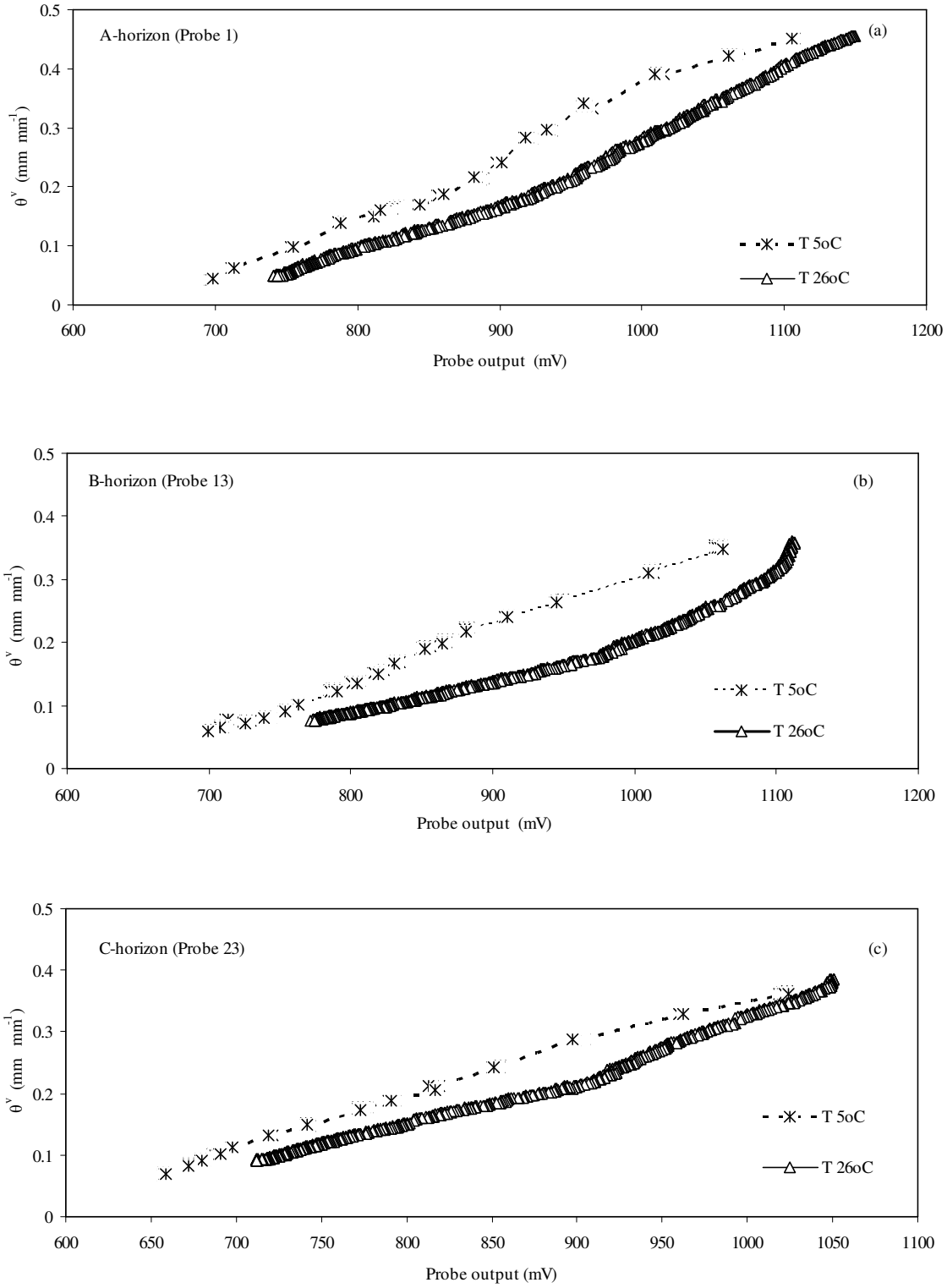

Figure 3.2 Relationship between probe output (mV) of randomly selected ECH_2O-TE probes and volumetric soil water content measured during the desorption of the A (probe 1), B (probe 13) and C (probe 23) horizons at 5 and 26^{o}C treatments

Mathematical functions (linear and nonlinear) that best describe the relationship probe output and volumetric soil water content for each temperature treatment are summarized in Table 3.3. The results indicated that each probe responded uniquely to changes in soil water content as Table 3.3 shows that the same probe had significantly different results when calibrated in another temperature treatment. It must be noted however, that no one type of curve function uniquely provided the best fit and the precision (R^2) for most of the probes were high at 99% with only probe #2 out of the eleven selected ECH_2O-TE probes with a slightly lower precision of 0.97% at the 5^{o}C drying cycle. Table 3.1 provided evidence that temperature affected the probes significantly under wet-to-dry conditions, hence; the calibration equations in Table 3.3 could not just be applied owing to the large errors under these conditions. Therefore, temperature compensated calibration equations (θ_{tc}) had to be developed to compensate for temperature sensitivity of the ECH_2O-TE probes.

Table 3.2 K-S test comparison predicted soil water content values between laboratory equations derived at 5 and 26^{o}C

Diagnostic horizon	Probe pairs	θ_5 versus θ_{26}	
A-horizon	1 - 1	0.2136*	0.0000
	2 - 2	0.4918*	0.0000
	3 – 3	0.4412*	0.0000
	4 - 4	0.4900*	0.0000
B-horizon	13 – 13	0.5000*	0.0000
	17 – 17	0.3439*	0.0000
	18 – 18	0.1697*	0.0000
	19 – 19	0.1884*	0.0000
C-horizon	20 - 20	0.3176*	0.0000
	22 – 22	0.2112*	0.0000
	23 - 23	0.5909*	0.0000

*Significantly different at $\alpha = 0.05$; ^{ns} not significantly different at $\alpha = 0.05$

Table 3.3 Laboratory calibration equations that describe the relationship between volumetric soil water content and probe output (mV) for the ECH_2O-TE probes calibrated (n = 284 per probe) separately at 5 and 26°C soil temperatures

Horizon	Probe no.	Linear or nonlinear equations at 5°C	R^2	Linear or nonlinear equations at 26°C	R^2
	1	$\theta_5 = 0.001x - 0.7168$	0.984	$\theta_{26} = 0.001x - 0.7081$	0.984
	2	$\theta_5 = 2\ x^{-10}x^4 - 8 \times 10^{-7}x^3 + 0.001x^2 - 0.6075x + 134.32$	0.968	$\theta_{26} = 2 \times 10^{-21}\ x^{6.7485}$	0.995
A-horizon	3	$\theta_5 = 0.0009x - 0.511$	0.995	$\theta_{26} = 8 \times 10^{-4}x - 0.5763$	0.982
	4	$\theta_5 = 2 \times 10\text{-}^{11}x^4 - 8 \times 10^{-8}x^3 + 0.0001x^2 - 0.0554x + 10.916$	0.900	$\theta_{26} = 8 \times 10^{-4}x - 0.4969$	0.994
	13	$\theta_5 = 0.0009x - 0.5421$	0.994	$\theta_{26} = 4 \times 10^{-13}x^{3.9117}$	0.995
B-horizon	17	$\theta_5 = 0.0009x - 0.5990$	0.987	$\theta_{26} = 8 \times 10^{-18}x^{5.493}$	0.991
	18	$\theta_5 = 0.0008x - 0.5696$	0.981	$\theta_{26} = 1 \times 10^{-17}x^{5.4044}$	0.982
	19	$\theta_5 = 0.0009x - 0.5074$	0.989	$\theta_{26} = 1 \times 10^{-7}x^{2.0033}$	0.994
	20	$\theta_5 = 0.001x - 0.6227$	0.995	$\theta_{26} = 4 \times 10^{-9}x^{2.6635}$	0.978
C-horizon	22	$\theta_5 = 0.0007x - 0.447$	0.994	$\theta_{26} = 4 \times 10^{-10}x^{2.9827}$	0.994
	23	$\theta_5 = 0.0008x - 0.4664$	0.996	$\theta_{26} = 6 \times 10^{-12}x^{3.5725}$	0.998

*Units for θ_{lab} are mm mm^{-1}; x represents probe output units in mV

3.3.2 Temperature compensated equations

Table 3.4 showed that all the temperature compensated equations had a high precision (R^2 varied between 93 to 99%). These temperature compensated equations are applicable to soil conditions with temperatures ranging between 5 to 26^{o}C. Table 3.5 shows the percentage in days measured by van Rensburg *et al*, (2002) and also in Chapter 4 of this study in whereby the temperature was between 5 and 26^{o}C; < 5^{o}C and > 26^{o}C for the A, B and C-horizons. The results revealed that soil temperature was below 5^{o}C for about 1.4% (between 3 to 4 days) in the A-horizon; from the soil surface to a depth of 75 mm). Therefore, this means that approximately 99% of the time in the A-horizon the soil temperature fell between 5 and 26^{o}C. For the B and C-horizons the soil temperature was always between 5 and 26^{o}C. The whole profile during these measurement periods was never higher than the reference room temperature of 26^{o}C. From the depth of 150 to 1050 mm, the soil temperature fell within the required range (5 and 26^{o}C) for the Bonheim soil.

Table 3.4 Temperature compensated equations for the eleven ECH_2O-TE probes calibrated at two drying cycles of 5 and 26^{o}C, respectively (n = 968 per probe)

Horizon	Probe no.	Temperature compensated equations	R^2
A-horizon	1	θ_{tc} = 0.000982x – 0.00297T - 0.61849	0.981
	2	θ_{tc} = 0.00133x – 0.00724T - 0.81222	0.932
	3	θ_{tc} = 0.0008x – 0.00752T - 0.40987	0.983
	4	θ_{tc} = 0.000815x – 0.00632T - 0.38328	0.970
B-horizon	13	θ_{tc} = 0.000756x – 0.00319T - 0.45009	0.964
	17	θ_{tc} = 0.000814x – 0.00171T - 0.5333	0.977
	18	θ_{tc} = 0.000766x – 0.00069T - 0.53522	0.975
	19	θ_{tc} = 0.000787x + 0.006447T - 0.49762	0.992
C-horizon	20	θ_{tc} = 0.001005x + 0.00384T - 0.62234	0.991
	22	θ_{tc} = 0.000703x + 0.001791T - 0.44054	0.995
	23	θ_{tc} = 0.000857x – 0.00172T - 0.48699	0.986

Table 3.5 The percentage of days measured by van Rensburg *et al*, (2002) and Chapter 4 whereby the soil temperature (^{o}C) levels are: 5↔26^{o}C; < 5^{o}C and > 26^{o}C

Diagnostic horizon	Soil depth (mm)	Soil temperature variation (%)					
		5↔26^{o}C		< 5^{o}C		> 26^{o}C	
		*Van Rens	*Chapter 4	Van Rens	Chapter 4	Van Rens	Chapter 4
A-horizon	25	99.4	98.6	0.6	1.4	0	0
	75	99.2	98.6	0.8	1.4	0	0
	150	100	100	0	0	0	0
B-horizon	450	100	100	0	0	0	0
	750	100	100	0	0	0	0
C-horizon	1050	100	100	0	0	0	0

*Data from van Renburg *et al*, (2002) from DOY 101 to 217 (2002) and chapter four from DOY 168-293 (2008)

3.3.3 Evaluation of calibration equations

Figure 3.3 shows the relationship between measured volumetric soil water content and predicted soil water content using (i) temperature compensated and (ii) manufacturers' equations. The graphs showed clearly that temperature compensated equations predicted soil water content within the ±10% error lines for all the probes. The accuracy index (D in Table 3.6) indicated that the accuracy ranged between 48.1 to 83.9% when manufacturer's equations were compared with measured independent values of soil water content. According to Willmott (1992) for a modelled equation to be acceptable the ratio of RMSEu/RMSE should be higher or equal to 0.65 and RMSE be as close to zero as much as possible.

Table 3.6 showed clearly that only probes #19 and #20 satisfied the above mentioned criteria when manufacturer's equations were applied. The precision coefficient's (R^2) for the remaining nine probes were between 0.95 and 0.99, but this means that they were consistent in predicting water contents inaccurately with RMSE's much more than zero. Czarnomski *et al*. (2005) concluded that these probes needed to be calibrated in the particular mediums where its to be used for the calibration equations to be accurate.

Table 3.6 indicated that temperature compensated equations were accurate, precise and consistent in prediction of soil water content. All temperature compensated probes throughout had accuracies (D-indices) that ranged from 0.94 to 0.99; and RMSE/RMSEu ratios varied

between 0.74 and 1.00 satisfied the criteria for a good model. The lowest RMSE was at 0.015 mm mm^{-1} for temperature compensated compared to 0.107 mm mm^{-1} for manufacturer's equations for probe #23. Most manufacturers' equations had standard errors higher than 20% and this phenomenon was also observed by Czarnomski *et al.* (2005) for the ECH_2O-TE probe. However, the error ranged between 0-2 percent thus a 5% improvement in the measurement of soil water content when using temperature compensated equations. This may suggest that the ECH_2O-TE probe manucfacturers internal compensation design mechanism for temperature is not adequate enough hence the 40% temperature sensitivity displayed by the different probes in this study as shown in Table 3.1.

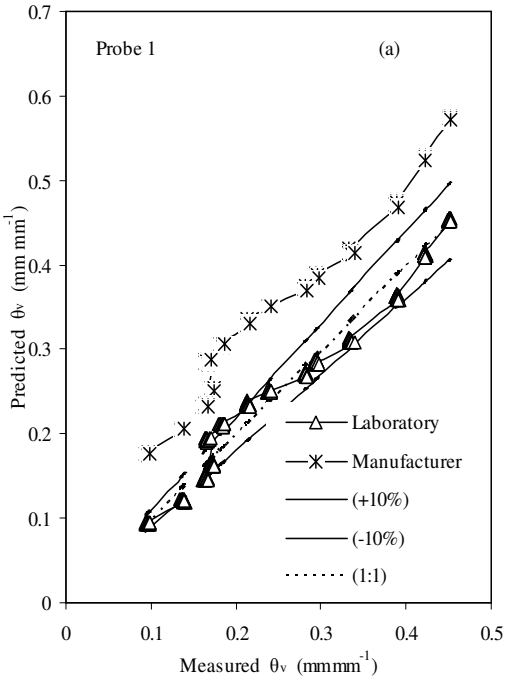
Probe 1
(a)
Predicted θv (mm mm-1)
Measured θv (mm mm-1)
Laboratory
Manufacturer
(+10%)
(-10%)
(1:1)

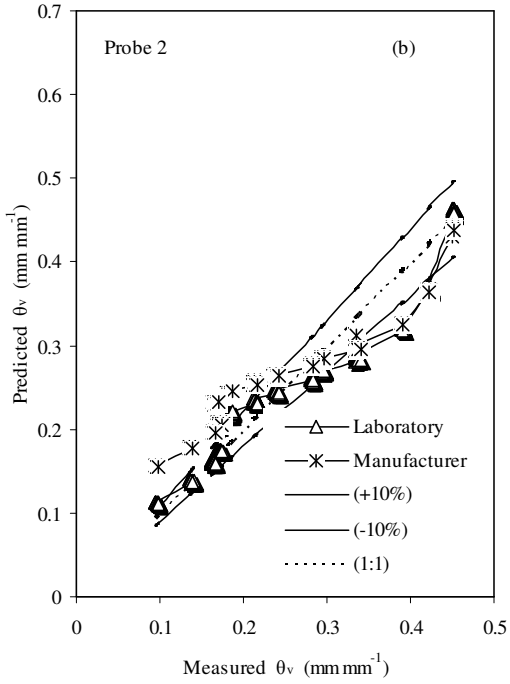
Probe 2
(b)
Predicted θv (mm mm-1)
Measured θv (mm mm-1)
Laboratory
Manufacturer
(+10%)
(-10%)
(1:1)

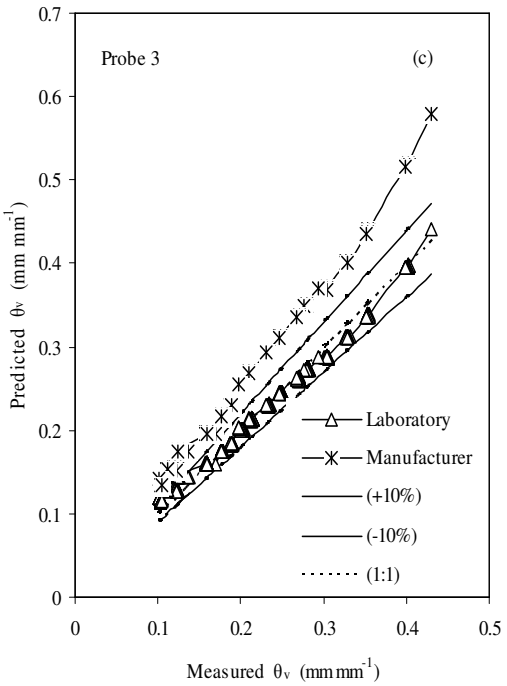
Probe 3
(c)
Predicted θv (mm mm-1)
Measured θv (mm mm-1)
Laboratory
Manufacturer
(+10%)
(-10%)
(1:1)

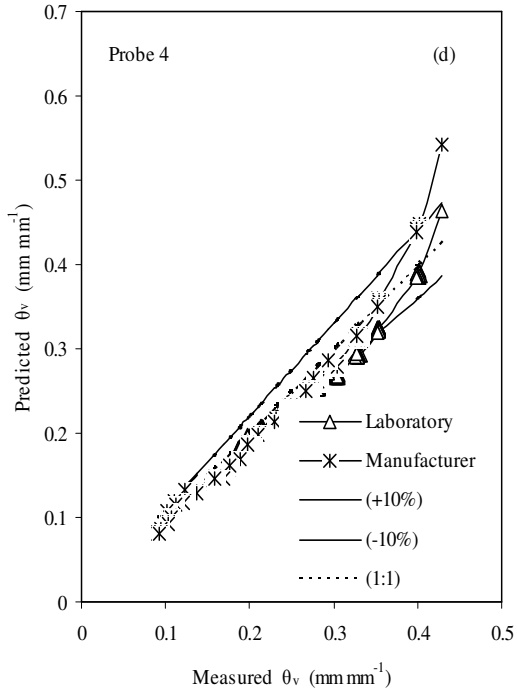
Probe 4
(d)
Predicted θv (mm mm-1)
Measured θv (mm mm-1)
Laboratory
Manufacturer
(+10%)
(-10%)
(1:1)

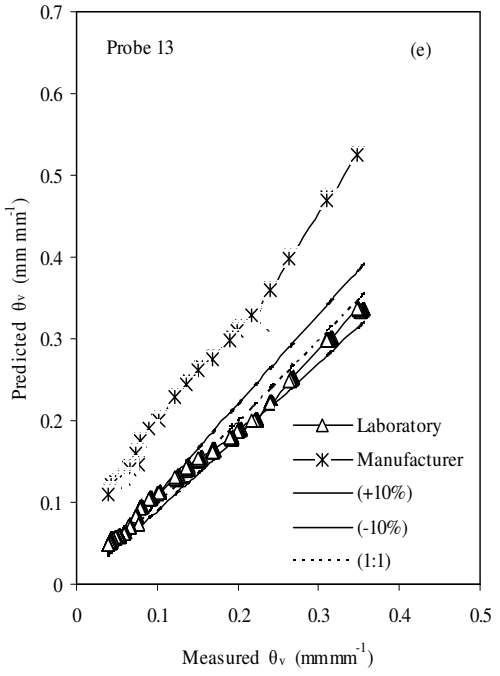
Probe 13
(e)
Predicted θv (mm mm-1)
Measured θv (mmmm-1)
Laboratory
Manufacturer
(+10%)
(-10%)
(1:1)

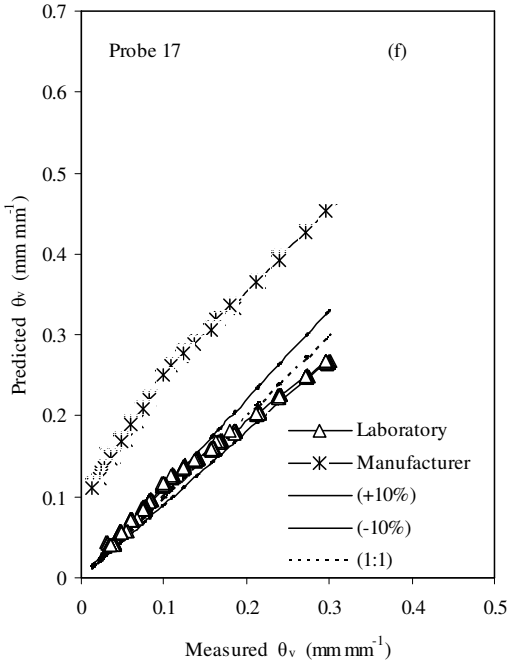
Probe 17
(f)
Predicted θv (mm mm-1)
Measured θv (mm mm-1)
Laboratory
Manufacturer
(+10%)
(-10%)
(1:1)

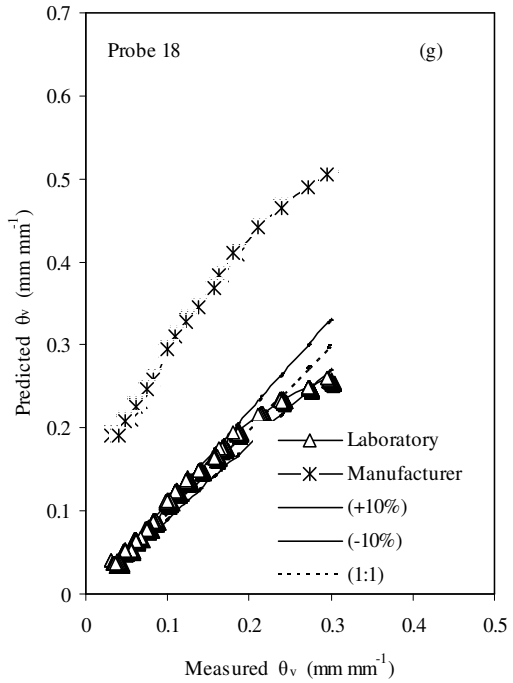
Probe 18
(g)
Predicted θv (mm mm-1)
Measured θv (mm mm-1)
Laboratory
Manufacturer
(+10%)
(-10%)
(1:1)

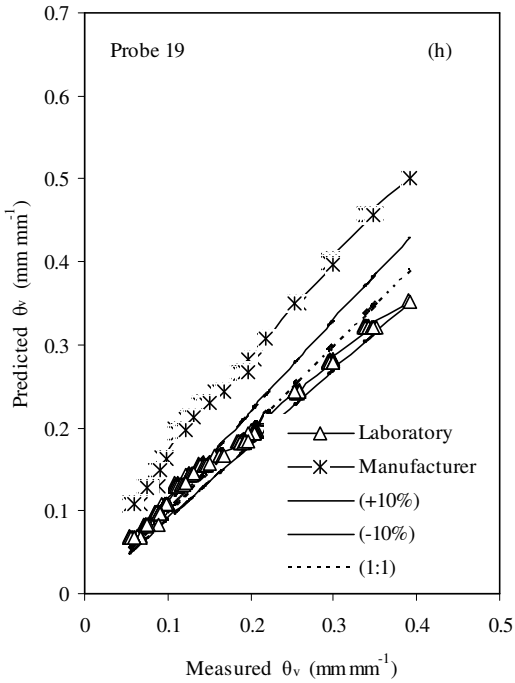
Probe 19
(h)
Predicted θv (mm mm-1)
Measured θv (mm mm-1)
Laboratory
Manufacturer
(+10%)
(-10%)
(1:1)

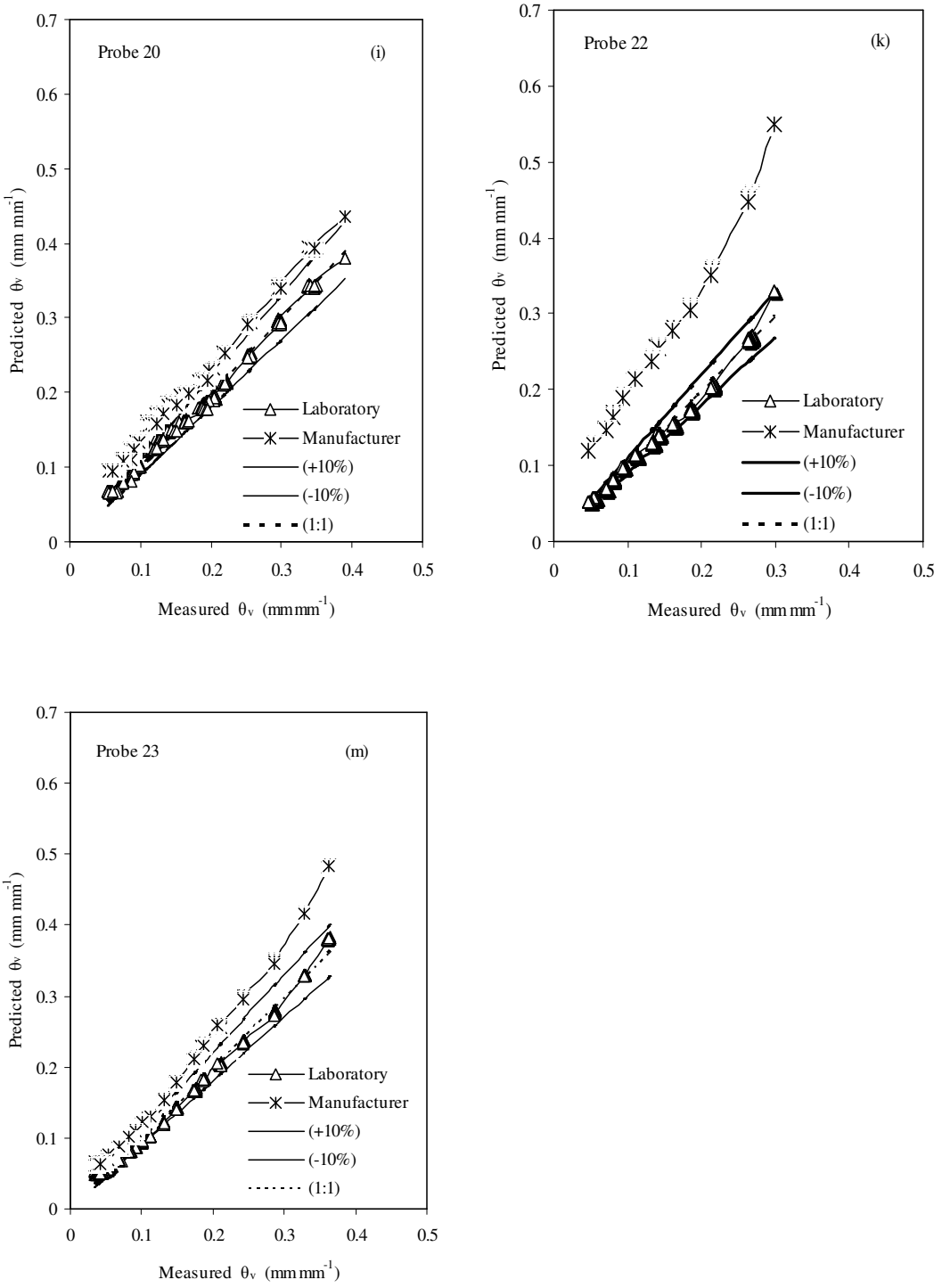

Figure 3.3 Relationships between volumetric soil water content versus predicted soil water content using (i) manufacturers and (ii) combined laboratory calibration equation values for each of the 11 ECH_2O-TE probes calibrated at 5 and 26^oC (average n per probe = 220)

Table 3.6 Quantitative measures evaluating the relationship between measured soil water content (θ_v) versus (i) manufacturer's and (ii) temperature compensated (θ_{tc})*

		A-horizon				B-horizon				C-horizon		
Probe number		1	2	3	4	13	17	18	19	20	22	23
(i) θ_v versus θ_m	RMSE	0.168	0.172	0.215	0.126	0.218	0.191	0.217	0.093	0.080	0.118	0.107
	RMSEs	0.165	0.145	0.201	0.108	0.214	0.196	0.212	0.069	0.042	0.099	0.106
	RMSEu	0.031	0.093	0.075	0.065	0.042		0.044	0.063	0.068	0.064	0.018
	MAE	0.166	0.162	0.209	0.113	0.214	0.186	0.213	0.065	0.049	0.095	0.102
	R^2	0.985	0.935	0.973	0.996	0.954	0.976	0.173	0.985	0.979	0.993	0.980
	D-index	0.717	0.617	0.574	0.782	0.502	0.563	0.481	0.833	0.839	0.728	0.822
	Slope (b)	1.076	0.755	1.305	1.346	1.447	1.363	1.415	1.406	1.073	1.566	1.251
	Intercept (a)	0.148	0.195	0.125	0.019	0.133	0.143	0.151	-0.184	-0.063	-0.018	0.049
	RMSEs/RMSE	0.983	0.843	0.937	0.857	0.981	1.030	0.979	0.737	0.521	0.814	0.985
	RMSEu/RMSE	0.182	0.538	0.349	0.515	0.192		0.205	0.676	0.853	0.541	0.171
(ii) θ_v versus θ_{tc}	RMSE	0.025	0.089	0.090	0.089	0.041	0.023	0.059	0.064	0.070	0.020	0.015
	RMSEs	0.003	0.013	0.060	0.061	0.002	0.003	0.004	0.003	0.002	0.000	0.002
	RMSEu	0.024	0.088	0.067	0.065	0.040	0.023	0.059	0.064	0.070	0.020	0.014
	MAE	0.014	0.045	0.067	0.068	0.020	0.014	0.026	0.020	0.022	0.006	0.011
	R^2	0.985	0.935	0.972	0.996	0.954	0.975	0.973	0.985	0.979	0.993	0.980
	D-index	0.990	0.868	0.823	0.841	0.940	0.981	0.875	0.884	0.862	0.985	0.995
	Slope (b)	0.972	0.924	0.962	1.008	1.006	1.020	0.997	1.018	0.992	1.006	0.979
	Intercept (a)	0.007	0.008	-0.051	-0.063	-0.003	0.000	-0.004	-0.008	0.000	-0.001	0.004
	RMSEs/RMSE	0.140	0.141	0.668	0.682	0.057	0.144	0.072	0.041	0.033	0.025	0.149
	RMSEu/RMSE	0.990	0.990	0.744	0.731	0.998	0.990	0.997	0.999	0.999	1.000	0.989

*The terms b and R^2, D-index, RMSEs/RMSE, RMSEu/RMSE are dimensionless, while the remaining terms have the units mm mm^{-1}

3.4 Conclusions

The ECH_2O-TE probes were calibrated to measure the effect of soil temperature on the probes at room reference temperatures of 5 and 26^oC as treatments. Temperature affected soil water measurements between wet to dry soil conditions to about 48, 62 and 34% for the A, B and C-horizons, respectively. Secondly, temperature compensated equations predicted soil water content measurements with an accuracy, precision and repeatability at 99, 99 and 95%, respectively. Thirdly, manufacturer's generic equation tended to over predict soil water content measurements and lacked accuracy with errors ±40% and repeatability. Hence, the equation provided by Decagon Devices (2006) holds a low validity for the soil used in this study. Furthermore, temperature compensated equations yielded accurate and repeatable results when compared with the manufacturer's equations. It is advisable therefore that each ECH_2O-TE probe be calibrated at different temperatures in order to develop probe specific temperature compensated equations thus avoiding the use of one generic calibration equation for this type of ECH_2O-TE probe. The study revealed that the temperature compensated equations improved measurements to an error of ±1% as it compensated for a range of temperatures. In contrast, work carried out by Kizito *et al.* (2008) and Bogena *et al.* (2007) concluded that standard equations can be used to accurately estimate soil water content, but the results from this study show clearly that their assumptions may lead to errors of ±10% as soils differ in their physical and chemical properties. For scientific purposes it was concluded that ECH_2O-TE probes be calibrated under conditions that are as close as possible to field conditions as the calibration soil temperatures fell within the required range of between 5 and 26^oC. This study concludes that with careful calibration the ECH_2O-TE probe can be deployed in reactive clay soils thereby reducing research costs.

CHAPTER 4

INFLUENCE OF MULCH TYPE AND SURFACE COVERAGE ON TEMPERATURE REGIMES IN A CLAY SOIL UNDER SEMI-ARID CONDITIONS

Abstract

Temperature plays a significant role in evaporation. This study investigates ways of limiting evaporation by investigating how mulch type and percentage cover influences temperature, both above and below the soil surface. The mulching treatments were: bare soil surface (Ba, control), 50% reed mulch cover (50% R), 50% stone cover (50% S) and 100% reeds mulch cover (100% R). Temperature measurements were made at 25, 75, 150, 450, 750 and 1050 mm below the soil surface using ECH_2O-TE sensors and at 75, 160 and 1400 mm above the soil surface using HMP-50 probes. K-S statistical test results and cumulative distribution function (CDFs) revealed that 100% R mulch had small soil temperature variation throughout the year long measurement period. Results show there were no significant temperature differences between 50% S and bare treatments at $\alpha = 0.05$; at the depths of 25, 75 and 150 mm, however 100% R affected soil temperature significantly more than 50% R. Mulch did not influence air temperature at height of 160mm above the soil. Percentage coverage affected soil temperature at depths: 25, 75 and 150 mm, but not at the deeper depths of 450, 750 and 1050 mm. The variation for all depths in the soil temperature gradient was lowest (0.00^oC per half hour) for the 100% R with the highest at 0.49^oC per half hour for the bare soil (control). The 100% R influenced soil temperature more than the other treatments in the following order: 100% R, more than 50% R, more than 50% S and greatest difference from bare soil.

Key words: bare soil, stone, reed

4.1 Introduction

In the south eastern part of the Free State Province of South Africa there is a semi-arid area that covers 800 000 hectares with a population of approximately 500 000 people. The characteristics of this area include heavy clay soils; erratic rainstorms and high evaporation rates. Hensley *et al.* (2000) reported that water loss through evaporation for this area can amount up to 75% of the annual rainfall under maize production and 69% for sunflower; hence they developed a crop production technique known as In-field Rain Water Harvesting (IRWH). This technique is used by households in this area to grow maize and vegetables in their backyard gardens (Kundhlande *et al*., 2004). The IRWH technique minimises runoff, thus promoting infiltration both during the fallow and growing periods; however, the major loss of water is still through evaporation from the soil surface. Mulching has been widely used by researchers to conserve soil water and moderate the field microclimate (Novak *et al*., 2000; Stigter *et al*., 2005; Zhang *et al*., 2009). Hence, this study investigates how reed and stone mulches affect the soil thermal properties. The shortened energy balance at the soil surface is given by the equation (Wu *et al*., 1996):

$$R_n + H + \lambda \mathrm{E} + G = 0 \tag{4.1}$$

where R_n is the net radiant flux (W m^{-2}), H is the sensible heat flux (W m^{-2}), λ is the soil thermal conductivity (W m^{-1} K^{-1}), λE is the latent heat flux (W m^{-2}), and G is the soil heat flux (W m^{-2}). These parameters are different for the bare soil surface and mulched soil surface. The net radiant flux for a bare soil surface is given by the equation:

$$R_n = (1 - a_s)R_s + \in_s R_a - \in_s \sigma T^4 \tag{4.2}$$

where a_s is the soil albedo, R_s is the measured global radiation (W m^{-2}), $\in_s$ is the soil emissivity, R_a is the atmospheric long wave radiation (W m^{-2}), T is the surface temperature (K) and σ is the Stefan-Boltzmann constant (5.67 x 10^{-8} W m^{-2} K^{-4}). The net radiant flux at the mulched soil surface (Wu *et al*., 1996) is determined as follows:

$$R_n = R_s\tau_s(1-a_s)/(1-\rho_s a_s) + \in_s R_a\tau_1/(1-\rho_1+\rho_1\in_s) + \in_s\in_m\sigma T^4/(1-\rho_1+\rho_1\in_s \\ -(1-\rho_1)\in_s\sigma T^4/(1-\rho_1+\rho_1\in_s) \quad (4.3)$$

where ρ_1 is reflectivity of the mulch to long wave radiation, ρ_s is the reflectivity of the mulch to solar wave radiation,$\in_m$ is the mulch emissivity, τ_1 is transmissivity of the mulch to long wave radiation and τ_s is transmissivity of the mulch to solar short wave radiation. Weiss and Hays (2005) observed that a major driving force in most evaporation processes is temperature. Therefore, soil management regimes that can change the characteristics of the soil surface, and hence influence the soil thermal properties can be used as solutions to limit evaporation in the IRWH.

Several investigators have reported that the soil thermal regime under mulching is different from that of a bare soil, with soil temperatures often being lower under mulched surfaces than in non-mulched soils (Bristow, 1988; Sarkar *et al*., 2007; Zhang *et al*., 2009; Hou *et al*., 2010). Others have documented the fact that mulch can increase the top layer soil temperature for example under high weed infestation on groundnut fields in Vietnam (Ramakrishna *et al*., 2006) and under plastic film between maize row crop in China (Wang *et al*., 2003; Zhou *et al*., 2009). These conflicting results may be due to timing of soil temperature measurements, soil properties, the type of mulch used as well as other undocumented factors. Many researchers' note that the effect of mulch on soil temperature varies in that it may increase or decrease temperatures during the growing season from the fallow period through to full canopy stage (Ma and Li, 1996; Cheng and Zhang, 2000). The usual purpose of surface treatments is to influence soil temperature favorably, to prevent water loss by evaporation, to check soil erosion by wind and runoff as well as to enhance soil structure. Traditionally mulch consists of a well aerated, and therefore poor thermal conducting surface cover such as straw, leaf litter and wood chips (Katan, 1979; Maurya and Lal, 1981; Gurnah, 1987; Sui *et al*., 1992). Crop residues, when left as mulch, influence soil water content and soil temperature because they decrease the

energy available to the soil from the incoming solar radiation, and therefore reduce the amount of heat entering the soil. This, occurs due to changes in the surface shortwave reflective properties, as well as an increase in the resistance to vapor or heat diffusion as seen in equation 4.3 from Wu *et al*. (1996). The mulch properties that determine these changes are its type, amount, thickness, and percentage ground covered, as well as its shortwave reflectivity, porosity and tortuosity (Van Doren and Allmaras, 1978). The objectives of this study were (a) to evaluate the effect of percentage cover and type of mulch on the diurnal profile of both the soil and air temperatures; and (b) to determine the change in temperature gradients with soil depth and during a day-night cycle.

4.2 Materials and methods

4.2.1 Experimental design

Soil description and experimental site details are fully discussed in chapter 2, section 2.2.1. There were four treatments as shown in Figure 4.1 and (Appendix 3), namely (i) bare soil or no mulch on the soil surface (Ba), (ii) mulch of reeds covering 50% of the area (50% R), (iii) mulch of reeds covering 100% of the area (100% R), and (iv) mulch of stones on the soil surface covering 50% of the area (50% S). There was also a two meter fetch area around the experimental plot. There was no replication as the instruments are expensive hence a very detailed measurement process was conducted over a long period. Before the instruments were installed in the field a test experiment was conducted to make sure that the instruments are placed in areas representative of the treatments and thus provide valid results. The common reed *Phragmites australis* was used as reed mulch which has hollow and rigid woody stalks with diameter of reeds ranging between 11-29 mm, with an average diameter of ±19 mm. The stones used were approximately round dolerite stones with a diameter ranging from 90 to 160 mm, with an average of 113 mm.

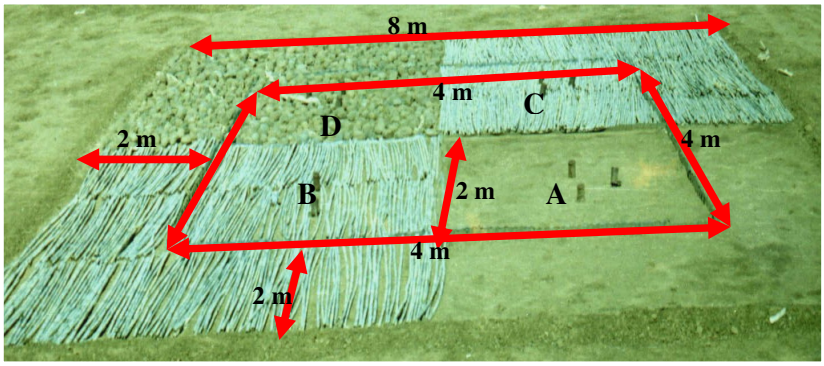

Figure 4.1 Experimental layout showing the four mulch treatments viz Bare soil (B), mulch of reeds covering 50% (B) of the surface area (50% R), mulch of reeds covering 100% (C) of the surface area (100%), mulch of stones covering 50% (D) of the area (50% S) and 2 m fetch area

4.2.2 Measurement period and instruments used

The experimental measurement period lasted from 17 June 2009 to 20 October 2009 (DOY 168 to 188; 205 to 207; 221 to 236; 244 to 245; 261 to 293); with measurements on a total of 70 days. Days missing were due to data logger failure. Winter and spring periods are represented by DOY182-207 and DOY274-293 respectively. DOY 205 (24 July 2009) and DOY 288 (15 October 2009) were chosen at random to represent diurnal winter and days spring respectively. Temperature was recorded every 30 minutes at several positions in each treatment, both above (+) the soil surface (Ab) and below (-) the soil surface (Be). Measurements were taken at heights (+) or depths (-) of +1400, +160, +75, -25, -75, -150, -450, -750 and -1050 mm. Soil temperature measurements were collected using ECH$_2$O-TE probes (Decagon Devices Inc., Pullman, WA) and air temperature measurements were made with HMP-50 probes protected by small radiation shield with an accuracy of ±3% and 99% precision (Campbell Scientific, Logan, UT) both connected to a CR1000 logger via a multiplexer (Campbell Scientific, Logan, UT).

The ECH$_2$O-TE probes were calibrated for temperature sensitivity at 5 different temperatures (2, 14, 27, 31 and 40^{o}C) in a waterbath in the laboratory.

4.2.3 Temperature calculations

Daily maximum temperature (*T*): these values were used in the calculation of mean temperature values for each ten day period for each mulch treatment and elevations (above and below soil surface) using the following equation:

$$T = \frac{\sum_{i=1}^{10} T_i}{10} \tag{4.4}$$

where *i* is the day, T*i* is the daily maximum temperature value for day *i* (^{o}C). Each of the 10-day periods were grouped as follows: 1st (DOY 168-177), 2nd (178-187), 3rd (DOY 188 and 205-206 and 221-226), 4th (DOY 232-236 and 244-245 and 261-263), 5th (DOY 264-273) and 6th (DOY 274-283). Temperature gradient: For this study the amount of energy entering or leaving a particular soil depth over time; during the day and night cycles is expressed as a temperature gradient (TG) or rate of change of soil or air temperature. The TG during the night-time cycle (cooling phase) is termed TG*n* and during the daytime known as TG*d* (warming phase) and can be negative or positive. An equation describing TG*d* and TG*n* for any of the treatments and elevations is as follows:

$$TGd = \frac{T_{18h00} - T_{6h30}}{12} \tag{4.5}$$

$$TGn = \frac{T_{6h00} - T_{18h30}}{12} \tag{4.6}$$

Where: T_{6h00} is the temperature at 06h00 local time per treatment (^{o}C)

T_{6h30} is the temperature at 06h30 local time per treatment (^{o}C)

T_{18h00} is the temperature at 18h00 local time per treatment (^{o}C)

T_{18h30} is the temperature at 18h30 local time per treatment (^{o}C)

TG is the rate of change of temperature (^{o}C h^{-1}) with subscripts *n* and *d* representing night and day periods.

4.2.4 Cumulative distribution functions and statistical analysis

The daily maximum temperature values for the measurement period were arranged in ascending order. The cumulative probability for each treatment or measurement depth was then plotted as the probability of the particular value including the sum of the probabilities of the values ranked below it. Cumulative distribution functions (CDFs) were then constructed as the probabilities against the corresponding maximum temperature values. To test the degree to which cumulative distributions were statistically different from each for each of the treatments, the Kolmogorov-Smirnov (K-S) two sample tests were applied (Steel *et al*., 1997; Langyintuo *et al*., 2002). According to the K-S test, two distributions are significantly different if the maximum vertical (D-statistics) deviation between them exceeds the critical value at the specified significance level (α). In other words, the hypothesis that temperatures at different depths and across different treatments are similar (H_o) is tested, using the K-S test.

4.3 **Results and discussion**

4.3.1 Daily maximum temperatures for the measurement period

Generally, the temperature profiles (Figures 4.2a; 4.2b; 4.2c and 4.2d) indicate downward energy entering the soil and influencing the soil profile down to the -450 mm level; with the greatest influence being at depths (-25 and -75 mm), followed by -150 mm and lastly -450 mm depth. Figures 4.2a; 4.2b; 4.2c and 4.2d also indicate that when the weather station temperature at +1400 mm was higher than 15^{o}C; the temperature values at +75 and +160 mm levels were continuously higher than the station air temperature by approximately 4^{o}C for all the four treatments (100% R, 50% R, 50% S and bare). The higher temperature values maybe attributed to an intermediate layer of still (warmer) air just above the soil surface due to the amount of terrestrial radiation leaving the surface; reflective albedo of the mulch or soil and the slow transfer of sensible heat into the soil caused air temperature at these heights to be higher than the station air temperature.

Figure 4.2b shows that at depths (+25, +75 and +150 mm) below the soil surface, the soil temperature values for the 100% R were lower than those of the bare treatment (Figure 4.2a) which had temperatures above 15^{o}C. This is due to the fact that, the mulch absorbs most of solar radiation and heats up and then transmits little energy downward by conduction thus resulting in a lower soil temperature underneath it. A similar trend was observed by Stigter *et al*. (2005) as the influence of mulch on microclimate. At the depths -25 and -75 mm the bare soil's maximum temperatures were higher than those from any of the mulch treatments, 100% R, 50% R and 50% S treatments during the same period. Table 4.1 also indicates that the soil temperature values at depths -25 and -75 mm for the bare treatment were not significantly different from each other, at a significance level of $\alpha = 0.05$ thus the profiles downward heat flux through the top 75 mm of soil was similarly affected when no mulch was present. At depths of -150 and -450 mm below the soil, there was less variation in soil temperature for the 100% R (Figure 4.2b), than the bare soil treatment throughout the measurement period (Figure 4.2a).

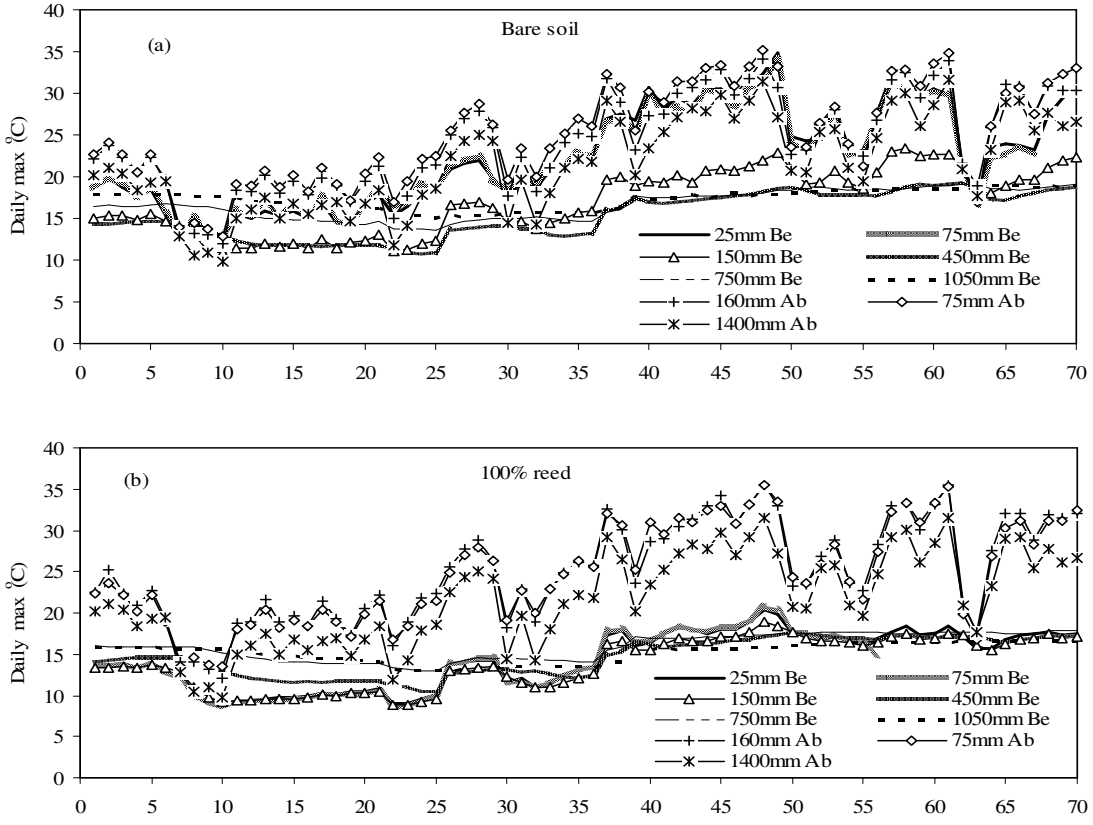

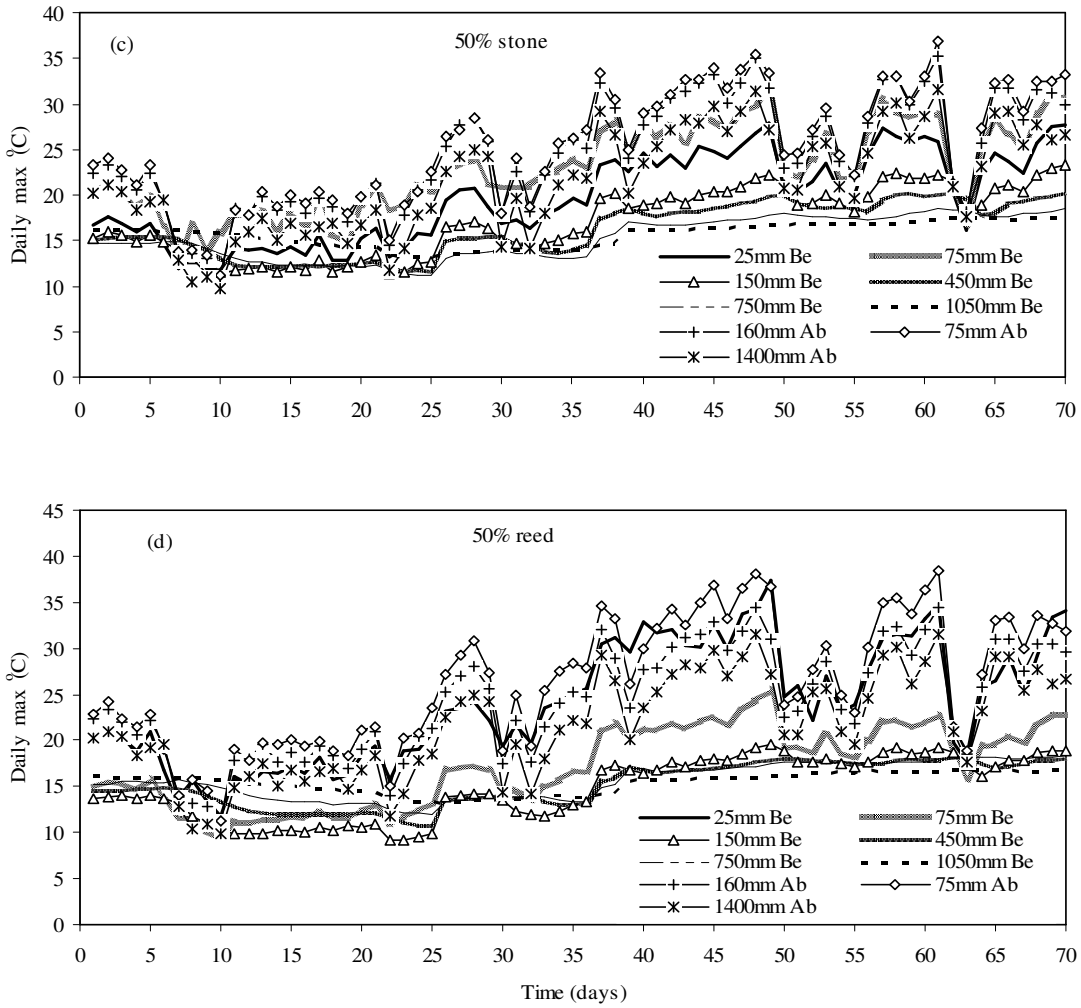

Figure 4.2 Daily maximum temperature variation above (Ab) and at depths below (Be) the soil surface over the whole measuring period for (a) bare soil, (b) 100% reed, (c) 50% stone and (d) 50% reed treatments, starting at DOY 168

Figures 4.2b; 4.2c and 4.2d show that, at the depth of -750 mm the soil temperature values were lower than soil temperatures at the -1050 mm depth during the winter period due to the fact that there is still downward heat movement into the deeper layers of the soil. But, the opposite was observed during the spring period whereby the soil temperature values at -750 mm were higher than soil temperatures at depth -1050 mm (Figure 4.2). It maybe due to the downward heat flow during the day as the heat moves downward through the profile faster than during the warmer periods, thus releasing some of the energy to the layers above it during the night. The K-S comparison results (Table 4.1) indicate that for the bare soil treatment, the temperature

profile from the height of +1400 mm above the soil downwards to the depth of -75 mm below the soil surface were not significantly different ($\alpha = 0.05$). For the other treatments (100% R, 50% R and 50% S) the temperature values were significantly different. Within each of the following treatments: 100% R, 50% R and 50% S at depths -25, -75, -150, -450, -750 and -1050 mm temperature values were significantly different from each other at $\alpha = 0.05$ (Table 4.1) throughout the measurement period. This confirms the influence of different mulch types and cover on soil temperature regimes.

4.3.2 CDFs for daily maximum air and soil temperature between treatments

Figures 4.3a and 4.3b and Table 4.2 show that the daily maximum air temperature values at heights (+75 and +160 mm) above the soil surface for different treatments were not significantly different from each other at $\alpha = 0.05$ throughout the measurement period. This means that mulch type and percentage cover of the mulch did not influence air temperature at these heights above the soil surface. CDF graphs show clearly that the 100% R had the greatest effect on lowering soil temperature at depths of -25, -75, -150 and -450 below that of other treatments followed by the 50% R. This was consistent with work of Horton *et al*. (1996) who observed that mulch cover normally has a higher albedo and therefore lower thermal conductivity than bare soil, and consequently it reduces the solar energy reaching the soil, and finally reduces the temperature increases during warm conditions.

Table 4.1 K-S comparisons of daily maximum temperatures at different heights and depths

Pairs above (+) and below (-) soil	Bare		100% R		50% R		50% S	
	D-stats	P value	D-stats	P value	D-stats	P value	D-stats	P value
(+) 1400 vs (+) 160	0.2143^{ns}	0.0690	0.2571*	0.0160	0.2000^{ns}	0.1060	0.2286*	0.0430
(+) 1400 vs (+) 75	0.2571*	0.0160	0.2714*	0.0090	0.2000^{ns}	0.1060	0.2286^{ns}	0.0430
(+) 1400 vs (-) 25	0.1571^{ns}	0..3260	0.6426*	0.0000	0.2429*	0.0260	0.1857^{s}	0.4430
(+) 1400 vs (-) 75	0.1029^{ns}	0.844	0.6286	0.0000	0.3857*	0.0000	0.1429*	0.0000
(+) 1400 vs (-) 150	0.4143*	0.0000	0.7000*	0.0000	0.6429*	0.0000	0.4143*	0.0000
(+) 1400 vs (-) 450	0.6571*	0.0000	0.7429*	0.0000	0.7000*	0.0000	0.5714*	0.0000
(+) 1400 vs (-) 750	0.6571*	0.0000	0.7286*	0.0000	0.6857*	0.0000	0.6714*	0.0000
(+) 1400 vs (-)1050	0.6571*	0.0000	0.8000*	0..0000	0.7714*	0.0000	0.7429*	0.0000
(+) 160 vs (+) 75	0.1143^{ns}	0.7250	0.0714^{ns}	0..9920	0.2286*	0.0430	0.1429^{ns}	0.443
(+) 160 vs (-) 25	0.2000^{ns}	0.1060	0.8286*	0.0000	0.1143^{ns}	0.7250	0.3714*	0.0000
(+) 160 vs (-) 75	0.2206^{ns}	0.062	0.8286*	0.0000	0.5000*	0.0000	0.2143^{ns}	0.0629
(+) 160 vs (-) 150	0.5286*	0.0000	0.8714*	0.0000	0.7429*	0.0000	0.5714*	0.0000
(+) 160 vs (-) 450	0.7857*	0.0000	0.9143*	0.0000	0.8143*	0.0000	0.7143*	0.0000
(+) 160 vs (-) 750	0.7857*	0.0000	0.9000*	0.0000	0.81436*	0.0000	0.8143*	0.0000
(+) 160 vs (-) 1050	0.7857*	0.0000	0.9286*	0.0000	0.9286*	0.0000	0.9143*	0.0000
(+) 75 vs (-) 25	0.2571*	0.0160	0.8143*	0.0000	0.1571^{ns}	0..3260	0.3714*	0.0000
(+) 75 vs (-) 75	0.2647*	0.0140	0.8000*	0.0000	0.5857*	0.0000	0.2429*	0.0000
(+) 75 vs (-) 150	0.5714*	0.0000	0.8714*	0.0000	0.8143*	0.0000	0.6143*	0.0000
(+) 75 vs (-) 450	0.8429*	0.0000	0.9000*	0.0000	0.9143*	0.0000	0.7429*	0.0000
(+) 75 vs (-) 750	0.8571*	0.0000	0.9000*	0.0000	0.9000*	0.0000	0.8571*	0.0000
(+) 75 vs (-) 1050	0.8571*	0.0000	0.9429*	0.0000	0.9286*	0.0000	0.9286*	0.0000
(-) 25 vs (-) 75	0.1029^{ns}	0.8440	0.2286*	0.0430	0.5000*	0.0000	0.2714*	0.009
(-) 25 vs (-) 150	0.4286*	0.0000	0.2286*	0.0430	0.7000*	0.0000	0.3571*	0.0000
(-) 25 vs (-) 450	0.6000*	0.0000	0.2857*	0.0050	0.7857*	0.0000	0.4857*	0.0000
(-) 25 vs (-) 750	0.6143*	0.0000	0.4000*	0.0000	0.7571*	0.0000	0.5714*	0.0000
(-) 25 vs (-) 1050	0.6143*	0.0000	0.4000*	0.0000	0.8143*	0.0000	0.6000*	0.0000
(-) 75 vs (-) 150	0.3824*	0.0000	0.2286*	0.0430	0.4000*	0.0000	0.4857*	0.0000
(-) 75 vs (-) 450	0.4286*	0.0000	0.4286*	0.0000	0.4714	0.0000	0.6857*	0.0000
(-) 75 vs (-) 750	0.6176*	0.0000	0.5714*	0.0000	0.4571*	0.0000	0.7714*	0.0000
(-) 75 vs (-) 1050	0.6324*	0.0000	0.5286*	0.0000	0.5000*	0.0000	0.8571*	0.0000
(-) 150 vs (-) 450	0.4000*	0.0000	0.0260*	0.0000	0.2286*	0.0430	0.2571*	0.0160
(-) 150 vs (-) 750	0.4143*	0.0000	0.4571*	0.0000	0.2714*	0.0090	0.4571*	0.0000
(-) 150 vs (-) 1050	0.4143*	0.0000	0.3714*	0.0000	0.4429*	0.0000	0.4857*	0.0000
(-) 450 vs (-) 750	0.3857*	0.0000	0.3429*	0.0000	0.1857*	0.1590	0.3429*	0.0000
(-) 450 vs (-) 1050	0.5143*	0.0000	0.3429*	0.0000	0.3857*	0.0000	0.4571*	0.0000
(-) 750 vs (-) 1050	0.3286*	0.0010	0.4571*	0.0000	0.3857	0.0000	0.3000*	0.0030

*Significantly different at $\alpha = 0.05$; ^{ns} not significantly different at $\alpha = 0.05$

The stones have good contact with the soil surface and therefore can conduct the heat received from solar radiation on the upper surface through the stone and directly into the soil profile. Stone mulch acts similarly to the bare soil with a continuous contact surface for conduction of heat received from solar radiation. The stones physical system is different from that of the reed mulch. The reeds are laying on the surface of the soil, but they are hollow which discourages the conduction of heat. So, although the upper surface of the reeds may reach a high temperature, this heat cannot be easily conducted directly across the air space of the hollow reeds. Thus they provide a thermal conduction discontinuity and so the temperatures below the 100% R mulch are much lower than the other treatments (Figure 4.3).

At depths of -75, -150, -450 mm the bare and 50% S treatments had a similar effect on soil temperature as they were found to be not significantly different (i.e: similar) at $\alpha = 0.05$, they were only significantly different from each other at the surface (-25 mm) and at the deepest measurement depths of -750 and -1050 mm (Figures 4.3d; 4.3e; 4.3f and Table 4.2). The 50% stone and bare treatments had the similar effect on temperature; and were significantly different from other mulch treatments 50% R and 100% R at depths -75, -150 and -450 mm, this means that they probably allow similar amounts of radiation onto the soil surface hence heat conductivity into the soil profile is probably similar. Depths -25 and -75 mm (Figure 4.2) show that there was diurnal and daily temperature variation, at -150 and -450 mm less variable and at -750 and -1050 mm little variation. These results indicate that the mulch had more influence on soil temperature through to the depth of -450 mm than in the deeper layers as also observed by Dahiya *et al*. (2007). These results indicate that temperature and mulch had an effect up to -450 mm contrary to Botha (2006) findings: who stated that Es only occurs between soil depths (0-300 mm). Therefore, this means that the effective zone of evaporation from the soil (0-450 mm).

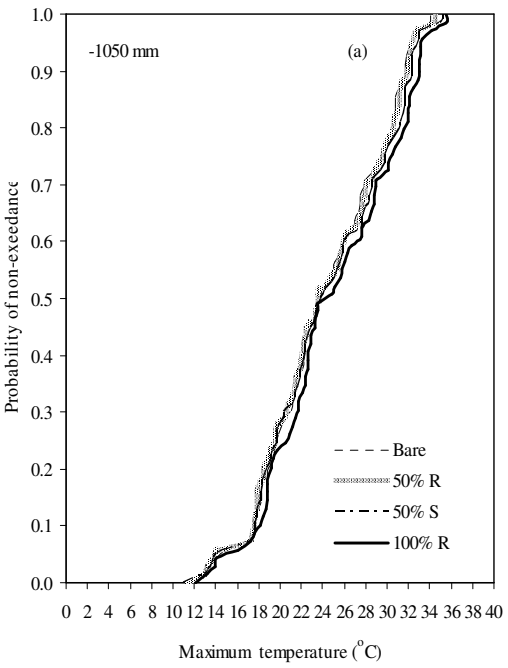
-1050 mm
(a)
Probability of non-exeedance
Maximum temperature (°C)
Bare
50% R
50% S
100% R

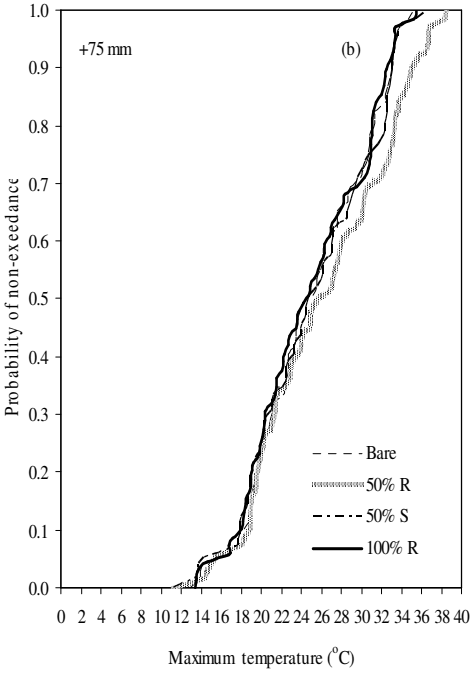
+75 mm
(b)
Probability of non-exeedance
Maximum temperature (°C)
Bare
50% R
50% S
100% R

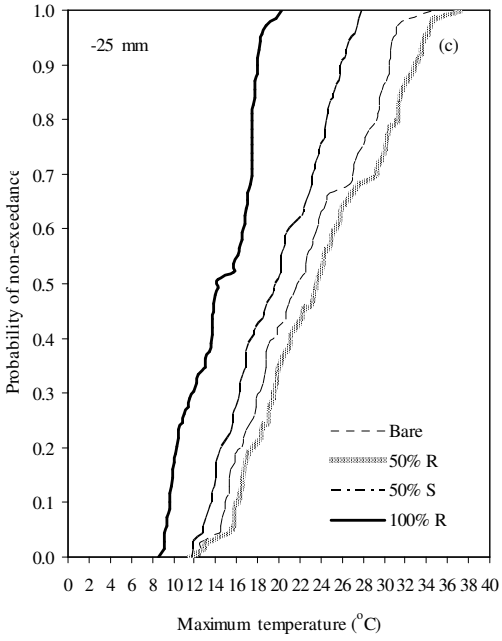
-25 mm
(c)
Probability of non-exeedance
Maximum temperature (°C)
Bare
50% R
50% S
100% R

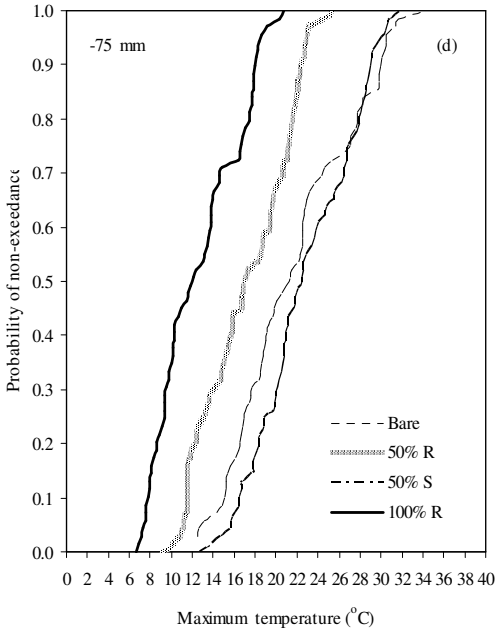
-75 mm
(d)
Probability of non-exeedance
Maximum temperature (°C)
Bare
50% R
50% S
100% R

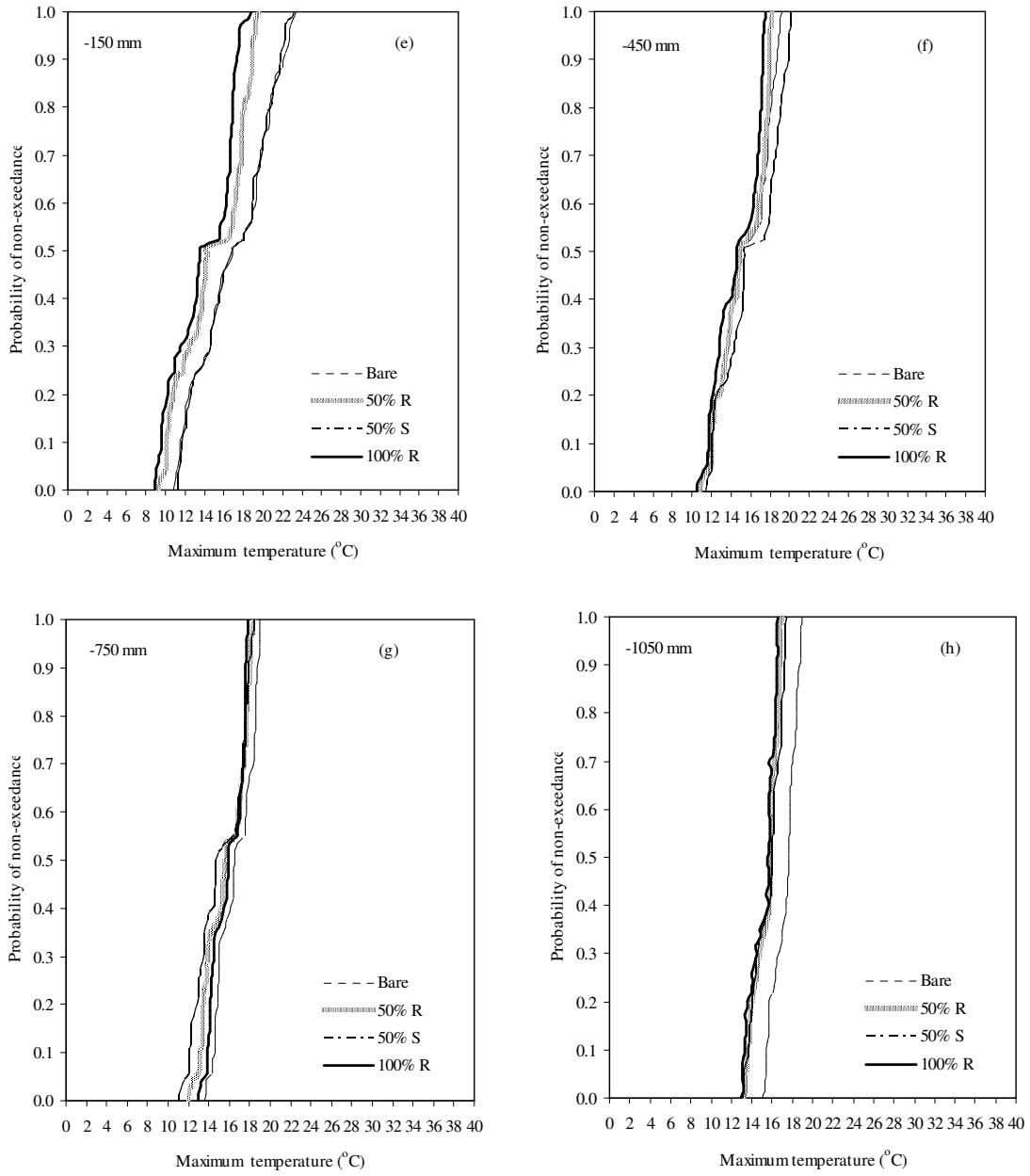

Figure 4.3 Cumulative distribution function graphs of daily maximum temperature for heights above (+) and depths below (-) the soil surface as influenced by the mulch treatments

Table 4.2 K-S paired comparison of maximum temperatures for the mulching treatments at various levels above (+) and below (-) the soil surface over the measurement period

Comparisons	Sensor level relative to soil surface: (+) above and (-) below							
	+160 mm		+75 mm		-25 mm		-75 mm	
	D-statistics	P-value	D-statistics	P-value	D-statistics	P-value	D-statistics	P-value
Bare vs 100R	0.1286^{ns}	0.5800	0.0714^{ns}	0.9920	0.6429*	0.0000	0.6555*	0.0000
Bare vs 50R	0.0571^{ns}	1.000	0.1571^{ns}	0.3260	0.1714^{ns}	0.2320	0.3567*	0.0000
Bare vs 50S	0.0714^{ns}	0.9920	0.0714^{ns}	0.9920	0.2714*	0.0090	0.1702^{ns}	0.2460
100R vs 50R	0.1143^{ns}	0.7250	0.1714^{ns}	0.2320	0.7286*	0.0000	0.4143*	0.0000
100R vs 50S	0.0714^{ns}	0.9920	0.1000^{ns}	0.8570	0.5286*	0.0000	0.7286*	0.0000
50R vs 50S	0.0714^{ns}	0.9920	0.1429^{ns}	0.4430	0.3143*	0.0010	0.4143*	0.0000
	-150 mm		-450 mm		-750 mm		-1050 mm	
	D-statistics	P-value	D-statistics	P-value	D-statistics	P-value	D-statistics	P-value
Bare vs 100R	0.4571*	0.0000	0.3286*	0.0010	0.3571*	0.0000	0.7000*	0.0000
Bare vs 50R	0.3857*	0.0000	0.1857^{ns}	0.1590	0.3000*	0.0030	0.6714*	0.0000
Bare vs 50S	0.0714^{ns}	0.9920	0.2143^{ns}	0.0690	0.3571*	0.0000	0.5714*	0.0000
100R vs 50R	0.2857*	0.0050	0.2714*^{s}	0.0090	0.2571*^{s}	0.0160	0.2143^{ns}	0.0690
100R vs 50S	0.4571*	0.0000	0.4571*	0.0000	0.3143*	0.0010	0.3143*	0.0010
50R vs 50S	0.3714*	0.0000	0.3857*	0.0010	0.1714^{ns}	0.2320	0.2714*	0.0090

*Significantly different at $\alpha = 0.05$; ^{ns} not significantly different at $\alpha = 0.05$

4.3.3 Air temperature

To illustrate the effect of the mulch treatments on the diurnal changes in air temperature, two separate days were randomly chosen for detailed analysis from each period viz. for winter DOY 205 and for spring DOY 288 (Figure 4.4). DOY 205 had a maximum weather station temperature of 11.8^{o}C and minimum of -6.6^{o}C. DOY 288 had a maximum of 29.1^{o}C and minimum of 16.5^{o}C.

DOY 205 (winter): At the +75 mm above mulch layer the 100% R, the night temperature was higher (by up to 4^{o}C) than other treatments. It seems that the 100% reeds provided insulation and retained heat such that the air does not cool down as much as compared to bare soil, 50% R or 50% S treatments (Figure 4.4a). However, the effect was absent at the +160 mm in all the treatments (Figure 4.4b). All mulching treatments had temperature values higher than station air temperature at the +1400 mm level (Figures 4.4a and 4.4b) during daytime. The Bare treatment had the highest temperatures at +75 mm (Figure 4.4a) due to terrestrial radiation making the soil surface hot, hence also warming the nearby air. From 09h00 to 18h00, the 50% treatments (50% R and 50% S) had at the +75 mm level similar maximum temperatures at 15.0^{o}C and (100% R and Bare) were similar at 17.0^{o}C (Figures 4.4a and 4.4b). Overall the results reveal that percentage cover and type of mulch did not have a significant effect on air temperature, except for the 100% reed mulch which caused an increase in temperature during the night and midday at +75 mm level.

DOY 288 (spring): At the +75 mm level, Figure 4.4c shows that 100% R and Bare treatments had similar trends in their response to temperature both with a maximum of 30^{o}C at 12h00; however 50% R and 50% S both had a slightly higher maximum by 3^{o}C. Figure 4.3d at the +160 mm level illustrates clearly that the treatments applied did not influence air temperature though the temperatures were 4^{o}C higher than the weather station air temperature at +1400 mm during the morning only. Results for both DOY 205 and 288 show, that the

different mulch treatments did not have a meaningful effect on air temperature at heights +75 or +160 mm.

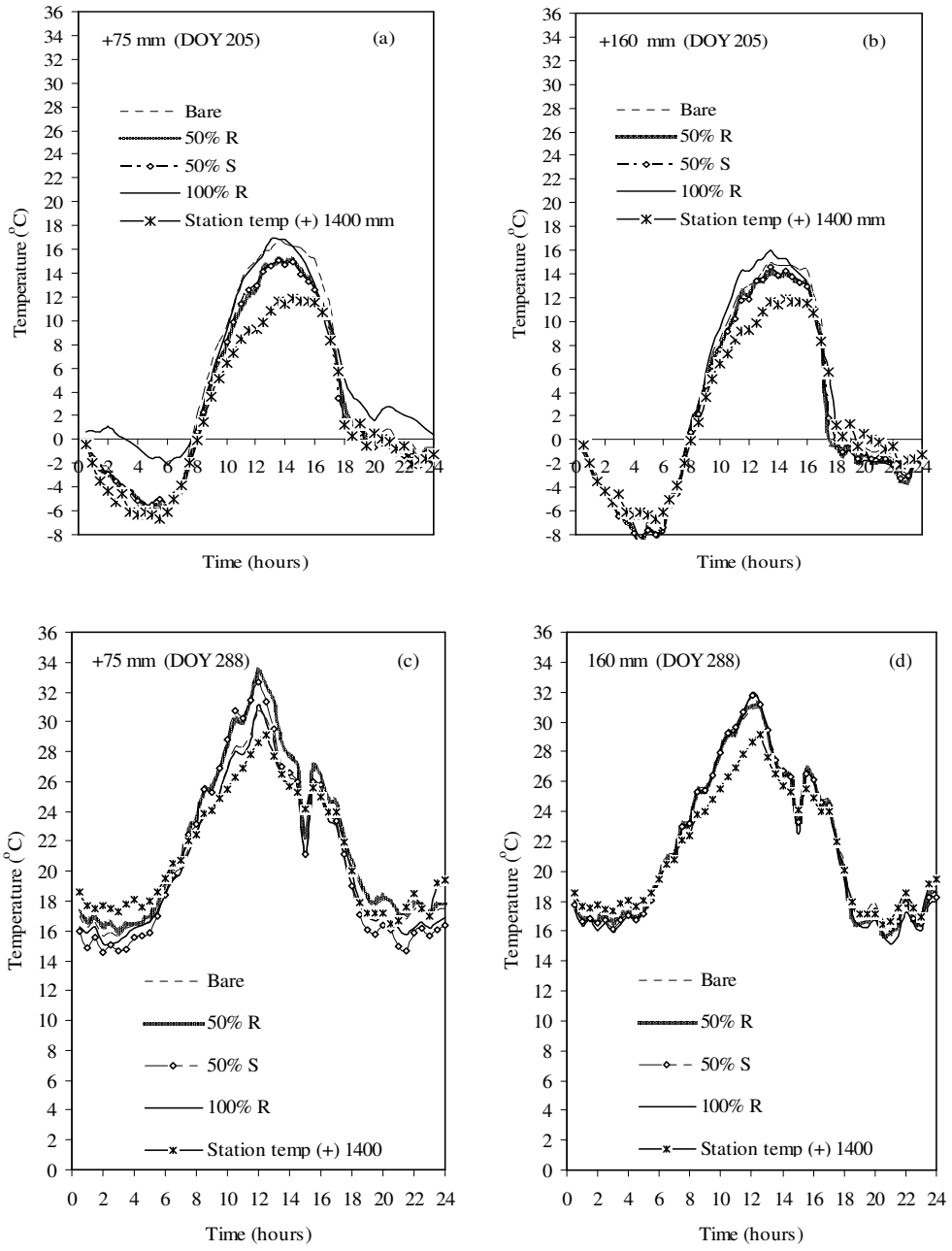

Figure 4.4 Diurnal changes in air temperatures at heights +75 and +160 mm on DOY 205 and DOY 288 as affected by the mulch treatments

4.3.4 Soil temperature

DOY 205 (winter): The diurnal changes in soil temperature displayed in Figure 4.5a shows that at depth -25 mm, the 100% R treatment had daily maximum and minimum soil

temperatures of 9.1 and 6.3°C, respectively thus a daily variation of only 2.6°C; yet the 50% R, 50% S and Bare had daily variations of 13.3, 11.0 and 15.2°C, respectively. It seems that the 50% R mulch allows the most back radiation and escape of heat from the surface as it reached the lowest minimum temperature (-1.6°C) at -25 mm depth. The Bare showed a similar pattern with daytime high of 15.3°C and cooling down to 0.1°C at night; thus during the night, temperature of the bare soil falls rapidly because of radiative cooling such that the surface is the coldest location in the profile. The 100% R retains the most heat at -25 mm depth and thus has a small diurnal variation. This is due to the fact that some solar energy passes through the mulch and heats up the air within and soil beneath the mulch, and then the heat is trapped by the "greenhouse effect". Similar patterns are shown in Figure 4.5b for -75 mm depth, where the 50% S reached highest peak of 18.4°C, followed by bare with 16.5°C; then 50% R with 10.8°C and lastly 100% R with 8.7°C. The 100% R reduces the amplitude of daily temperature variations due to the insulating effect of mulch as also observed by Shinners *et al*. (1993). Throughout the study period the 100% R kept soil temperature peak variations to a minimum, far more than any of the other treatments throughout the day; followed by 50% S, then 50 % R and lastly the bare soil treatment had the highest diurnal variation. The 100% R mulch for the whole spring period seemingly had more insulation effect than any of the other three treatments both during the day and night. In general the soil temperature seemed to increase linearly from 07h00 to reach a peak at 15h00, from then on it gradually decreased again, compared to station air temperature more sudden cooling after 16h00. At -150 mm level, Figure 4.5c shows that 100% R, 50% R, 50% S and bare treatments reached maximum at 18h00 (8.9°C), 18h30 (9.1°C), 19h30 (11.4°C) and at 18h30 (11.0°C) and all had similar minimums of less than 8°C. The 50% S and bare treatments and 100% R and 50% R followed the same trends as shown in Figure 5c, though its important to observe that 50% S mulch reached its peak much later at 19h30, which may be due to the stones continuous transmission of stored heat in comparison to the bare treatment (the stones served as a storage place for heat to be released in the late afternoon).

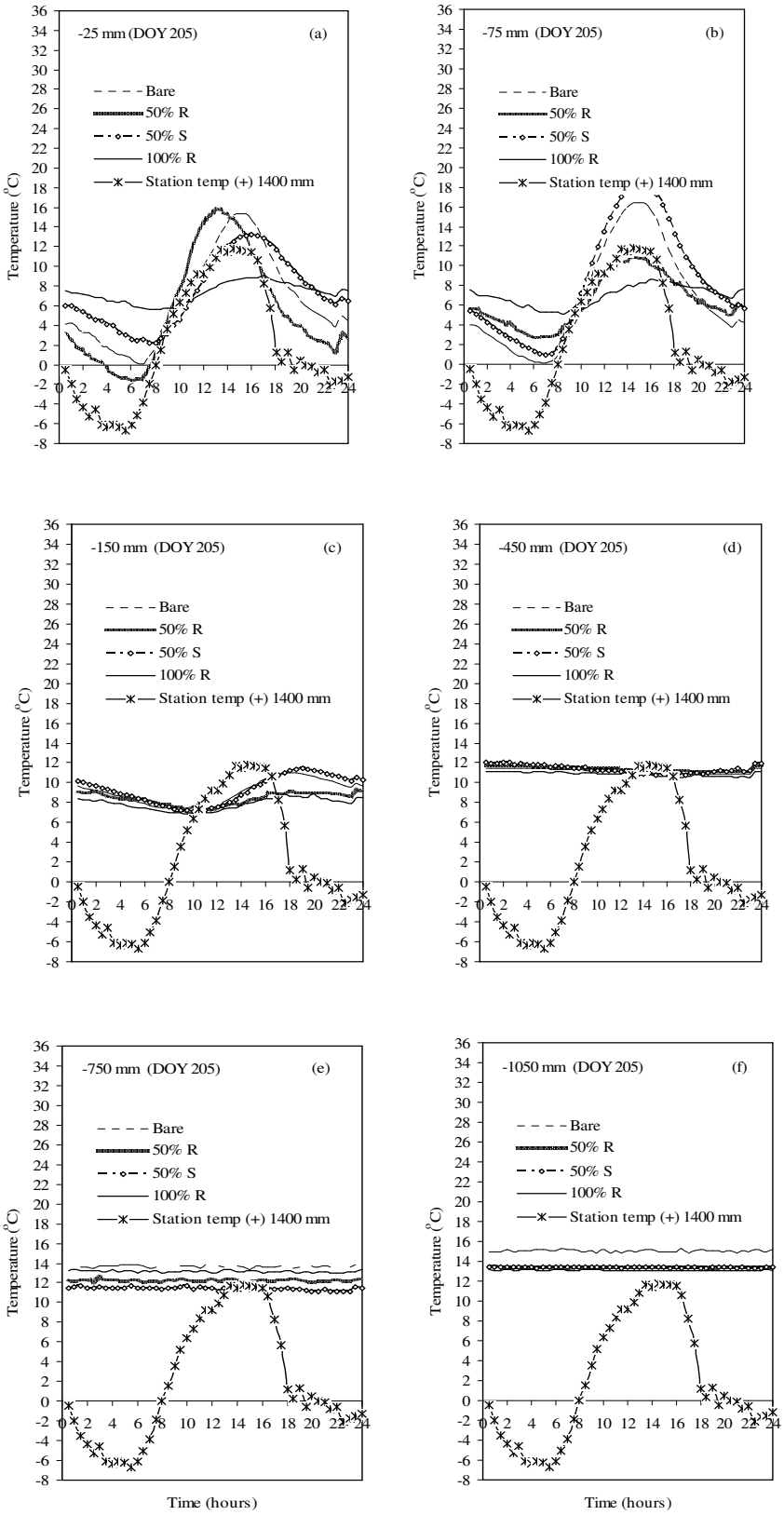

Figure 4.5 Soil temperatures values below (-) the soil at (a) -25, (b) -75, (c) -150, (d) -450, (e) -750 and (f)-1050 mm for DOY 205 representing winter values compared with station air temperature values at +1400 mm

At the depth of -450 mm (Figure 4.5d) there was little variation in soil temperature between treatments except that the 50% S had slightly higher temperature by 1°C compared to the other treatments. This meant that the stone mulch transmitted more solar radiation into the soil than the other treatments; due to the fact that the stones are a better conductor of heat than the reeds which are hollow inside, thus reducing heat transfer into the soil. At the depth of -750 mm (Figure 4.5e) the 100% R, 50% R, 50% S and bare treatments maintained almost constant average soil temperatures of 13.4, 12.3, 11.5 and 13.7°C, respectively; however for the depth of -1050 mm (Figure 4.5f) the 50% R and 50% S mulches had similar temperatures at 13.4°C throughout the day. The 100% R mulch at -1050 mm was lower by 0.2°C and the bare soil had a higher average temperature than the others by 1.7°C at 15.1°C. Throughout DOY 205 the 100% reed mulch imposed a more effective blanket or moderating effect on the temperature than the other treatments. This phenomenal agrees with the fact that during colder winter periods, the input of solar energy is lower and there is a net loss of soil heat energy to the atmosphere at night, resulting in temperature decrease in the soil profile. For the bare treatment conduction of heat through the surface is higher; hence it releases more heat during the night. The presence of mulch on the surface seems to insulate, to some degree, the soil from the colder atmosphere. Therefore, heat loss from the soil is somewhat lower under mulching (Figures 4.5a, 4.5b and 4.5c) than without mulching and soil temperatures consequently remain higher and have lower diurnal variation especially with the 100% R coverage.

DOY 288 (spring)**:** Figure 4.6a shows how 100% R influences soil temperature at -25 mm with a low diurnal variation in temperature of 1.4°C; with a low maximum at 13h00 of 17.0°C. Figure 4.6b shows clearly that the 50% S mulch continuously had higher temperatures throughout the cycle. The peak temperatures at 13h30 for the 50% S, bare, 50% R and 100% were at 26.1, 24.1, 21.0 and 17.0°C, respectively. The stones absorb solar energy and conduct heat into the soil much more efficiently than the other treatments due to the fact that it is in good contact with the soil surface. The 50% R at depth of -75 mm below the soil recorded the lowest temperatures between 24h00 and 08h00 (Figure 4.6b). The 50% S and Bare followed

the same trend in soil temperature at -25mm depth but only reaching a maximum of 23.0^{o}C. Once again, the 100% R continued to maintain almost constant soil temperatures at about 16.0^{o}C at -75, -150 and -450 mm depths (Figures 4.6b, 4.6c and 4.6d). At -150 mm depth, the maximum temperature diurnal variation was at 3^{o}C for all the treatments, showing little variation in soil temperature throughout the day, this is due to the damping effect of temperature with the increase in depth. However, the 50% S and bare treatments had higher temperature than the 100% R and 50% R. At -450 mm below the soil (Figure 4.6d), the temperatures were almost constant throughout the whole day at 16.5, 17.0, 18.5 and 17.5^{o}C for the 100% R, 50% R, 50% S and bare treatments, respectively. The 50% S soil temperatures were higher than the other treatments since the stones store heat when it's warm and then release it slowly into the soil. Figures 4.6e and 4.6f for depths -750 and -1050 mm show that soil temperature for 100% R, 50% R, and 50% S mulch treatments were similar throughout the day at 17^{o}C and bare soil was consistently higher by 1.0^{o}C. At depths -25, -75 and -150 mm (Figures 4.6a, 4.6b and 4.6c) soil temperatures under 100% R mulch concurred with results of Fabrizzi *et al*. (2005) and Olasantan (1999), as both indicated that their soil temperatures under mulching were higher than bare soil during colder weather. They concluded that the magnitude of the changes in soil temperature varies across studies, and attributed it to the mulch type, amount, soil properties as well as climate regions.

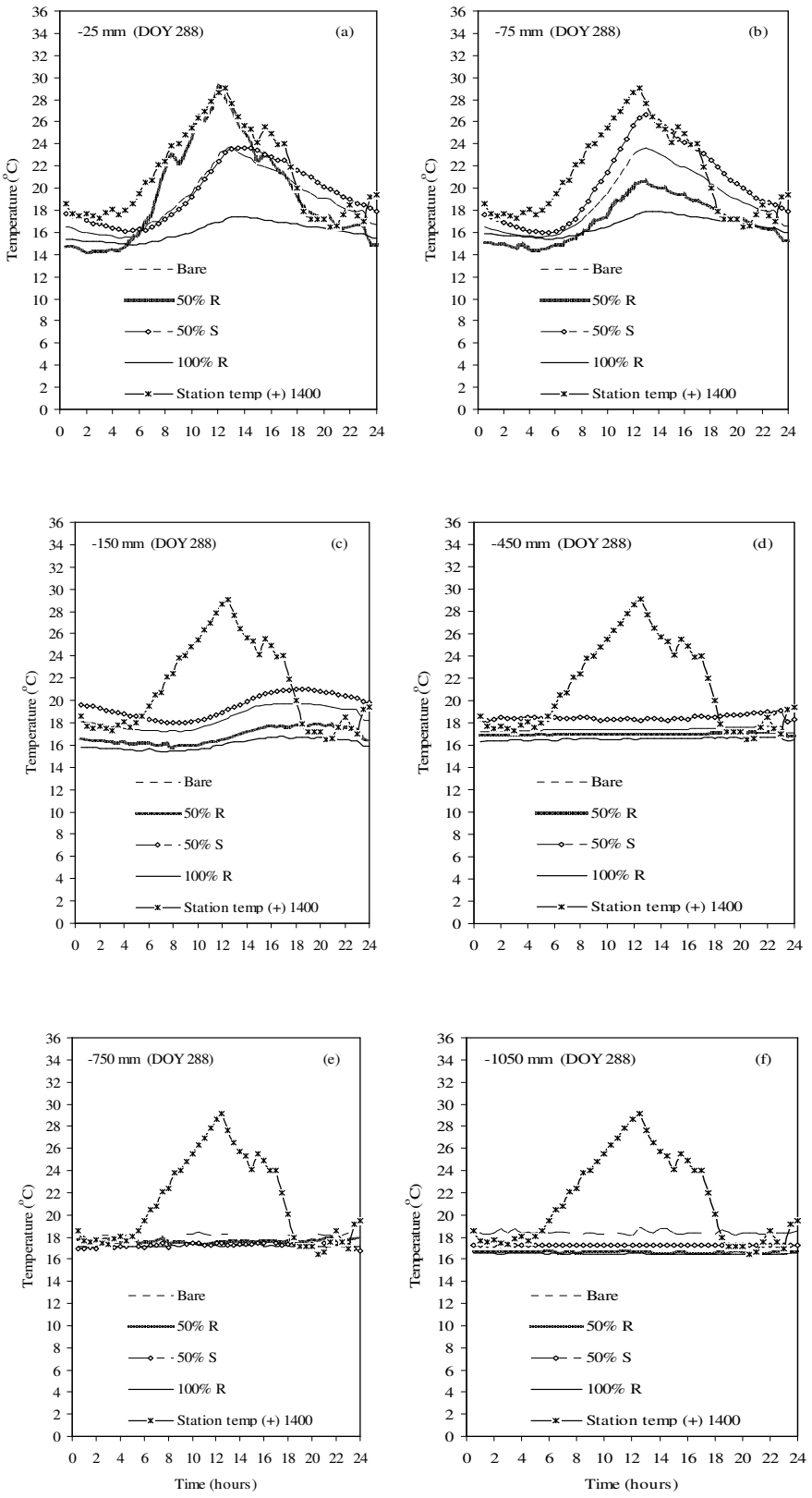

Figure 4.6 Soil temperatures below (-) the soil at (a) -25, (b) -75, (c) -150, (d) -450, (e) -750 and (f) -1050 mm for DOY 288 representing spring

4.3.5 Ten day periods of daily maximum temperature profiles

The results for the ten day periods of maximum temperature profiles as influenced by the mulch treatments are presented in Figure 4.7. In the topsoil (0-400 mm), Figures 4.7a, 4.7b, 4.7c, 4.7d, 4.7e and 4.7f show that the 100% R generally had lower soil temperature values than the 50% R, 50% S and bare soil. This was attributed to the insulation effect of reeds, as they are hollow and hence poor conductors of heat. The temperature values from the 50% R were similar to those of the 100% R, followed by the 50% S and lastly the bare. A similar trend was observed at depth -450 mm in all the treatments. All the other treatments had higher temperatures values than the 100% R, this can be logical in that their soil surfaces are heated more directly than the 100% R surface and can be attributed to the fact that the reeds provide a blanket effect. The 50% S had higher temperatures closer to the surface (-25, -75 and -150 mm) owing to the fact that the stones conduct heat into the soil even during the night being better conductor but it did not go all the way to the deepest soil layers. Figure 4.7 and Tables 4.3 show clearly that bare soil had higher soil temperatures than the 100% R, 50% R and 50% at the depth of 1050 mm; the effect of solar radiation passes through to the deeper profile layer faster than the other treatments hence the higher temperatures. The lower temperatures could contribute positively to root growth and plant development due to the low variations in soil temperatures under mulched soil surfaces. Figures 4.7a, 4.7b, 4.7c, 4.7d and 4.7d during winter; show that at the depth of -750 mm the 50% S had lower soil temperatures than 100% R, 50% R and bare soil. Yet at depth -450 mm, throughout the measurement period, similar temperature values with a variation less than 1.5^{o}C. It was observed also that with approaching spring, temperatures values closer to the surface started increasing considerably from DOY 264 onwards.

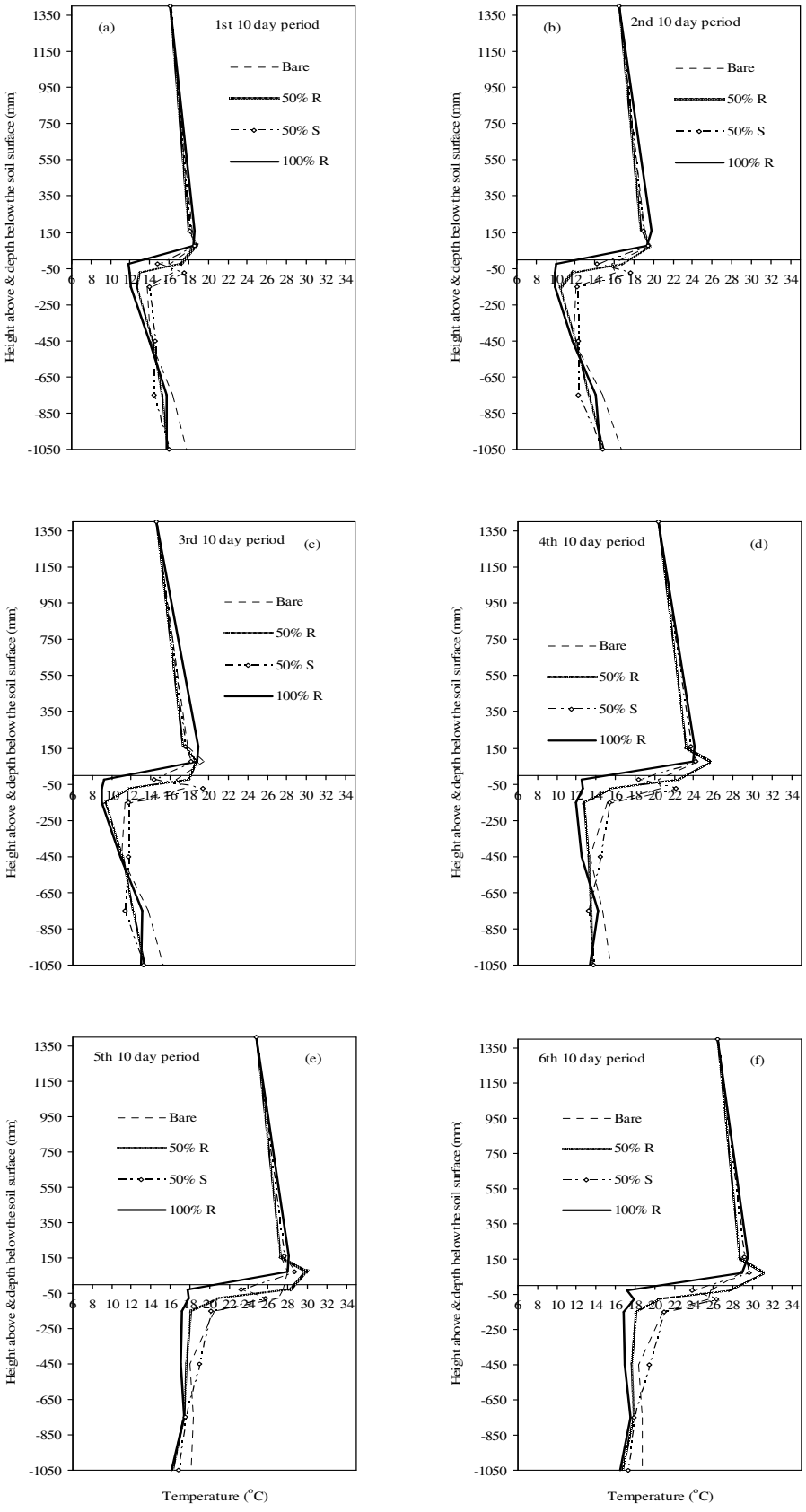

Figure 4.7 Ten day periods of maximum temperature (°C) per treatment for different levels above (+) and below (-) the soil surface

Table 4.3 10 day periods (1 to 6) of daily maximum temperature profile as influenced by the mulch treatments

Sensor level relative to soil surface in mm	Ten day periods of daily maximum temperature (°C) per treatment											
	1st ten day period (DOY 168-177)						2nd ten day period (DOY 178-187)					
	Bare	50% R	50% S	100% R	Sd**	CV*	Bare	50% R	50% S	100% R	Sd**	CV*
+1400	16.15	16.15	16.15	16.15	0.00	0.00	16.41	16.41	16.41	16.41	0.00	0.00
+160	18.32	18.04	18.16	18.64	0.26	0.01	19.02	18.68	18.98	19.81	0.48	0.03
+75	18.74	18.83	18.56	18.43	0.18	0.01	19.71	19.65	19.44	19.25	0.21	0.01
-25	16.06	17.07	14.79	11.87	2.25	0.15	15.73	16.99	14.23	10.07	3.01	0.21
-75	16.32	13.04	17.59	11.91	2.67	0.18	16.16	11.81	17.67	9.94	3.62	0.26
-150	13.73	12.62	13.95	12.02	0.92	0.07	12.00	10.34	12.20	9.90	1.16	0.10
-450	14.06	14.29	14.61	13.99	0.28	0.02	11.79	12.05	12.28	11.75	0.25	0.02
-750	16.40	15.31	14.40	15.70	0.83	0.05	14.78	13.36	12.33	14.08	1.05	0.08
-1050	17.75	15.90	15.98	15.74	0.94	0.06	16.76	14.90	14.74	14.57	1.02	0.07
	3rd ten day period (DOY 188-226)						4th ten day period (DOY 232-263)					
+1400	14.60	14.60	14.60	14.60	0.00	0.00	20.37	20.37	20.37	20.37	0.00	0.00
+160	17.86	17.30	17.60	18.86	0.68	0.04	23.24	23.21	23.70	24.07	0.41	0.02
+75	19.50	18.75	18.12	18.75	0.56	0.03	24.47	25.69	24.15	23.96	0.78	0.03
-25	16.68	17.91	14.36	9.26	3.82	0.26	20.33	22.50	18.31	12.51	4.29	0.23
-75	17.51	11.72	19.36	8.95	4.87	0.34	20.65	15.56	22.11	12.61	4.42	0.25
-150	11.40	9.31	11.77	8.98	1.43	0.14	15.18	12.82	15.33	12.00	1.68	0.12
-450	11.03	11.17	11.77	10.86	0.40	0.04	13.38	13.29	14.38	12.55	0.75	0.06
-750	13.77	12.26	11.42	13.16	1.03	0.08	14.73	13.52	13.24	14.18	0.67	0.05
-1050	15.33	13.45	13.32	13.10	1.03	0.07	15.49	13.61	13.77	13.33	0.98	0.07
	5th ten day period (DOY 264-273)						6th ten day period (DOY 274-283)					
+1400	24.74	24.74	24.74	24.74	0.00	0.00	26.45	26.45	26.45	26.45	0.00	0.00
+160	27.26	27.24	27.65	28.11	0.41	0.01	28.68	28.65	29.12	29.51	0.41	0.01
+75	27.95	29.96	28.64	27.96	0.94	0.03	28.81	31.17	29.69	28.96	1.08	0.04
-25	27.46	28.17	23.18	17.78	4.78	0.20	25.78	27.77	23.78	17.22	4.58	0.19
-75	27.05	20.85	25.79	17.86	4.29	0.19	25.47	20.35	26.27	17.88	4.04	0.18
-150	20.46	18.13	20.13	17.14	1.59	0.08	20.89	18.12	20.98	16.77	2.09	0.11
-450	18.05	17.63	18.99	17.10	0.80	0.04	18.37	17.67	19.39	16.97	1.03	0.06
-750	18.38	17.44	17.55	17.47	0.45	0.03	18.71	17.88	17.94	17.56	0.49	0.03
-1050	18.15	16.26	16.76	16.10	0.93	0.06	18.67	16.70	17.23	16.45	0.99	0.06

**CV is the coeffient of variation and *Sd is standard deviation

4.3.6 Temperature gradients

Generally heat is continually moving into or out of the soil and the thermal energy being continually redistributed through the soil. Heat will not flow under isothermal conditions (no temperature gradient) and the rate of heat flux into the soil is determined by the temperature gradient (TG) and thermal conductivity of the soil. During the day and night time (Table 4.4) at heights (+160 and +1400 mm) above the soil, the highest TG was 0.27^{o}C h^{-1} and the lowest was 0.27^{o}C h^{-1} in all four treatments on DOY 288. On the contrary for the same day, at the depths (-25, -75 and -150 mm) the TG between the day and night phases was highest at nearly 0.58^{o}C h^{-1} for 50% S and the other treatments (bare, 50% R and 100% R) were at most 0.47^{o}C h^{-1}. An indication that the stones store energy (good conductor) during the day and release it during the night, hence the higher TG for 50% S. It was important to observe that deeper layers (-450, -750 and -1050 mm) experienced near isothermal conditions for the 100% R, 50% R and 50% S treatments during the day and night phases on DOY 288. Only the bare soil exhibited a negative gradient (-1.51^{o}C h^{-1} at -1050 mm) during the day and night times on both DOY 205 and 288, when compared to the 100% R, 50% R and 50% S mulch treatments. This is due to the fact that the bare soil allows more radiation to penetrate deeper into the soil profile than the other treatments; hence the heat (cold) wave reaches to deeper soil depths.

Below the soil surface at depth of -75 mm on DOY 205, the TG for the Bare (0.95^{o}C h^{-1}) and 50% S (1.12^{o}C h^{-1}) treatments were higher than those of 50% R (0.51^{o}C h^{-1}) and 100% R (0.23^{o}C h^{-1}) during the daytime (Table 4.4). The highest negative gradient is in the night being that of 50% S due to the fact that it has very good contact with the soil hence a good conductor of heat during the day and cooling at night. In general the temperature gradient is greater in the topsoil (0 to 150 mm) than in the deeper soil layers (-450 to -1050 mm). Overall the gradient value for 100% R was less than other daytime gradients being nearer zero than others during nighttime.

Table 4.4 Temperature gradient profiles (TG, $^{o}C\ h^{-1}$) for both the warming and cooling phases for DOY 205 (summer day) and DOY 288 (spring day) in 2009 as influenced by mulching treatments at heights above (+) or below (-) the soil surface

Sensor level relative to soil surface in mm	Temperature change ($^{o}C\ h^{-1}$)															
	DOY 288 (Spring)								DOY 205 (Winter)							
	Daytime phase				Night phase				Daytime phase				Night phase			
	100%R	50%R	50%S	Bare	100%R	50%R	50%S	Bare	100%R	50%R	50%S	Bare	100%R	50%R	50%S	Bare
+1400	0.21	0.21	0.21	0.21	-0.12	-0.12	-0.12	-0.12	0.98	0.98	0.98	0.98	-0.66	-0.66	-0.66	-0.66
+160	0.19	0.18	0.21	0.20	-0.13	-0.13	-0.17	-0.17	0.82	0.62	0.77	0.71	-0.63	-0.62	-0.67	-0.62
+75	0.21	0.26	0.22	0.27	-0.15	-0.25	-0.17	-0.25	0.80	0.94	0.77	0.95	-0.55	-0.71	-0.56	-0.70
-25	0.15	0.37	0.47	0.40	-0.15	-0.31	-0.45	-0.38	0.23	0.77	0.81	0.89	-0.18	-0.63	-0.72	-0.76
-75	0.13	0.31	0.58	0.44	-0.15	-0.31	-0.54	-0.40	0.23	0.51	1.12	0.95	-0.19	-0.43	-0.97	-0.82
-150	0.07	0.12	0.22	0.19	-0.09	-0.13	-0.22	-0.19	0.12	0.05	0.23	0.25	-0.09	-0.07	-0.23	-0.24
-450	0.02	0.00	0.00	0.01	-0.01	-0.02	-0.02	-0.01	-0.02	-0.03	-0.07	-0.04	0.03	0.04	0.07	0.05
-750	0.01	0.00	0.02	0.00	-0.01	-0.02	-0.02	-1.51	0.01	0.00	-0.02	-0.01	0.00	0.00	0.02	-1.15
-1050	0.00	-0.02	0.00	-1.53	0.01	0.01	0.00	0.02	-0.01	0.00	0.00	0.00	0.00	0.00	0.01	-0.01

4.4 Conclusions

Mulch type and percentage cover do not affect air temperature significantly at +75 and +160 mm above the soil. However, 100% R and 50% R mulching treatments reduced soil temperature diurnal variations during daytime conditions and encouraged higher soil temperatures during cold weather when compared to 50% S and bare soil. The 100% R mulch cover had minimal temperature diurnal variation throughout the study period. Mulching treatments affected soil temperature in the following order: 100% R; 50% R, 50% S and Bare. However, 50% S had higher temperature values than the 100% R, 50% R and bare treatments at the depths of -25, -75, -150 and -450 mm below the soil surface. The variation in the temperature gradient below the soil surface was ($-1.53^{o}C\ h^{-1}$) for the bare soil at 1050 mm depth (control) with the highest at $1.12^{o}C\ h^{-1}$ for the 50% S soil treatment at -75 mm depth, and the 100% R had the least variation with a maximum at $0.23^{o}C\ h^{-1}$. Overall, the results indicate that mulch had less effect on soil temperature with the increase in depth from -25, -75, -450, -750 and -1050 mm. The results also show clearly that percentage cover affects soil temperature. Considering the abundant availability of reed mulch material in the region, it is recommended that mulching can help reduce evaporation by controlling soil thermal properties.

CHAPTER 5

CHARACTERIZATION OF THE HYDRAULIC PROPERTIES OF A BONHEIM SOIL

Abstract

There is a distinct lack of knowledge with respect to the hydraulic properties of the South African Bonheim soil, also referred to as a vertic phaeozem in other countries. The aim of this study was to fill the gap by determining some of the most important hydraulic properties (drainage patterns, soil water-hydraulic conductivity and soil water-matric suction) of a modal Bonheim soil sampled at Glen Agricultural Institute near Bloemfontein. Desorption measurements were carried out on each horizon to obtain a series of soil water content (θ)–matric suction (h) values from which the "soil water release curve" (SWRC) was derived. Hillel's internal drainage method was used to obtain the *in situ* drainage pattern as well as the relationship between soil water content (θ) and the hydraulic conductivity (K) for each master horizon. Structural and textural pore domain classes were identified in each horizon by using the *in situ* internal drainage (ISID) method. The structural (macro) pores of the three horizons were associated with very low suctions (<1.1 kPa) and were found to hold between 12-19% of the total pore volume and conduct water at rates between 1 and 20 mm hr^{-1}. A second pore class was identified as transitional pores, which fell between the structural and textural domain pore classes and these pores occupied between 17 and 20% of total pore volume and conducted water at rates between 3.9-12.6 mm hr^{-1}. Lastly, textural pores represent a third class of pore domain which conducted water at rates between 3.3-10.4 mm hr^{-1}. The results showed that the transitional pores (upper boundary pore class) is associated with very low suctions (> 1.3 kPa) and thus a suggestion was made that the θ within this class is associated with the drained upper limit (DUL). The lower boundary (textural pores) is associated with soil water contents at 1500 kPa. A sizeable amount of water can be stored between these two boundaries which are of great importance for crop production.

Key words: hydraulic conductivity, soil water, water release, instantaneous, drainage

5.1 Introduction

Bonheim soils (Bo) have a melanic A, pedocutanic B and saprolite C horizons, which are associated with gentle or flat-lying areas and formed from sedimentary or igneous rocks. A mean annual precipitation of 550 - 800 mm and an aridity index of 0.2 - 0.5 (semi-arid) are particularly conducive for the formation of these soil forms (Soil Classification Working Group, 1991; van der Merwe *et al*., 2002). It is by definition a well-structured, dark-coloured margalitic clay soil with marked swell-shrink properties (le Roux *et al*., 1997; Hensley *et al*., 2006). The South African Bo is similar to the vertic phaeozem of the international classification system belonging to the mollic group of soils (World Reference Base, 1998). This soil form can be found throughout the world, for example: Ethopia (Zekele *et al*., 2004); Russian Federation (Meidema *et al*., 1999); United States of America (Blanco-Canqui *et al*., 2007); from the Thabankulu border of Swaziland through to Zimbabwe (van der Merwe *et al*., 2002). In South Africa, soils with a melanic A horizon cover an area of approximately 2.3 million ha or 2% of the total area of 122.8 million ha (van der Merwe *et al*., 2002). This soil has a high porosity and water holding capacity. The relatively high levels of organic matter and near-neutral pH make these soils very fertile (van der Merwe *et al.*, 2002).

The Free State Province covers 12.9 million ha of which 3.82 million ha are arable. Yet, it produces one third of South Africa's total grain crop, mainly maize and wheat. Of this entire grain crop produced none is from areas south, east and north-east of Bloemfontein, in spite of the more favourable rainfall of between 500 - 600 mm. The potential is limited by the clay and duplex soils which are dominant and have properties which render them unfavourable for cropping with conventional tillage practices. This is due to a dry soil water regime caused by excessive water losses through runoff and evaporation (Hensley *et al*., 2006). Eloff (1994) classified these soils as having a very low potential for agricultural production, and recommended them for grazing despite the fact that they cover about 2.8 million ha. Field experiments were conducted on the Bo north-east of Bloemfontein to test appropriate

production techniques, in an attempt to deal with the problem of soils east of Bloemfontein (Hensley *et al*., 2000). Botha and van Rensburg (2004) demonstrated from their findings over six seasons that the in-field rainwater harvesting (IRWH) crop production technique, when compared to conventional production practices (ploughing with mouldboard) increased maize and sunflower yields by as much as 50%. Tekle (2005) identified about 80 000 ha in the Free State where the IRWH technique could be applied. This technique has proved to be particularly suitable and acceptable by the subsistence farmers in Thaba Nchu area for selected field and vegetable crops (Kundhlande *et al*., 2004; Botha *et al*., 2007). These farmers are considered extremely vulnerable, because the majority of the people suffer from poverty (56%), unemployment (31%) and food insecurity (54%) (Department of Agriculture - Free State Province, 2006).

A number of researchers, as listed in Table 5.1, have done some studies on clay soils in South Africa and internationally. The review shows clearly that, though some work has been done on the Bo, none of these studies have determined the hydraulic properties of this soil. Hillel (1998) and Dirksen (1999) stated that a soil's hydraulic conductivity (K) is one of the most important physical properties; as it varies over many orders of magnitude not only between different soils, but also within the same soil. It is envisaged in this study that the characterization of the inter-relationships between hydraulic conductivity (K)-soil water content (θ) [K(θ)] and θ-matric suction [θ(h)] for the Bo will provide insightful information, fill a gap in knowledge, and contribute to the understanding of the soil water balance of the IRWH system. This in turn could improve peoples life's throughout South Africa and other semi-arid zones in the world. Some studies on the determination of hydraulic properties using the instantaneous drainage method of Hillel (1972) have been done for other soil forms in the Free State (South Africa): notably the works of Fraenkel (2008) on the Tukulu, Arcadia, Sepane and Bloemdal soils; Chimungu (2009) on the Tukulu and Bainsvlei soils and Bothma (2009) on the Bloemdal and Sepane soils (Table 5.1).

Table 5.1 Soil hydraulic studies on melanic and duplex soils [(+) indicates work done and (-) indicates work not carried out on the topic]

Country	Author(s)	Dominant soil form	Soil water balance						Particle distribution (%)			Soil hydraulic properties		Other soil physical properties	
			ΔS	I	Es	Ev	dr	R	Cc	Si	Sa	θ(*h*)	K(θ)	ρ_b	ρ_o
South Africa	Hensley *et al*. (2000);	Bonheim; Swartland	+	-	+	+	+	+	+	+	+	-	-	+	+
South Africa	Botha *et al*. (2003)	Bonheim; Swartland	+	-	+	+	+	+	+	+	+	-	-	+	+
South Africa	Botha, (2006)	Bonheim; Swartland	+	-	+	+	+	+	+	+	+	-	-	+	-
South Africa	Anderson, (2007)	Bonheim	+	-	+	-	-	+	+	+	+	-	-	+	-
South Africa	van Rensburg *et al*. (2002)	Bonheim	+	-	+	-	-	+	+	+	+	-	-	+	-
South Africa	Chimungu, (2009)	Bainsvlei; Tukulu	-	-	-	-	-	-	+	+	+	+	+	+	-
South Africa	Fraenkel, (2008)	Tukulu; Sepane Bloemdal	-	-	+	-	+	-	+	+	+	+	+	+	+
South Africa	Bothma, (2009)	Bloemdal; Sepane	-	-	-	-	+	-	+	+	+	+	+	+	+
South Africa	van der Merwe *et al*. (2002)	Melanic A horizon	-	-	-	-	-	-	+	+	+	-	-	+	-
Ethopia	Welderufael, (2006)	Bonheim	+	+	+	-	+	+	+	+	+	-	-	+	+
Russian Federation	Miedema *et al*. (1999)	Mollic A horizon	-	+	+	-	-	-	+	+	+	-	+	-	+
Ethopia	Zekele *et al*. (2004)	Mollic Andosol	-	+	-	-	-	-	+	+	+	-	+	+	+
USA	Blanco-Canqui *et al*. (2007)	Mollic	-	+	-	-	-	-	+	+	+	-	+	+	+

where: ΔS: change in soil water storage; I: irrigation; Es: soil surface evaporation; Ev: evapotranspiration; R: runoff; Cc; Sc, Sa: Clay; Silt, and Sand contents; dr: drainage curves; ρ_o: porosity; ρ_b: bulk density

Unfortunately, these findings cannot be extrapolated to the Bo with it's melanic A horizon, that differs in many ways from those soils. The aims of the study were to:

(i) describe the profile of a typical Bonheim soil and

(ii) relate pedological attributes of the master horizons to measured hydraulic properties.

5.2 Material and methods

5.2.1 Soil sampling

Site location and soil classification are detailed in chapter 2 (section 2.2.1). Undisturbed soil core samples were taken from the profile pit under wet conditions at the depths of 150 mm (representing the A-horizon), 550 mm (representing the B-horizon) and 850 mm with three replications using a modified hydraulic jack as described in Chapter 2, section 2.2.2.2. The dimensions of the core sampler were 105 mm (diameter) with a height of 77 mm. Each sample was properly sealed and used for both the bulk density (ρ_b) and soil water retention determinations. For ρ_b the samples were dried in an oven at 105^{o}C for 24 hours.

5.2.2 Soil water release measurements

To prepare the soil samples for retention measurements, the first step was to saturate the soil cores using a two way vacuum saturation chamber system as discussed in chapter 2 (section 2.2.2.2). The system is made up of two vessels (chambers), one of them filled with water and a stirrer placed at the bottom of the vessel to continually stir the water in the vessel during the de-airing process. In the other vessel, three core samples were placed on a 3 mm high platform gauge wire-mesh and both vessels de-aired using a vacuum pump sucking at -70 kPa at room temperature for 48 hours. Thereafter the vacuum pump has turned off; hence, ensuring the two-way chamber system remains air tight. The de-aired water was allowed to gradually flow into the chamber containing the de-aired core samples until the water level was just below the top of

the core samples. Soil samples were then left for a further 24 hours in the chamber, thus ensuring that full saturation was achieved. The gravimetric weights of the saturated samples were determined by weighing the samples immediately after taking them out of the saturation vessel.

After saturation, the soil water release curves (SWRC) were determined in three steps: Step 1 used the hanging water column tension cup method of Dirksen (1999) on undisturbed core samples with ranges from 0 up to 9 kPa (Note: absolute kPa values used hereafter). For this study the 0.01 kPa was assumed to represent 0 kPa. The suction levels differed amongst horizons, but a total of 10 suction levels were achieved for each of the three soil horizons. Step 2 involved the equilibration of undisturbed soil samples from the three soil horizon using the pressure plate apparatus of Jury *et al.* (1991) set at 10, 20, 40, 70, and 100 kPa. In step 3 disturbed soil samples from the three horizons on the pressure plate apparatus were used at settings of 100, 300, 500, 1500 kPa. Steps 1, 2 and 3 lasted approximately 6, 8 and 11 days, respectively until equilibrium at each pressure setting. Soil samples were weighed after each equilibration to determine the gravimetric water content and the volumetric water content was then calculated using the measured bulk density. Then soil water retention curves were drawn from the data for each horizon.

5.2.3 Specific water capacity

The slope of the SWRC, which is a change of water content per unit change of matric potential, is generally termed the specific (or differential) water capacity (C_θ). C_θ values were calculated for each soil horizon at different sections of the SWRC and the separated sections were as follows: (i) 0-1 kPa, referred to as $C_{\theta\,(0\text{-}1)}$;

(ii) 1-10 kPa: referred to as C_θ (1-10);

(iii) 10-1500 kPa: referred to as $C_{\theta\,(10\text{-}1500)}$.

C_θ were calculated using the equation below (Hillel, 1998):

$$C_\theta = -d\theta / dh \quad (5.1)$$

where $d\theta$ (mm mm^{-1}) is the slope of wetness and dh (mm) is the change in matric suction.

5.2.4 Internal drainage method

In this study, the internal drainage method (IDM) of Hillel *et al*. (1972) was used to determine the K(θ) relationship as it has come to be accepted as a standard *in situ* procedure (Marion *et al*., 1994). The main advantage is that it is non-destructive, and can be applied simultaneously at several soil depths under natural conditions that include swelling and shrinking, and normal field suction heads (Hillel *et al*., 1972; Zhang *et al*., 2007). The internal or instantaneous drainage experiment was carried out on the Bonheim soil using an area of 4000 mm x 4000 mm. A metal frame of 400 mm in height was inserted to a depth of 300 mm into the soil to prevent lateral water movement from the surrounding soil. Within this plot, soil water and *in situ* matric suction measurements were taken at depths: 25, 75, 150, 450, 750 and 1050 mm from the soil surface level. The volumetric soil water content was recorded hourly using calibrated ECH$_2$O-TE probes connected to a CR1000 logger via multiplexer (Campbell Scientific, Logan, UT). The matric suction was also recorded hourly using Watermark 200 sensors. Four neutron access tubes were also inserted to a depth of 1300 mm to assist only in monitoring soil wetness during water ponding. Water was ponded on the soil surface until the ECH$_2$O-TE probe readings indicated saturation for the entire profile and which was achieved three days after continuous ponding. Then, the whole plot was completely covered by a sheet of black plastic to stop water entering or evaporating from the plot. During the experiment it was discovered that the Watermark 200 was not sensitive enough in the wet range at suctions between 0-10 kPa and matric potentials in this range were estimated from the laboratory obtained SWRC. These curves were used to estimate matric suction from the soil water content measured with the ECH$_2$O-TE probes during drainage.

5.2.5 Data processing for internal drainage method

The processing of the data obtained during the IDM experiment was carried out as described by Hillel *et al.* (1972); first *in situ* θ values were plotted with time for each depth (Figure 5.2). Secondly, *q* was calculated through each depth increment by integrating the θ-time curve, with respect to depth (Appendix 4). Thirdly, the hydraulic gradient $\partial H / \partial z$ was determined using three different SWRC each specific for each depth to estimate *h* from *in situ* determined values of θ. Gravitational head was then added to *h* to obtain the change in hydraulic gradient (ΔH). Fourthly, K(θ) was calculated at each depth (Appendix 5 and 6) and for the different θ values by dividing the flux (*q*) with the corresponding $\partial H / \partial z$ values. Finally, K was plotted against θ values and a curve was fitted.

5.2.6 Partitioning of pores into structural and textural components

A new method for separating structural and textural pores is proposed based on the *in situ* internal drainage characteristic of the profile, abbreviated as the ISID method. The ISID method partitions data into classes, by using successive "critical levels" and their associated R^2 values as described by Cate and Nelson (1971). The partitioning occurs where the R^2 reaches its maximum. The technique consists of the following steps:

(i) Arrange the (X, Y) pairs from smallest to the highest based on the X-values; where X is time (hours) and Y is volumetric soil water content (mm mm^{-1}) at X.

(ii) Secondly, calculate the correction factor (C) using the following equation:

$$C_f = \frac{(\sum Y)^2}{n} \tag{5.2}$$

(iii) Thirdly, calculate the total corrected sum of squares (D) using the following equation:

$$D_d = \frac{(\sum Y^2 - (\sum Y)^2}{n} \tag{5.3}$$

(iv) Fourthly, calculate the D deviations from the means of two populations that result from each successive X value, for example:

$$\left[A_1 = \frac{(Y_1 + Y_2)^2}{2}\right] + \left[B_1 = \frac{(Y_3 + Y_n)^2}{n-2}\right] \quad (5.4)$$

then; not;

$$\left[A_2 = \frac{(Y_1 + Y_2 + Y_3)^2}{3}\right] + \left[B_2 = \frac{(Y_4 - Y_n)^2}{n-3}\right] \quad (5.5)$$

(iv) Thereafter, add the sum of squares of the pooled sum of squares at each X level and then subtract the correction factor and divide by D expressed as a percentage of D or as R^2 with the equation:

$$R^2 = \left[\frac{A_n + B_n - C}{D}\right] \quad (5.6)$$

By this interactive process obtain a series of R^2 values by increasing number of samples by one each time until a critical level of X is reached, where R^2 is at its maximum and thereafter starts reducing.

5.2.7 Statistical analysis

The accuracy of fitted soil water release curves was evaluated using the Willmott procedure which is detailed in chapter 2, section 2.2.3.

5.3 **Results and discussion**

5.3.1 Profile attributes of the Bonheim

The soil description of the Bonheim soil at Glen [Table 2.1 (chapter 2)] is supported with a photo of the profile [Figure 2.1 (chapter 2)] and the soil attributes are summarised together with other Bo soils reported by Turner (2000), sampled in KwaZulu-Natal and Mpumalanga (n = 13 profiles). The melanic horizon at Glen is a clay soil with dark brown angular blocked peds,

characterized by a high proportion of smectite clay minerals to a depth of 400 mm. It has a strongly developed structure with a high CEC value at 24.3 $cmol_c\ kg^{-1}$ soil characterized by marked swell-shrink properties with a bulk density at 1.48 mg mm^{-3}. The exchangeable Na content at 2.5% is fortunately low and therefore cannot be blamed for exacerbating the swell-shrink properties. The Mg content (12.2 $cmol_c\ kg^{-1}$) is relatively high compared to an average of 9.7 $cmol_c\ kg^{-1}$ for other the melanic layers. The 56% exchangeable Mg may be a factor that contributed to the high plasticity index (P*i*) value at 31.

The pedocutanic layer (B-horizon at Glen) is a dark brown soil classed as clay soil from a depth of 400 up to 800 mm and graded as having well-developed angular and sub-angular blocked structure and characterized by the presence of high proportion of smectite clay minerals, hence the P*i* value of 33, which is higher than the value of 31 for the melanic horizon. This confirms the strong structure of this expanding clay, which enables it to retain more water. The pedocutanic layer at Glen has a clay content of 41.3%, with other-pedocutanics (n = 13) at 58.0% and a bulk density of 1.33 mg mm^{-3}. It has a lower CEC (23.6 $cmol_c\ kg^{-1}$) value compared to other-pedocutanic layers at 36.8 $cmol_c\ kg^{-1}$ with a standard deviation (Sd) of 9.4 $cmol_c\ kg^{-1}$. The pedocutanic layer at Glen is typically similar to other pedocutanic layers in the country as most of the textural and structural properties were similar.

The C-horizon is a calcium carbonate enriched sandstone saprolite sufficiently weathered to a depth of at least 1200 mm and offers no significant impedance to root development to that depth. The parent material is a mixture of dolerite and sandstone colluvium, with dolerite dominating. The exchangeable Na content in the profile is fortunately low (ESP < 5%) and does not cause swell-shrink properties like the overlying pedocutanic layer. The clay, silt and sand contents for this layer were at 37.7, 20.0 and 40.9%, respectively. It is textural classified

as clay loam and has an exchangeable Mg and Na values at 36 and 4.9%, respectively. The P*i* value was 28, considerably more than the overlying horizons.

Comparing the attributes of the Bonheim at Glen with that of the other Bonheim's from Turner (2000) (Table 5.2), revealed that CEC, carbon (C) and clay content, compared well within the A-horizons, but not for the B-horizons. These attributes are closely related to the structural pores in the horizons i.e. the volume of the macro pores, while the clay content and the type of clay are associated with textural pores (micro pores) (Luxmoore, 1981). Macro and meso pores are very conductive and are responsible for water flow and fluxes between saturation and the drained upper limit of horizons. On the other hand, micro pores are slow conductive pores which operate below the drained upper limit and lower suctions. Thus, it can be predicted that the hydraulic properties of the melanic horizon of Glen were comparable to that from Turner (2000). Due to apparent differences in the soil attributes of the B-horizons, the structural and textural pores will differ and hence the hydraulic properties. Hydraulic conductivity is also related to chemical attributes such as salt concentration (expressed as resistance in Table 5.2) and exchangeable sodium percentage (ESP) of the horizons (McNeal and Coleman, 1966). Unfortunately the ESP attribute was absent from the chemical data from Turner (2000), which makes comparisons impossible. However, the chemical properties are dynamic and depend on management. Overall, it can be expected that the A-horizons will exhibit similar hydraulic properties and the B-horizons can be slightly different.

5.3.2 Characterization of drainage patterns of horizons

Drainage data were obtained from the internal drainage experiment, which lasted 30 days, by selecting all the hourly data over the first 100 hours (4.2 days) of the experiment and thereafter only measurements taken daily at 08h00 were used for the remaining period.

Table 5.2 Comparison of physical and chemical properties of Bonheim at Glen with other Bonheim (n = 13) soils described in Turner (2000)

Property	Parameter	Melanic			Pedocutanic			Saprolite
		Glen	Other	Sd	Glen	Other	Sd	Glen
Physical	Sand (%)	44.40	31.00	9.48	44.4	30.0	10.18	40.9
	Silt (%)	9.50	29.00	13.79	12.9	28.0	10.68	20.0
	Clay (%)	43.50	40.0	2.47	41.3	58.0	11.81	37.7
	Texture class	Cc	Cc-CcLm		Cc	Cc-CcLm		CcLm
	ρ_b (mg mm^{-3})	1.58	-	-	1.33	-	-	1.47
	Swelling (%)	11	-	-	13	-	-	6
	Plasticity Index	31	-	-	-	-	-	28
Chemical	Carbon (%)	0.57	1.0	0.30	0.2	0.5	0.14	-
	Resistance (ohms)	340	900	396	280	420	98.99	240
	pH (H_2O)	7.56	6.6	0.68	8.25	7.20	0.74	8.49
	pH (KCl)	6.11	5.6	0.36	7.06	6.00	0.75	7.21
	Na ($cmol_c$ kg^{-1})	0.56	4.0	2.28	1.05	9.00	5.62	1.19
	K ($cmol_c$ kg^{-1})	0.65	1.0	0.25	0.59	1.00	0.29	0.58
	Ca ($cmol_c$ kg^{-1})	8.33	8.5	0.12	7.98	12.10	2.91	13.77
	Mg ($cmol_c$ kg^{-1})	12.22	9.7	1.78	11.74	48.30	25.85	8.86
	*Clay-S value	21.76	-	-	21.35	-	-	24.4
	CEC ($cmol_c$ kg^{-1})	24.30	27.4	2.19	23.58	36.80	9.35	26.21
	Exch. Na ESP (%)	2.5	-	-	4.9	-	-	4.9
	Exch. Mg ESP (%)	56	-	-	-	-	-	36

where: Sd = standard deviation; Cc = clay; CcLm = Clayloam; ρ_b = bulk density; *(Σ exchangeable cations x 100/ % clay)

A power function was fitted through the data and the curves are depicted in Figure 5.1 for each of the three horizons. The associated regression results are summarized in Table 5.3. From the regression data it is clear that the power function fitted the data well for all horizons ($R^2 > 0.98$) which explains the similar shapes of the curves. However, the coefficients of the equations differed markedly amongst horizons, indicating that they are unique for each horizon. The

regression functions indicated slightly higher values of porosity in the field than porosities calculated based on the ρ_b of the three horizons. Laboratory and field porosities for the A, B and C horizons were similar for each horizon: 0.40, 0.50, 0.45 mm mm^{-1}, and 0.46, 0.51 and 0.48 mm mm^{-1}, respectively.

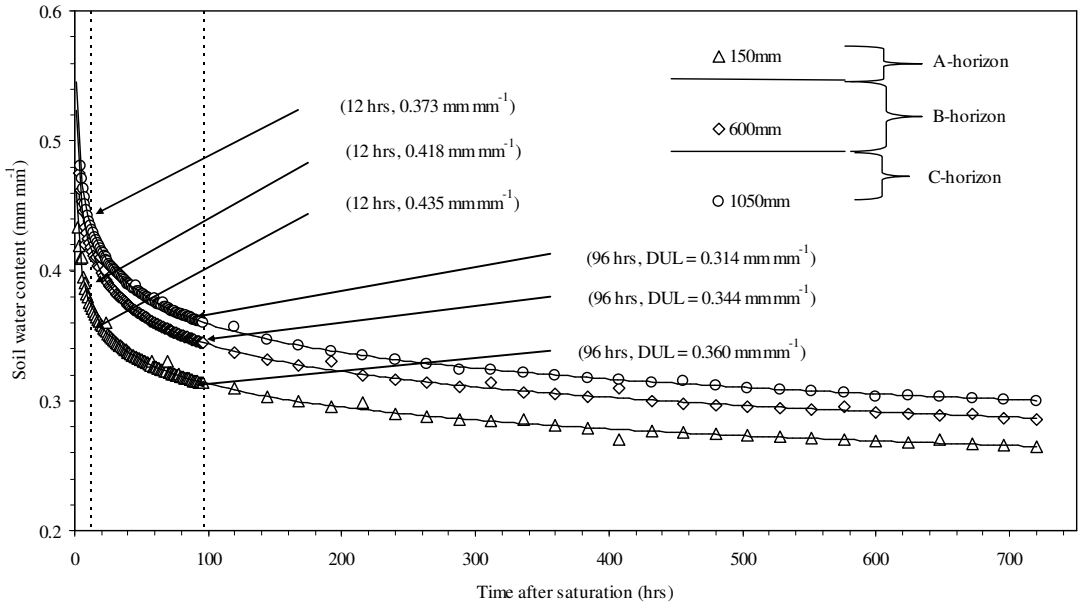

Figure 5.1 Drainage patterns of three horizons for the Bo soil at Glen for a 30-day period

Table 5.3 Regression functions describing drainage patterns over time for a 30-day period for the horizons of the Bonheim soil at Glen

Diagnostic soil horizon (mm)	Regression function	R^2
A-horizon (0-400)	$\theta = 0.4594\ t^{-0.0837}$	0.988
B-horizon (400-800)	$\theta = 0.5056\ t^{-0.0927}$	0.998
C-horizon (800-1050)	$\theta = 0.4958\ t^{-0.0905}$	0.996

θ is the soil water content in mm mm^{-1} and t is time after field saturation in hours

The *in situ* internal drainage method (ISID) was used in partitioning the drainage curves into relatively high flow (macro pores), moderate flow (meso or transitional pores), and low flow (micro pores) hydraulic classes (Figures 5.1 and 5.4). The dotted lines in Figure 5.4 represent the cut-off points or partitioning of pores into classes. For each of the three horizons, all the macro pores were drained after 12 hours and the meso pores drained after 96 hours (4 days) and

these being determined using the ISID method. This study proposes that the drained upper limit (DUL) occurs after the meso pores have been completely drained, opposed to the method described by Ratliff *et al.* (1983). They defined the DUL where the drainage curve has attained a negligible drainage rate (about 0.1 to 0.2% per day). Typically, the Ratliff *et al.* (1983) method suggested that most soils reach DUL in between 2 to 12 days and fine-textured soils and soils with restrictive layers required up to 20 days of drainage. This approximation of determining the DUL by Ratliff *et al.* (1983) is refined in this study by using the ISID method to accurately determine the 'critical level' were DUL is reached. For comparison, based on a 20 day (480 hours) drainage cycle of Ratliff *et al.* (1983) the DUL values for A, B and C horizons were: 0.274% (110 mm), 0.297% (119 mm) and 0.311% (93 mm), respectively, with a profile total of 322 mm (Figure 5.1). DUL values obtained using the ISID method for the same horizons were: 0.360% (144 mm), 0.344% (138 mm) and 0.314% (94 mm), respectively, with a total profile of 376 mm (Figure 5.1). Compared to the ISID method, the Ratliff *et al.* (1983) method under estimated the DUL for the A, B and C horizons by 24, 14, and 1%, respectively. Botha (2006) using the Ratliff *et al.* (1983) method found that the DUL values for the A, B and C horizons were 0.305, 0.344 and 0.260 mm mm^{-1} respectively, compared to ISID DUL values of 0.314, 0.344 and 0.360 mm mm^{-1}. Because the ISID method is based on a statistical procedure that can be applied and repeated on any drainage curve, it is suggested that the method should be used as an alternative to the Ratliff *et al.* (1983) method.

5.3.3 Characterisation of K(θ) relationships of horizons

Soil hydraulic conductivity (saturated and unsaturated), typically varies by orders of magnitude in space, and unsaturated values can change dramatically in time with the state of the water content of the soil. The relationship between measured K and θ for the Bonheim soil is presented in Figure 5.3 and results of regression functions for each of the three horizons are given in Table 5.4. The mathematical relationships between conductivity [K (mm hr^{-1})] and soil

water content [θ (mm mm^{-1})] could be best described by exponential equations (Table 5.4 and Figure 5.2). The linear relationships on the semi-log scale suggests that the K(θ) relationships are unique for each horizon because they have different slopes and intercepts. It seems that the vertical flow in the profile is controlled by the C-horizon when flow rates are above 0.35 mm mm^{-1}, and controlled by the A-horizon when flow rates are between 0.27-0.31 mm mm^{-1}.

Table 5.4 Regression functions describing the K(θ) relationships for the three master horizons for the Bo soil

Diagnostic soil horizon	Soil depth (mm)	Regression functions	R^2
A-horizon	150	$K = 5 \times 10^{-6} e^{44.76(\theta)}$	0.997
B-horizon	600	$K = 6 \times 10^{-7} e^{37.452(\theta)}$	0.977
C-horizon	1050	$K = 1 \times 10^{-3} e^{21.108(\theta)}$	0.994

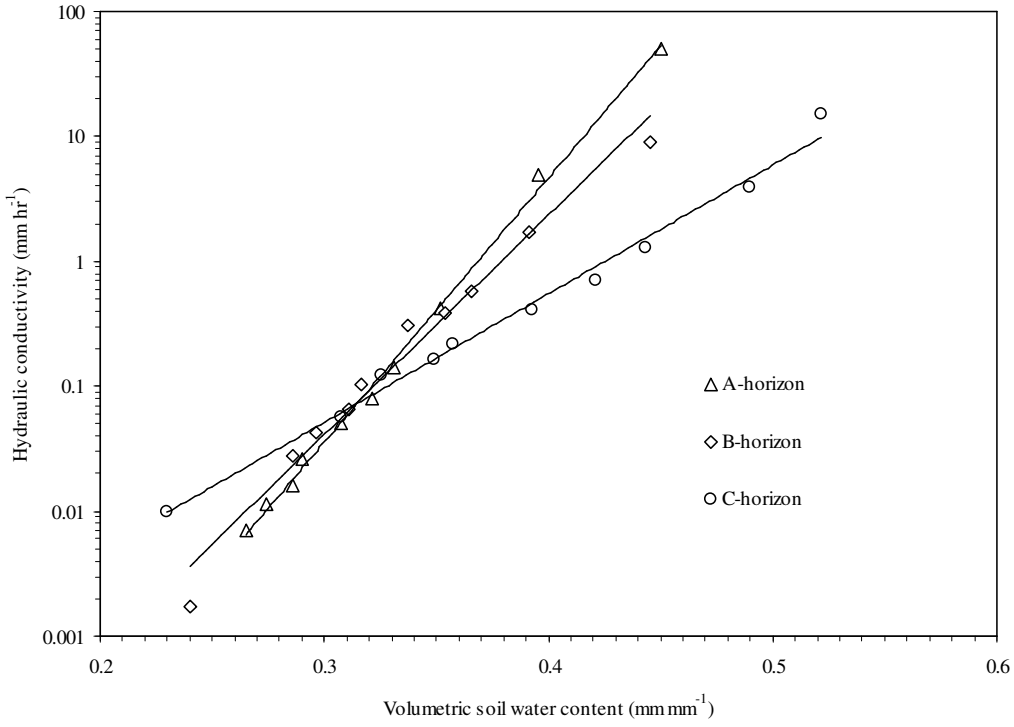

Figure 5.2 K(θ) relationships for the A, B and C horizons of the Bonheim at Glen

5.3.4 Characterisation of θ(h) relationships of horizons

The relationships of volumetric soil water content versus matric suction for the different soil horizons are shown in Figure 5.3. From the shape of the curves and slope being the specific water capacity (C_θ), it is clear that the three horizons exhibit unique soil water release characteristics. For example, over the 0-1 kPa suction range the specific water release [$C_{\theta\ (0\text{-}1)}$] was higher in the C horizon (C_θ = 0.1613), followed by the B (C_θ = 0.0803) and then the A horizon (C_θ = 0.0407). The situation changed dramatically from 1-10 kPa, where the highest specific water release capacity [$C_{\theta\ (1\text{-}10)}$] was experienced by the A horizon (C_θ = 0.0196), followed by the B (C_θ = 0.0172) and then the C horizon (C_θ = 0.0100). Between the suction ranges of 10 to 1500 kPa [$C_{\theta\ (10\text{-}1500)}$], all three master horizons held and released a similar amount of water, hence, the similar specific water release capacity at (C_θ = 0.0001).

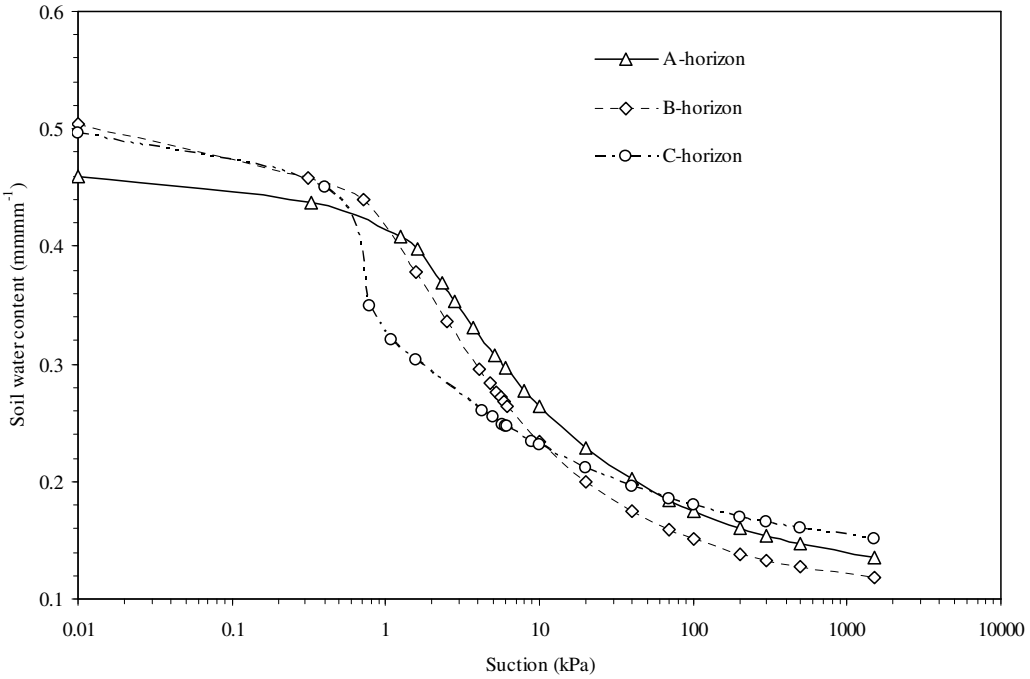

Figure 5.3 Soil water release curves for the three horizons for the Bo soil

5.3.5 Hydraulic properties and its relation to pedological features

The pedological features in this study are the structural and textural properties of the diagnostic horizons of the Bo soil. The relationship between these pedological features and hydraulic properties referred as Pedotransfer function (PTF) were deduced from the integration: of the:

(i) hydraulic information obtained using the IDM of Hillel e*t al*. (1972) and SWRCs;

(ii) proposed ISID method in the partitioning of pore classes into structural and textural pores as shown in Figures 5.1 and 5.4.

The melanic horizon is described as a dark brown, well developed, moderately course and angular blocky structured clay (44%) soil, and characterized by structural pores with a volume of water of 0.085 mm mm^{-1} (Table 5.5) (0.459-0.374 mm mm^{-1}) or 19% of the total air space (Figure 5.4a). This space is associated with the voids between structural units or peds and as such conduct water at very low suctions (0-1.1 kPa), resulting in relatively high flow rates of 10.5 to 12.7 mm h^{-1} (Figure 5.4a) and according to Luxmoore (1981) these pores are mainly >1 mm in diameter and are responsible for channel flow through the horizon under surface ponding and/or perched water table conditions. The meso pores occupy a smaller volume of space (16% of the total space) over a volumetric water content range from 0.373 to 0.314 mm mm^{-1} (Table 5.5) and holds water at suctions between 1.1-1.3 kPa, with flow rates between 3.9-10.5 mm h^{-1} (Table 5.5). The meso pores in this study are considered to be transitional between structural and textural pores. According to Luxmoore (1981) this pore diameter size range is found between 0.01 and 1 mm. Textural pores are in general related to the clay content of a soil and are known as micro pores. The textural pores associated with the melanic prevailed between soil water content range of 0.314 (DUL) to 0.135 mm mm^{-1} as shown in Figures 5.3; 5.4 and Table 5.5 between the suction ranges of 1.3 to 1500 kPa. Therefore an amount of 0.085 mm mm^{-1} (34 mm per 400 mm) of water was made available by the melanic A-horizon. This is a very important property of this soil in dryland farming, an aspect which is often neglected in

agronomical evaluations. The pedocutanic layer (B-horizon) is a dark brown layer, strong course characterised by both angular and medium sub-angular blocked structured clay (41%) soil. The average flows of water within the pedocutanic layer structural pores were moderate between 8.5-9.1 mm hr^{-1} (Table 5.5) and water occupied a volume of 0.092 mm mm^{-1} (35 mm per 400 mm and 17% of the total air space) and conducted between suctions (0-1.1 kPa). This pore class according to Luxmoore (1981) is associated with drainage; hysteresis and gravitational driving force. The structural pores of the melanic released 1% more soil water than the pedocutanic horizon.

Table 5.5 Measured values of K and θ at different pore class domain for Bo soil

Hydraulic property	Pore class		A-horizon	B-horizon	C-horizon
K (mm hr^{-1})	Macro	Max	12.700	9.120	15.030
		Min	10.527	8.471	12.573
		Mean	11.614	8.796	13.802
	Meso	Max	10.527	8.471	12.573
		Min	3.973	6.971	10.405
		Mean	4.833	7.721	11.489
	Micro	Max	3.973	6.971	10.405
		Min	3.353	4.863	6.648
		Mean	3.663	5.917	8.527
θ (mm mm^{-1})	Macro	Max	0.459	0.510	0.496
		Min	0.374	0.418	0.435
		Total available	0.085	0.092	0.061
	Meso	Max	0.374	0.418	0.435
		Min	0.314	0.344	0.360
		Total available	0.060	0.074	0.075
	Micro	Max	0.314	0.344	0.360
		Min	0.135	0.119	0.151
		Total available	0.179	0.225	0.209

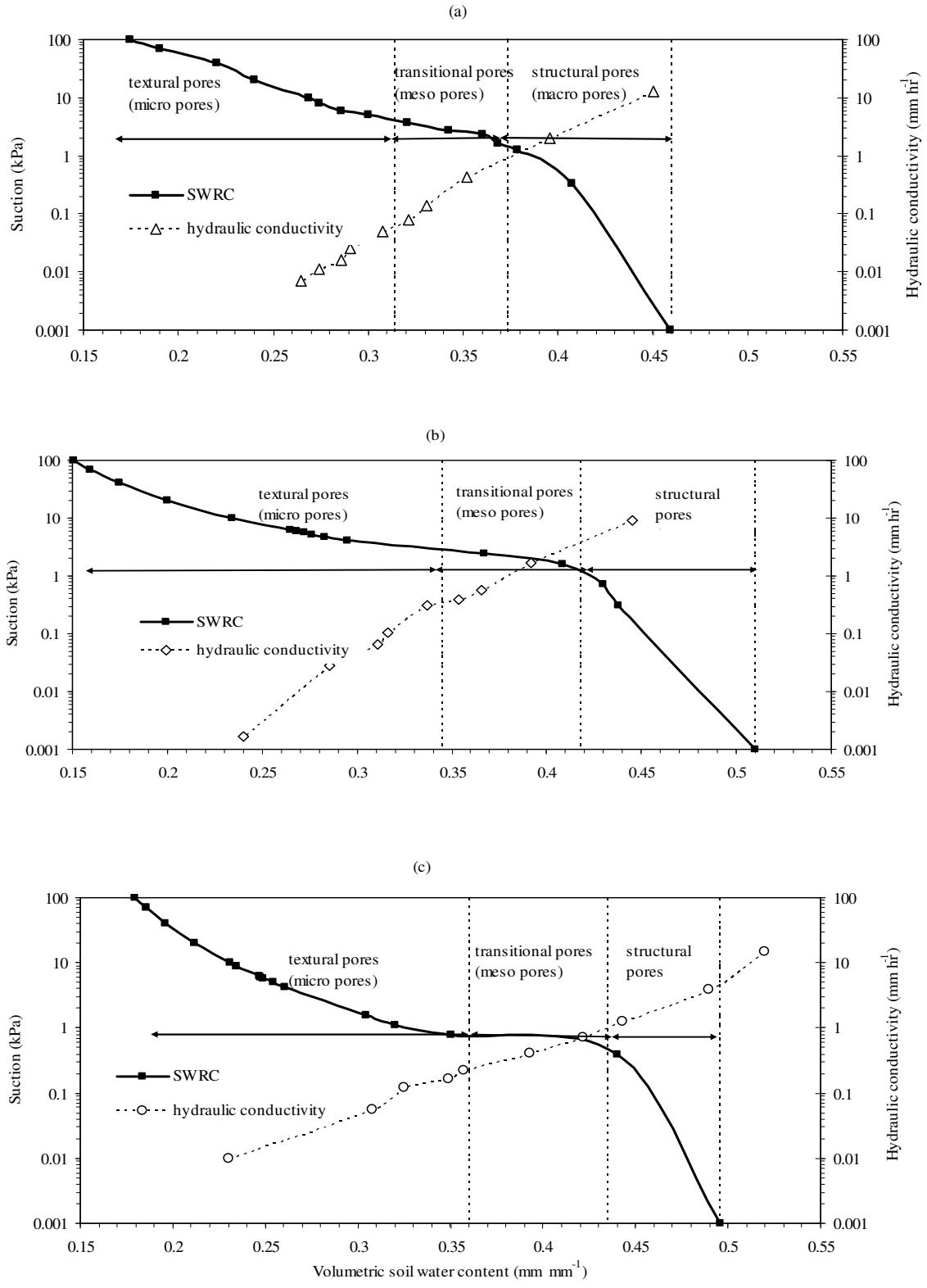

Figure 5.4 Field determined hydraulic conductivity, volumetric soil water content, and pore classes (structural and textural) for the A, B and C horizons for the Bo soil

The transitional (meso) pores of the pedocutanic occupy 18% of the total air space, 2% more than the melanic layer and the flow rates through the soil were 7.0-8.5 mm hr^{-1}. These pores held 29.6 mm per 400 mm of soil water [(0.418-0.344 mm mm^{-1}) x 400 mm], or 20% more water than those held by the melanic. The measured DUL value for the B-horizon was 0.344 mm mm^{-1}. The flow through the micro pores of the pedocutanic ranged from 0.344 to 0.119 mm mm^{-1}, which means these pores held 0.225 mm mm^{-1} equivalent to 90 mm per 400 mm soil water. This is typical of the pedocutanic layer which has relatively high smectic clays coupled with a plasticity index of 33 and a swelling percentage of 13%. Thus it holds much more water than melanic for this pore class. The pedocutanic released 20% more water than the melanic layer at this pore class and this feature is important in sustaining crop growth and development until the next rainfall event. The flow rates through the pedocutanic were between 6.6-10.4 mm hr^{-1} (Table 5.5).

The saprolite layer belongs to a clay loam texture class (38% clay) and does not have distinct structural properties as in the case of the overlying horizons. Despite this fact, the results showed that it had a considerable amount of structural related pores (12%) between the ranges of 0-1 kPa. The pores conduct water at a rate that varies between 12.6 and 15.0 mm hr^{-1}. The meso pores released 23 mm of soil water per 300 mm at flow rates of between 11.5 - 12.6 mm hr^{-1}. The DUL value for the saprolite was found to be at 0.360 mm mm^{-1} (Figure 5.1). The micro pores of the saprolite held 63 mm per 400 mm depth of soil and the water flow was between 0.360-0.151 mm mm^{-1} (Table 5.5).

Overall, the Bonheim soil provides a good environment for plant growth and development especially the pedocutanic layer, followed by the melanic. The pedocutanic layer stores and

releases more soil water through its structural and textural pores compared to the other soil horizons which is an important property in dryland crop production.

5.4 Conclusions

From the drainage curves, soil water-hydraulic conductivity relationships and soil water – matric suction curves, it was concluded that the hydraulic relationships were unique for the melanic, pedocutanic and saprolite horizons. The challenge, however, was to relate these hydraulic properties to structural and textural pore domains. Pore domains were identified in each horizon by applying the statistical procedure of Cate and Nelson (1971) on the *in situ* determined drainage patterns. Based on the separation procedure (referred to as the ISID method) several conclusions were drawn.

Firstly, the structural (macro pores) were associated with very low suctions (between 0 and 1.1 kPa) for all horizons. Apparently they occupied a small amount of pore volume of between 12-19% and with a storage capacity of 0.085 mm mm^{-1} with flow that ranged between 8-15 mm hr^{-1}. Secondly, the pore class that fell between the structural and textural domain is referred to in this study as transitional or meso pores and occupied about the same volume of the total pore space as that of the structural pores (between 17 and 20% of total pore space), characterised by low K values. Thirdly, textural pores started at low suctions in all of the horizons, >1.3 kPa for the melanic, > 1.1 for the pedocutanic and >0.8 kPa for the saprolite. These pores are very important for water storage and hence crop production. Accordingly, plants can extract water from the textural related pores up to suctions of 1500 kPa, also referred to as the laboratory determined lower limit of plant available water. The ISID method allows agronomists to obtain accurate field values of the DUL of soil horizons. These values can be used as pedo-transfer functions.

CHAPTER 6

DETERMINATION OF EVAPORATION FROM THE MELANIC HORIZON USING A WEIGHING LYSIMETER

Abstract

The knowledge of daily evaporation rates (Es) both in irrigated and dryland crop production is important especially under semi-arid conditions, as most of the water is lost through evaporation and thus considered to be unproductive. The objective of the study was to use a continuous weighing lysimeter to give a standard soil surface evaporation rate measurement [Es(lys)] with a precision of 1 mm rainfall added or Es loss and evaluate the following five estimation methods, using Willmot test statistics for paired values namely: (1) Field hydraulic conductivity [Es(k)], (2) Darcy equation [Es(q)], (3) Hydraulic diffusivity [Es(*d*)], (4) Ritchie [Es(ri)], (5) Rose [Es(ro)] and (6) FAO-56 Penman-Monteith (ETo). Three evaporation (drying) cycles were identified and selected. The first (2008: DOY 270 - 281), second (2009: DOY 62 - 72) and third (2009: DOY 199 - 210) drying cycles lasted for 11, 10 and 11 days, respectively. An automatic weather station within the vicinity of the experimental area provided climatic data. The Es(k) method performed better than the Es(q), Es(*d*), Es(ri) and Es(ro) during the first drying cycle, with mean absolute error (MAE) and root mean square error (RMSE) of 1.3871 and 1.5067 mm d^{-1} respectively, followed by the Es(q) method at 1.3656 and 1.5741 mm d^{-1} both indicating a good performance. The FAO-56 Penman-Monteith method only provided estimates of the atmospheric potential. The indices of agreement for the Es(k) and Es(q) methods during the first cycle were 0.8775 and 0.85195 respectively. During the second cycle, the Es(q) method offered a better performance than the Es(k) as it predicted closer to lysimeter measurements. During the third cycle all the methods underestimated Es close to each other by 1.3 mm d^{-1}. The methods evaluated can be put in order from the most to the least accurate for the conditions of this experiment as follows: Es(k), Es(q), Es(ro), Es(*d*) and lastly Es(ri). The Es(k) method is recommended for use in estimating Es for Bonheim soils.

Key words: evaporation, lysimeter, hydraulic conductivity, soil water content

6.1 Introduction

The evaporation rate from a bare soil surface (Es) is the process by which water is lost as water vapour into the atmosphere over time. It is one of the most important water losses from semi-arid croplands in South Africa as this water cannot contribute to crop water use. It has a direct negative impact on crop yields in dryland agriculture in semi-arid regions. The knowledge of the amount of evaporation is also important in the determination of rainfall-runoff relationships (Hensley *et al*., 2000; Botha *et al*., 2003). The water regime for the Bonheim soil has been studied in field experiments with crops over a period of 10 years. The aim of those experiments was water conservation for crop production using a production technique called "In-field Rain Water Harvesting" (IRWH) and was compared with a conventional full surface tillage method (mould board plough). The results of those experiments revealed that Es amounted to 75% of the annual rainfall for maize and 69% for sunflower production (van Rensburg *et al*., 2002; Botha *et al*., 2003). Thus it is a major problem in semi-arid areas. Bennie *et al*. (1994) also estimated that in semi-arid areas of South Africa between 60 and 80% of the rainfall evaporates before it can make any contribution to crop production.

Under unsaturated conditions Es occurs in three stages (Hillel, 1998). During the first stage Es is controlled by the evaporative demand of the atmosphere and the second stage occurs when the Es falls progressively below the potential atmospheric evaporation rate. This stage is dictated by the rate at which the soil can provide water towards the evaporation zone. The third stage comes after the surface zone has become so desiccated that further conduction of liquid water through it effectively ceases thus Es is almost zero. Soil water transmission through this desiccated layer thereafter occurs primarily by the slow process of vapor diffusion and this is controlled by the availability of water and the current atmospheric demand. According to Hillel (1998) for Es to occur three conditions are necessary: first, the existence of a vapor pressure

gradient between the soil and the atmosphere; second, the supply of energy needed for latent heat of vaporization of water and third, the supply of water to the surface. The first two conditions are influenced by meteorological factors, the soil water content of the surface horizon and the immediate horizon below it. The hydraulic property of the surface horizon influences the third condition. In this study it was important to measure and try to estimate Es from a bare surface of the melanic A-horizon of the Bonheim soil together with its hydraulic properties, viz. the relationship between hydraulic conductivity [K(θ)] and soil water content (θ); and the relationship [θ(h)] between matrix suction (h) and (θ) that control evaporation in the second and third stage. The previous chapter clearly described the relationships between these hydraulic properties. It was decided that a weighing lysimeter be used in the determination of Es as a standard measurement for the Es from the melanic layer of the Bonheim soil. This then provides an accurate independent measurement of Es so as to better understand this important clay soil widely distributed throughout the Free State Province of South Africa. If one characterizes the Es for this clay soil it can offer the possibility of extrapolating results to other geographical areas with similar soils in semi-arid regions. Extrapolation can done by applying and testing different equations already available in literature, for example Rose (1966), Hillel (1972), Ritchie (1972), Allen *et al*. (1998) and Hillel (1998) and possibly try to develop a predictive model for melanic soils.

The objective of this study was to evaluate six Es estimation methods against the lysimeter measurement of Es. It was envisaged that these different Es methods will provide insightful information, fill a gap in knowledge, and contribute to the understanding the evaporation dynamics of the IRWH system; which in turn could improve peoples livelihoods throughout South Africa.

6.2 Material and methods

6.2.1 Site location and soil classification

The field experiment was conducted at the University of the Free State (Free State Province, South Africa), on the Bloemfontein west campus research site, about two kilometers west of the main campus. The soil in the lysimeter is a melanic A-horizon transferred from the research site of the Glen Agricultural Institute about 25 km north of the main campus. The soil form of the melanic horizon used in this study was classified with the assistance of Hensley *et al.* (2000) in Chapter 2 (Section 2.2.1).

6.2.2 Description of the lysimeter

The weighing lysimeter made of non-heating fiber glass without a draining base had a diameter of 2.5 m and therefore a total surface area of 4.9063 m^2 with the depth available for filling with soil of 0.35 m, and thus soil filled volume of 1.7172 m^3. The volume of water 1 mm deep to cover the area of the lysimeter is the therefore 0.0049063 m^3. Assuming that the density of water at 20^oC, is 998.2071 kg m^{-3}, the mass of 1 mm = 0.001 m of rainfall over the lysimeter area is equal to 4.8975 kg (approximately 4.9 kg or 4.9ℓ of water). The total mass of soil placed in the lysimeter on DOY 172 of 2008 was 2 270 kg. Two samples of the melanic soil were taken just before adding to the lysimeter and oven dried at 105^oC for 24 hours to determine its gravimetric soil water content. It was found to be 11.89%. Therefore, the amount of water included in the soil on the day the lysimeter was filled was 269.903 kg and the total mass of oven dry soil added was therefore 2000.097 kg. The initial bulk density (ρ_b) (mass of oven dry soil/volume of soil in lysimeter) was 1160 kg m^{-3}. On DOY 270 when the first cycle was initiated, 339.6ℓ of water was added to the lysimeter between 17h00 and 18h00 and the bulk density changed to 1260 kg m^{-3}. To allow for good redistribution of soil water and minimal evaporation a plastic sheet was placed on the lysimeter on which to pour water using jerry cans to avoid disturbing the soil whilst adding the water.

6.2.3 Calibrating the lysimeter

The soil filled lysimeter was calibrated to cater for both increasing and decreasing masses (simulating additions by rainfall and losses by Es) on DOY 172 (2008) late in the afternoon to avoid high wind which could disturb the calibration process. For the purpose of calibration, output millivolt readings were read from a notepad logger connected to a CR10X data computer with readings taken every three minutes to ensure stabilization with loadcell accuracy at 0.99. Two liter (2ℓ) bottles were used for the calibration of the lysimeter, and the following steps were used:

(i) Forty-four two liter bottles were filled with water;

(ii) Each of the bottles were numbered, from number one to 44;

(iii) The mass of each numbered bottle (Appendix 7 and Appendix 8) was clearly written on the bottle's plastic body;

(iv) The initial millivolt reading (23482 mV) was then recorded, before placing any bottles onto the lysimeter;

(v) Thereafter, bottle No. 1 with a mass of 2024.3 g was placed onto the centre of the lysimeter and the corresponding millivolt reading was recorded;

(vi) Then, bottle No. 2 was placed onto the lysimeter and the corresponding millivolt output recorded;

(vii) Step (vi) was repeated for every two liter bottle placed onto the lysimeter until reaching bottle No. 44;

(viii) The final millivolt reading was 24119 mV and the 44 bottles had a total mass of 92.2731 kg;

(ix) Thereafter, bottle No. 44 was removed from the lysimeter and again the corresponding millivolt output recorded;

(x) The previous step (ix) was repeated by removing each of the bottles in numerical order from No. 43 down to bottle No. 1 and recording the corresponding millivolt output until there were no bottles on the lysimeter.

The series of millivolt readings obtained whilst increasing or decreasing the mass on the lysimeter during calibration is shown in Figure 6.1. They indicate that a single linear regression equation is appropriate as there is little effect of hysteresis, giving a very good R^2 value of 0.9995.

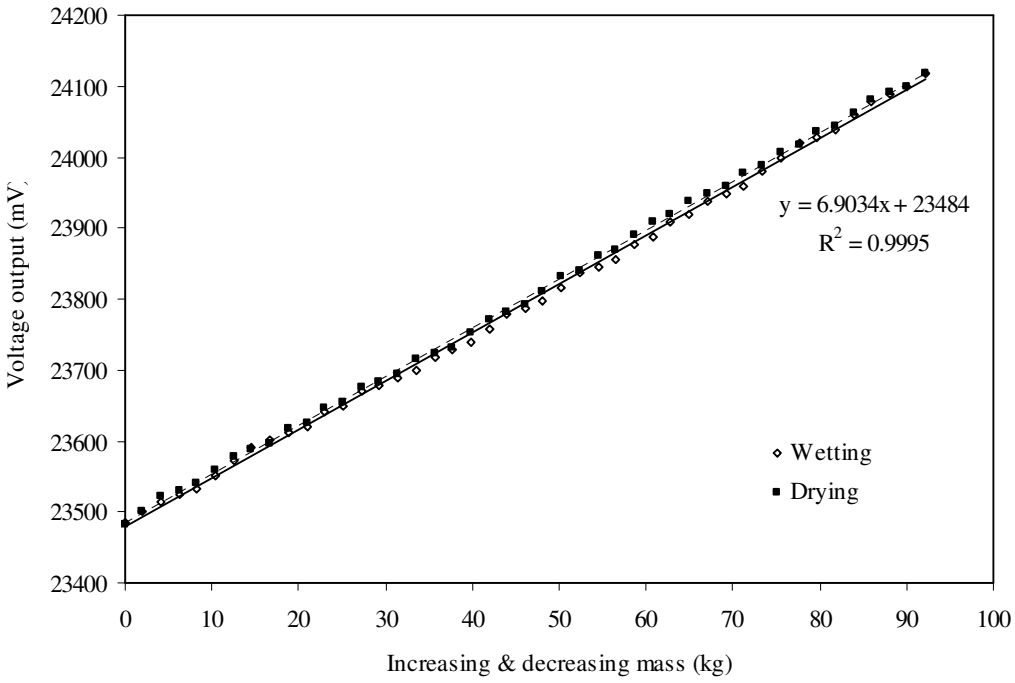

Figure 6.1 Series of millivolt outputs during the calibration process to represent wetting and drying phases

The series of millivolt readings obtained from the procedure above were used to make an equation to convert mass to Es loss from the lysimeter. Since, a change of 92.2731 kg in weight resulted in an increase in 637 millivolt and therefore, a mass of one kilogram in the lysimeter is equivalent to (conversion factor) 6.9034 millivolt per kilogram. Since, 1 mm of rainfall added

or Es loss on the lysimeter is equivalent to 4.9 kg of water, a change of 1 mm in the mass of the lysimeter will be signaled by a change in millivolt reading of (4.9 kg mm^{-1} x 6.903)mV = 33.83 mV mm^{-1}. Therefore daily lysimeter measurements Es(lys) from the lysimeter can be calculated using the equation:

$$Es(lys) = \frac{\sum_{i=1}^{24} \Delta mV_i}{33.83} \tag{6.1}$$

where Es(lys) is the daily Es measurement by the lysimeter (mm day^{-1}), mV_i is the millivolt output each hour *i*.

6.2.4 Measurements

The lysimeter was connected to a CR10X datalogger (Campbell Scientific, Logan, UT) via five loadcells. Millivolt output readings were recorded automatically every minute, averaged hourly and downloaded regularly. The Es measurement period lasted from 26 September 2008 (DOY 270) to 15 April 2009 (DOY 260) with a total of 320 days measured, with only 34 days when data was not available due to technical problems. An Es cycle was considered to be, initially from soil water content near to DUL until the next rainfall event after a minimum of 10 days had elapsed since the beginning of the Es cycle, and thereafter between consecutive rainfall events with cumulative amount(s) or rainfall events of between 19 and 25 mm. The selected drying cycles were as follows: 1st cycle 2008: DOY 270-281; 2nd cycle 2009: DOY 62-72 and 3rd cycle 2009: DOY 199-210.

6.2.5 FAO-56 Penman-Monteith

The equation for reference evapotranspiration as given by Allen *et al*. (1998):

$$ETo = \frac{0.408\Delta(Rn - G) + \gamma \frac{900}{T + 273} U_2 (e_s - e_a)}{\Delta + \gamma(1 + 0.34U_2)} \tag{6.2}$$

where ETo is the reference evapotranspiration (mm day^{-1}) for a well watered short grass surface calculated from standard automatic weather station measurements; Δ the slope of the

vapour pressure curve (kPa $^{o}C^{-1}$), 0.408 the conversion factor from energy values to equivalent depths of water (MJ m^{-2} day^{-1}); *Rn* is the net radiation at the crop surface (MJ m^{-2} day^{-1}); *G* is the soil heat flux density (MJ m^{-2} day^{-1}); T is the daily mean air temperature at 2 m height (^{o}C), U_2 is the wind speed at 2 m height (m s^{-1}); e_a is the actual vapour pressure (kPa); e_s is the saturated vapour pressure (kPa); $(e_s - e_\partial)$ is the vapour pressure deficit (kPa); γ is psychrometric constant (kPa $^{o}C^{-1}$). The inputs for the ET_o calculator (Raes, 2009) were: longitude, altitude, maximum temperature (T_{max}), relative humidity (RH) and wind speed.

6.2.6 Field hydraulic conductivity

A mathematical equation describing the relationship between hydraulic conductivity (K) and soil water content (θ) for the melanic A-horizon was derived in the field at Glen Agricultural Institute under field conditions (chapter 5: Table 5.5) and then applied in the lysimeter study. This equation was used to estimate Es(k) from the soil surface during stage two evaporation for the three drying cycles. Since, K(θ) equation was determined from the time just after the soil had reached DUL, it was assumed that water lost through Es was proportional to the change in K(θ). Therefore, Es equals K(θ). The derived K(θ) function and thus Es(k) is given by:

$$Es(k) = 5 * 10^{-6} \exp^{44.76(\theta)} \tag{6.3}$$

where θ is the soil water content for that day.

6.2.7 Darcy's equation - hydraulic conductivity method

The Darcy general equation describing flow was used to estimate Es(*q*) from the soil in the lysimeter so as to compare it with the other methods obtained from (Hillel, 1998):

$$Es(q) = K(\theta)\frac{\Delta H}{\Delta L} \tag{6.4}$$

where K(θ) is the daily hydraulic conductivity at a particular soil water content (mm day^{-1}); $\Delta H/\Delta L$ is the hydraulic gradient which is the difference between the daily soil water potential (h) in kPa at the depth of 200 mm and actual vapour pressure (e_a) in kPa at the soil surface. L

reflects on the distance in between these two points mentioned. The soil water potential (h) was obtained in the field from the relationship between h and θ in chapter 5 for the A-horizon from 1-1500 kPa (Figure 5.4) using equation 6.5:

$$h = 0.0023\theta^{-6.6341} \quad (6.5)$$

where h (kPa) is the soil potential and θ (mm mm^{-1}) is the measured soil water content from the lysimeter.

Actual vapor pressure was calculated using the following equation:

$$e_a = e_s(T_{\max})\frac{RH_{\min}}{100} \quad (6.6)$$

where e_a is the actual vapor pressure (kPa); T_{max} is the maximum air temperature (^oC) and RH_{min} is the minimum relative humidity, which usually occur at the same time using data obtained from an automatic weather station at 1.4 m and 15 m away from the weighing lysimeter.

6.2.8 Hydraulic diffusivity method

The hydraulic diffusivity method for semi-infinite soil columns subjected to infinite evaporation at the surface, was found to be a solution to flow equations, as it neglects gravity, and indicates that the evaporative flux Es(*d*) is proportional to the square root of time as given by Hillel (1998) as follows:

$$Es(d) = (\theta_i - \theta_{Le})\sqrt{D/\pi t} \quad (6.7)$$

where Es(*d*) is the daily Es calculated by the Hillel hydraulic diffusivity method; θ_i is the daily initial surface soil water content and θ_{Le} is the lower end (Le) at 1500 kPa of surface water content for the melanic soil and *D* is the hydraulic diffusivity (mm^2 day^{-1}) and *t* is time in days. A series of *D* values (Appendix 9) were determined in the laboratory by dividing K(θ) value with a corresponding specific water capacity (C_0) at a specific soil water content for the A-horizon. D values were estimated from an exponential function obtained from relationship

between a series of θ and D values (Appendix 10) using data from chapter 5 to get the following equation:

$$D = 0.691\exp^{17.189\theta} \quad (6.8)$$

where D is the hydraulic diffusivity ($mm^2\ d^{-1}$); θ is the mean daily soil water content.

Some scientists do not have sufficient detailed input data to use most of the equations of Es estimation mentioned above, and therefore the empirical methods of Ritchie (1972) and Rose (1966) have often been used and thus they are included in this study to test their reliability for the melanic A-horizon.

6.2.9 Ritchie method

Ritchie (1972) provided a cumulative Es equation to be used during stage two Es to predict ΣEs from the soil using the following equation as used by Bennie *et al*. (1998):

$$\Sigma Es = C_{ri} t^{0.5} \quad (6.9)$$

where ΣEs is cumulative Es (mm), t is time in days. C_{ri} (mm) is the calculated soil specific coefficient for each drying cycle obtained using the equation below:

$$C_{ri} = 26.11(\theta_i - \theta_{Le}) + 1.36 \quad (6.10)$$

Individual daily Es values from the Ritchie (1972) equation were obtained by using the following equation:

$$Es(ri) = (C_{ri} t^{0.5})_{day2} - (C_{ri} t^{0.5})_{day1} \quad (6.11)$$

where C_{ri} (mm) is a calculated soil specific coefficient for each of the drying cycles and θ_i (mm mm^{-1}) is the daily initial surface volumetric soil water content.

6.2.10 Rose method

The empirical method of Rose (1966) was used in this study to determine Es (mm day^{-1}) by first determining cumulative Es as described by Bennie *et al*. (1998) with the following equation:

$$\sum Es = ds * t^{0.5} + kt \quad (6.12)$$

where t (day) is the time; ds (mm) is the desorption coefficient and k is an empirical constant. Desorption coefficients (ds) was obtained using the equation:

$$ds = 20.951(\theta_i - \theta_{Le}) + 3.36 \quad (6.13)$$

where θ_i is the daily initial soil water content and θ_{Le} is the lower end soil water content. The lower end (θ_{Le}) was obtained using the following equation:

$$\theta_{Le} = 0.0012(Si - Cl) + 0.006 \quad (6.14)$$

where Si is measured percent silt (%) and Cl is measured percent clay (%).

The empirical constant (k) was obtained using the following equation:

$$k = 0.44 - 0.043(Si - Cl)^{0.5} \quad (6.15)$$

Then, Es(ro) could be calculated daily from the equation:

$$Es_{(ro)} = (ds * t^{0.5} + kt)_{day2} - (ds * t^{0.5} + kt)_{day1} \quad (6.16)$$

6.2.11 Soil evaporative coefficient for bare Bonheim soil

Daily soil evaporative coefficient (k_s) values for the bare Bonheim were determined by dividing Es(lys) values with daily ETo values obtained using Equation 6.2 as shown below:

$$k_s = \frac{Es(lys)}{ETo} \quad (6.17)$$

where Es(lys) is the daily Es measurement by the lysimeter (mm day^{-1}), ETo is the FAO 56 reference evapotranspiration (mm day^{-1}) calculated from standard automatic weather station measurements.

6.2.12 Statistical analysis

Es values measured by the lysimeter and those computed through various methods were compared by using simple regression analysis and statistics as proposed by Willmott (1982) for models for paired calculated and measured values. Lysimeter measurements [Es(lys)] were taken to represent measured values in this study. Error was calculated as:

$$RMSE = \left[N^{-1} \sum_{i=1}^{N} (P_i - Es(lys)_i)^2 \right]^{0.5} \quad (6.18)$$

where RMSE is root mean square error (mm day^{-1}); N the number of observations; P_i are estimated Es values using the various methods (mm day^{-1}); $Es(lys)_i$ are Es values measured (observed) from the lysimeter (mm day^{-1}). Willmot (1982) recommended the use of the mean absolute error (MAE) as a better measure of difference. The mean absolute error, which describes the average absolute deviation between measured and calculated data, was defined by Durar *et al*. (1995) as:

$$MAE = \frac{1}{N} \sum_{i=1}^{N} \left| P_i - Es(lys)_i \right| \quad (6.19)$$

where P_i and $Es(lys)_i$ are the paired calculated and measured values, respectively, and *N* is the total number of observations. The overall percentage error for any of the methods of estimating Es during a drying cycle was expressed as a percentage of the mean absolute error (MAE) over root mean square error (RMSE) measured [Overall method error (%) = MAE/RMSE]. The index of agreement (*D*) was also used as a relative measure of the difference among pairs, given by:

$$D = 1 - \left[\frac{\sum_{i=1}^{N} \left(P_i - Es(lys)_i \right)^2}{\sum_{i=1}^{N} \left(\left(P_i - Es(lys) \right) + \left(P_i - Es(lys) \right) \right)} \right] 0 \le D \le 1 \quad (6.20)$$

where $Es(lys)_i$ are lysimeter measured (observed) values by the lysimeter (mm day^{-1}). Perfect agreement would exist between Es(lys) and P if $D = 1$.

The Kolmogorov-Sminorv (K-S) two sample test statistical package was used to test the degree to which daily soil coefficients (K_s) were significantly different at a specified significant level (α) as applied by Steel *et al*. (1997).

6.3 Results and discussion

This chapter was embarked upon in order to fill a gap in knowledge and also to provide scientifically useful and applicable recommendations as to which one(s) of the six methods (detailed in section 6.2.5 to 6.2.10) of calculating daily Es from a bare Bo soil to recommend. This challenge was achieved by first identifying three drying (evaporation) cycles during the experimental period and these cycles were chosen on the basis that there was no risk of starting a cycle with water ponding at the bottom of the lysimeter. Six methods of Es estimation were selected from literature and their accuracy was evaluated using simple regression and Wilmott (1982) model test statistics for paired estimated and measured values. Estimated Es values were compared to daily standard weighing lysimeter Es measurements with a precision of 1 mm of rainfall added or Es loss from the lysimeter. It is important to mention that this chapter forms an integral part of this thesis in the quest to accurately determine Es which is a major (70%) loss of water from the soil surface of the bare Bo soil. The Bo soil form is predominate in the communities where the IRWH technique is being applied to grow a selected crops in the Free State Province, as a contribution to poverty alleviation, sustainable livelihoods and enhancing food security in these communities. Hence, approximately 2000 kg of the melanic A-horizon from the experimental site was carefully removed and transported to the University of the Free State, Bloemfontein West Campus weighing lysimeter to do an in-depth experiment to decide which of the tested Es calculation method(s) that can be used in the field to accurately estimate Es from Bo soils without a crop.

6.3.1 Lysimeter measurements of three Es drying cycles

The mass of oven dry soil in the lysimeter on DOY 270 was 2000 kg and 17ℓ of water. Hensley *et al*. (2000) reported that for a Bo soil, water occupies 30.5 mm per 100 mm depth at DUL. Since, the depth of soil in the lysimeter on DOY 270 was 350 mm, and 340ℓ of water was added to initiate the cycle and bring the soil in the lysimeter close to DUL, then this cycle

lasted 11 days. The second drying cycle started after a total of 25 mm of rain fell during three consecutive days; which was equivalent to 122.5ℓ of water in the lysimeter and so there was no chance that a water table would have accumulated at the bottom of the lysimeter; hence this period was chosen to start the second cycle lasting 10 days. The third drying cycle started after about 19 mm of rain fell over three consecutive days and was equivalent to 93.1ℓ of water added to the lysimeter and also lasted 10 days. Daily Es and rainfall amounts for the whole measurement period are shown in Figure 6.2. Es cycles depicted in Figure 6.2 were chosen on the basis that:

(i) there was no risk of a water table forming at the bottom of the lysimeter,

(ii) the amount of water in the lysimeter was close to the DUL value of 122 mm per 400 mm depth for the melanic soil,

(iii) the amount of water in the lysimeter soil was not more than 30 mm lower than DUL,

(iv) there was at least a minimum of 10 days without rain falling during the drying cycle.

The lysimeter measurements were taken as standard Es measurements in each of the three cycles identified as illustrated in Figure 6.2.

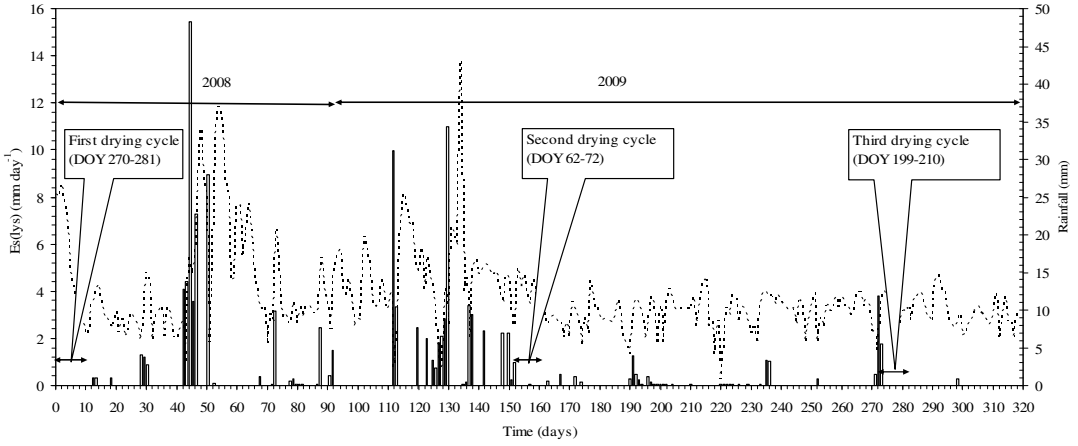

Figure 6.2 Es(lys) measurements of Es from 26 September 2008 (DOY 270) to 15 April 2009 (DOY 260)

The FAO-56 Penman-Monteith method provided an estimate of the initial stage of evaporation, which occurs while the soil is wet and conductive enough to supply water to the site of evaporation at a rate commensurate with the atmospheric evaporative demand. During this stage, the evaporation rate is limited by, and hence controlled by, external meteorological conditions rather than by the properties of the soil profile, hence Hillel (1998) referred to as the weather (atmospheric)-controlled stage. But during stage two evaporation, which Hillel (1998) referred to as soil profile-controlled stage, the evaporation rate is limited or dictated by the rate at which the gradually drying soil profile can deliver water towards the evaporation zone and can persist for a much longer time than the first stage.

6.3.2 Evaluation of Es calculation methods during the first drying cycle

Figure 6.3 shows the daily changes in Es with time during the first drying cycle (lasted 11 days) and indicates that the hydraulic diffusivity [Es(*d*)], Ritchie [Es(ri)] and Rose [Es(ro)] methods underestimated Es approximately by 5 mm d^{-1} for the second, third and fourth days after the beginning of the Es cycle. The difference gradually decreased such that on the fifth and sixth day, they underestimated by only 2 mm d^{-1}. On the seventh day underestimated by 1.8 mm d^{-1} and eighth and ninety by 1.5 mm d^{-1} and then the tenth and eleventh day by about 1 mm day^{-1}. On the other hand the Darcy [Es(q)] and field hydraulic conductivity [Es(k)] methods estimated Es closer to lysimeter measurements throughout the drying cycle than the other methods, but underestimated by 1.3 mm d^{-1} for the first five days and thereafter, by only 0.5 to 1 mm d^{-1}. The FAO-56 Penman-Monteith (ETo) method after the fourth day had higher Es values than lysimeter measurements [Es(lys)] by between 2.0 to 2.8 mm d^{-1} indicating the driving force of atmospheric evaporative demand.

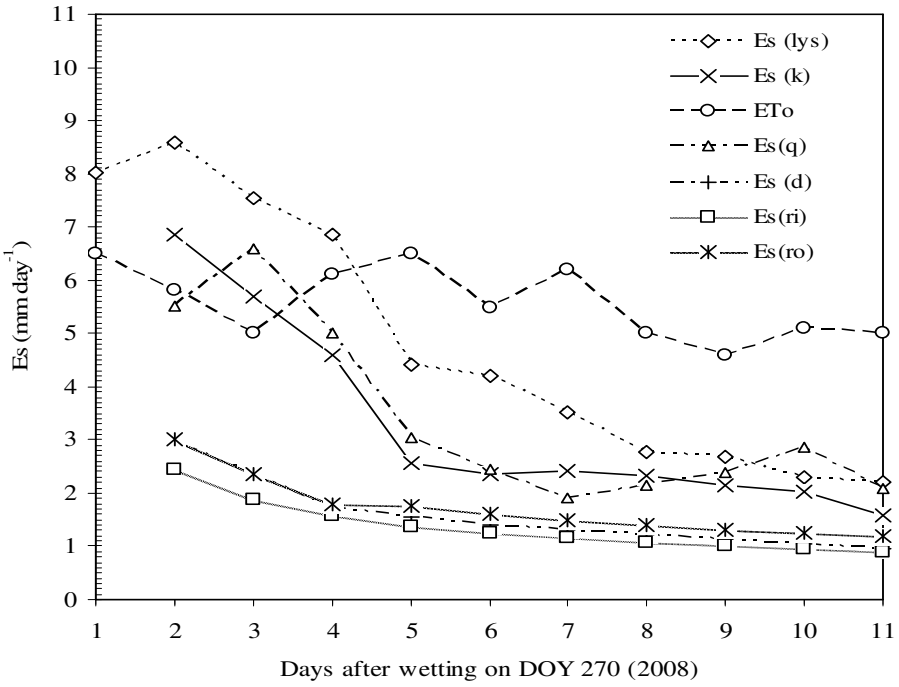

Figure 6.3 Lysimeter measurements, ETo and Es estimates from five methods plotted against time for the first drying cycle starting on DOY 270 in 2008

Willmott (1982) model test parameters, intercept, slope and coefficient of determination were used to compare the Es values from the different methods with lysimeter measurements as illustrated in Table 6.1 for the first drying cycle. Figure 6.4 further shows simple linear regression and 1:1 lines used as an evaluation tool between lysimeter measurements and Es estimated using six different methods. The Es(k) method was the best in estimating Es during the first drying cycle with the index of agreement (*D*), coefficient of determination (R^2) and percentage error at 0.8775, 0.9401 mm d^{-1} and 8%, respectively, indicating a small margin of error (Figure 6.4a). Wendroth *et al.* (1999) reported errors of between 30-40% when comparing the field hydraulic conductivity and lysimeter measurements, but an error of 8% was observed in this study indicating a good performance.

The Es(q) method performed second best during the first drying cycle with *D* and R^2 values of 0.8519 and 0.8349, respectively (Table 6.1). The RMSE and MAE of 1.5741 and 1.3656 mm d^{-1} were close indicating a good result in the estimation of Es (Table 6.1) with a difference of 0.2085 mm d^{-1}. The intercept and slope of 0.4407 and 0.6558 mm d^{-1} were not that different from zero and unity, respectively as shown in Figure 6.4c. The Es(*d*) method had a *D* value of 0.5301 (R^2 = 0.9103). The RMSE and MAE were 3.3719 and 2.9440 mm d^{-1}, respectively. The R^2 of 0.9103 was slightly lower than the 0.9289 obtained for the Es(ri) method. As was expected, the Es(ri) and Es(ro) methods performed similarly as they are based on similar theory with RMSE of 3.6153 and 3.2739 mm d^{-1}.

Table 6.1 Evaluation of the five methods of calculating daily Es during the first cycle

Method	Es (estimated) = a + b*[Es(lys)]			RMSE	MAE	*D*
	a	b	R^2			
Es(k)	-0.1123	0.7481	0.9401	1.5067	1.3871	0.8775
Es(q)	0.4407	0.6558	0.8349	1.5741	1.3656	0.8519
Es(*d*)	0.3880	0.2611	0.9103	3.3719	2.9440	0.5301
Es(ri)	0.4626	0.1990	0.9289	3.6153	3.1493	0.5030
Es(ro)	0.6983	0.2272	0.8760	3.2739	2.7862	0.5289

Willmot results of Es estimated by each method versus lysimeter measurements; a: ordinate at the origin (mm day^{-1}); b: slope; R^2: coefficient of determination; RMSE: root mean square error (mm day^{-1}); MAE: mean absolute error (mm day^{-1}); *D:* index of agreement; *: multiplication sign

Overall the results show an interesting trend in that during the first four days, lysimeter measurements were higher than those obtained using the ETo method which most scientists use as a evaporative demand of the atmosphere. It may be due to the fact that the ETo method assumes a grass cover hence may underestimate Es under bare soil conditions during the initial phase. However, this calls for further investigation in another study.

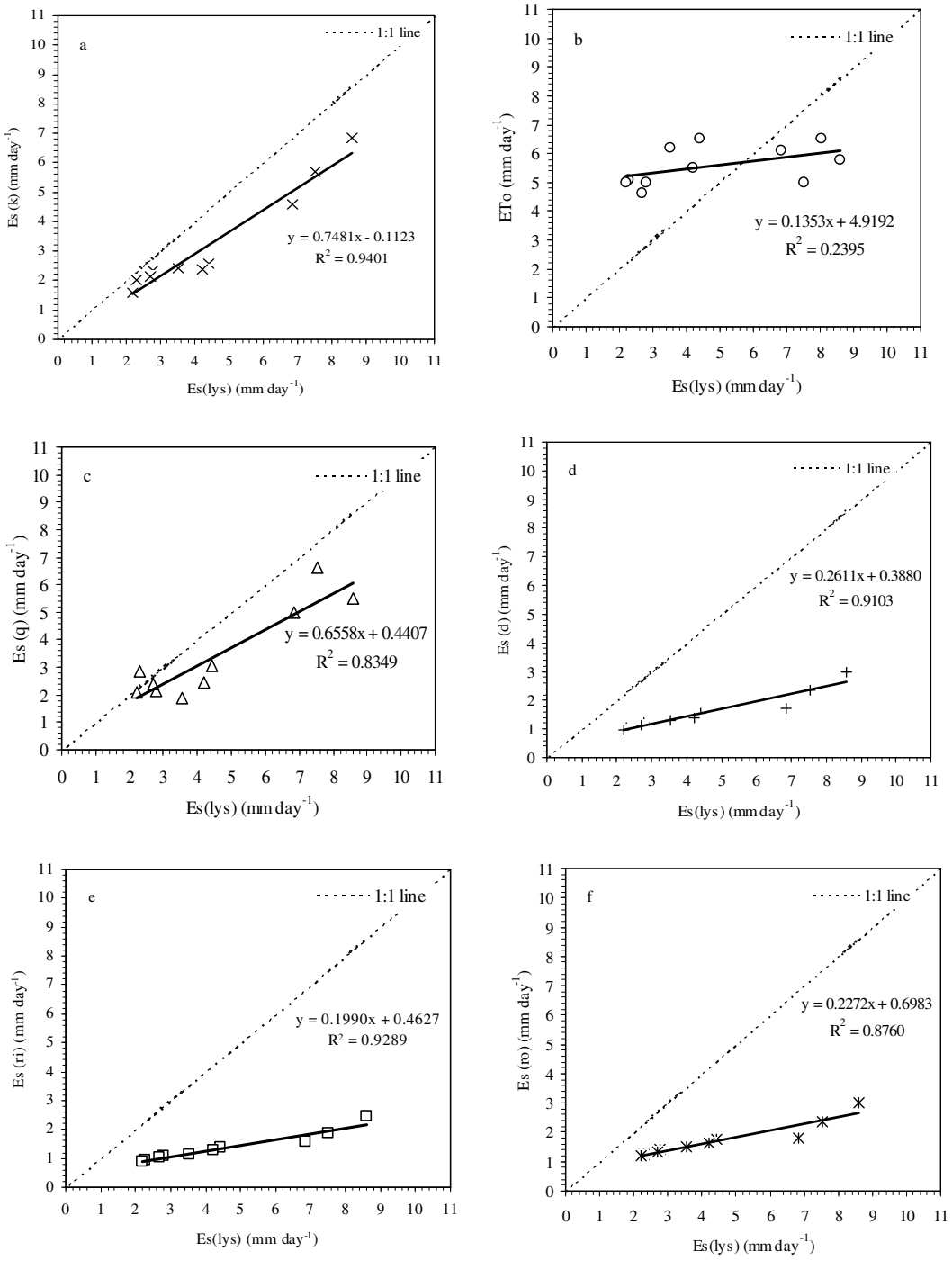

Figure 6.4 Simple linear regression and 1:1 lines showing the comparison between Es(lys) and those Es values obtained using six different methods of estimating Es for the first drying cycle namely: (a) Es(k), (b) ETo, (c) Es(q), (d) Es(*d*), (e) Es(ri) and (f) Es(ro)

6.3.3 Evaluation of Es calculation methods during the second drying cycle

During the second drying cycle the Es(k) and Es(q) methods had *D*-values (Table 6.2) more than 0.5, but the Es(q) estimated Es very close to lysimeter measurements during the last four days of this cycle (Figures 6.5; 6.6(b) and 6.6(c). The Es(ri) method underestimated lysimeter measurements more than all the other methods of estimation (Figure 6.5) just as in the first cycle (Figure 6.3) by an average of 2.7 mm d^{-1} throughout the second cycle hence the RMSE of 2.7313 mm day^{-1} (Table 6.2). The Es(k) method on the other hand estimated Es closer to lysimeter measurements but still not as good as in the first cycle, this maybe due to the differences in the soil water contents between the cycles.

Table 6.2 Evaluation of five methods of calculating daily Es values during the second cycle

Method	Es (estimated) = a + b*[Es(lys)]			RMSE	MAE	*D*
	a	b	R^2			
Es(k)	-0.9588	1.0622	0.2212	1.3711	1.2327	0.5170
Es(q)	0.9900	0.8980	0.3006	1.0036	0.6988	0.5915
Es(*d*)	-0.6893	0.5635	0.3223	2.4111	2.3495	0.3110
Es(ri)	-0.1630	0.3365	0.2992	2.7313	2.6869	0.2720
Es(ro)	-0.1321	0.5316	0.2992	1.9909	1.9138	0.3572

Willmot results of Es estimated by each method versus lysimeter measurements; a: ordinate at the origin (mm day^{-1}); b: slope; R^2: coefficient of determination; RMSE: root mean square error (mm day^{-1}); MAE: mean absolute error (mm d^{-1}); *D:* index of agreement; *: multiplication sign

However, it was interesting to note that the Es(q) method overestimated Es during the second cycle, only underestimated Es once by 0.5 mm d^{-1} during the cycle. Figure 6.6 also shows that the evaporation trends of underestimation by the Es(*d*), Es(ri) and Es(ro) methods were similar to the first cycle during the second evaporation cycle. The Es(q) method produced the best performance estimating Es closer to the lysimeter measurements when compared to the other

four methods. The Es(q) method had an RMSE and MAE close to each other at 1.0036 and 0.6988 mm d^{-1}, with a percent error of 30% and *D*-value of 0.5915.

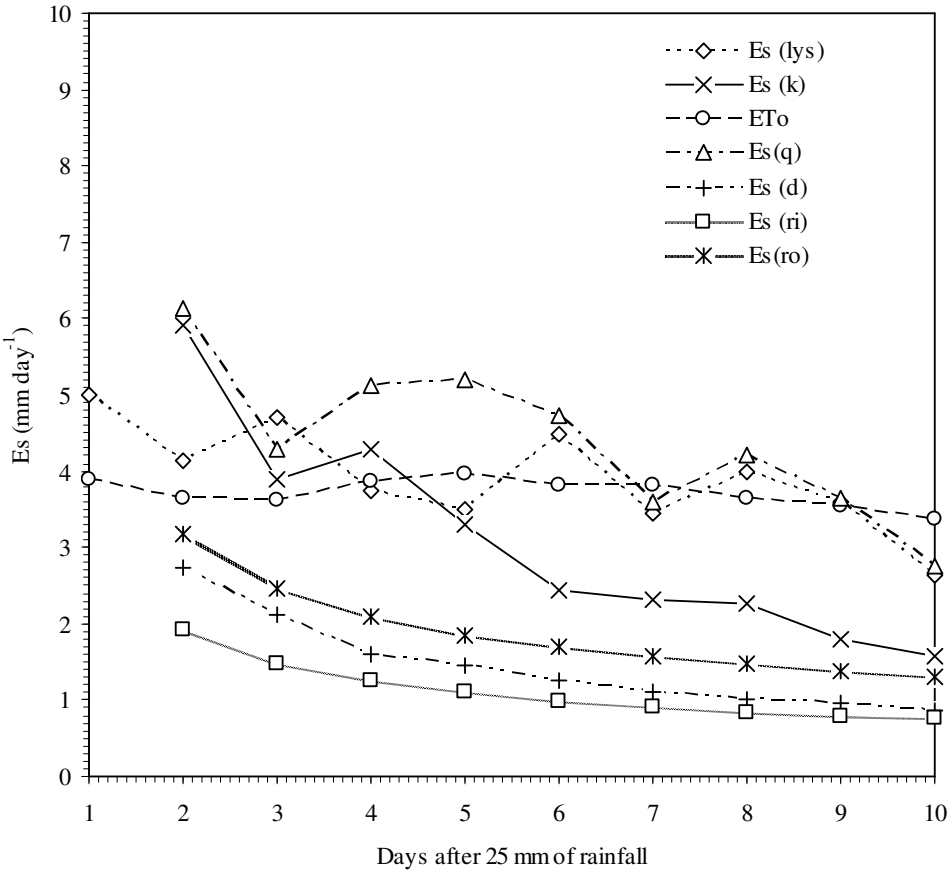

Figure 6.5 Lysimeter measurements, ETo and Es estimates from six methods plotted against time for the second drying cycle starting on DOY 62 in 2009

In the case of the Es(k) method, it performed fairly well during the second cycle with an index of agreement of 0.5170 and MAE of 1.2327 mm d^{-1}. However, the Es(*d*), Es(ri) and Es(ro) methods underestimated Es similarly even during the first drying cycle and depicted the same trend during the second cycle (Figure 6.5) and these methods generally underestimated Es below the 1:1 line as shown in Figure 6.6. The Es(*d*) method had an RMSE of 2.4111 and MAE of 2.3495 mm d^{-1} resulting in a difference of 0.0616 mm d^{-1}. The intercept and slope of -0.6893 and 0.5635 were close to zero as illustrated in Figure 6.6d, the R^2 value was low at

0.3223 showing poor correlation with the measured Es from the lysimeter. The Es(ri) and Es(ro) methods generally underestimated lysimeter measurements; however the Es(ro) method performed slightly better than the Es(ri) method indicated by the index of agreement of 0.3573 and 0.2720 for the Es(ro) and Es(ri) methods, respectively. The RMSE for the Es(ro) method was lower at 1.9909 mm d^{-1} than that of the Es(ri) method of 2.7313 mm d^{-1}. The difference between the MAE and RMSE for the Es(ro) was 0.0771 mm d^{-1} compared to 0.2607 mm d^{-1} for the Es(ri) method. But, neither method performed well and therefore would not be recommended to be used to estimate the Es under this drying cycle. Although, the Es(k) and Es(q) methods performed fairly well, they had lower agreement indices during the second cycle compared to the first cycle, most likely the decrease was due to the total amount of soil water present at the beginning of the second cycle and secondly due to the fact that a few days before the cycle began a heavy hail storm (Appendix 11) might have compacted the soil surface causing surface sealing thus further reducing Es from the melanic A-horizon.

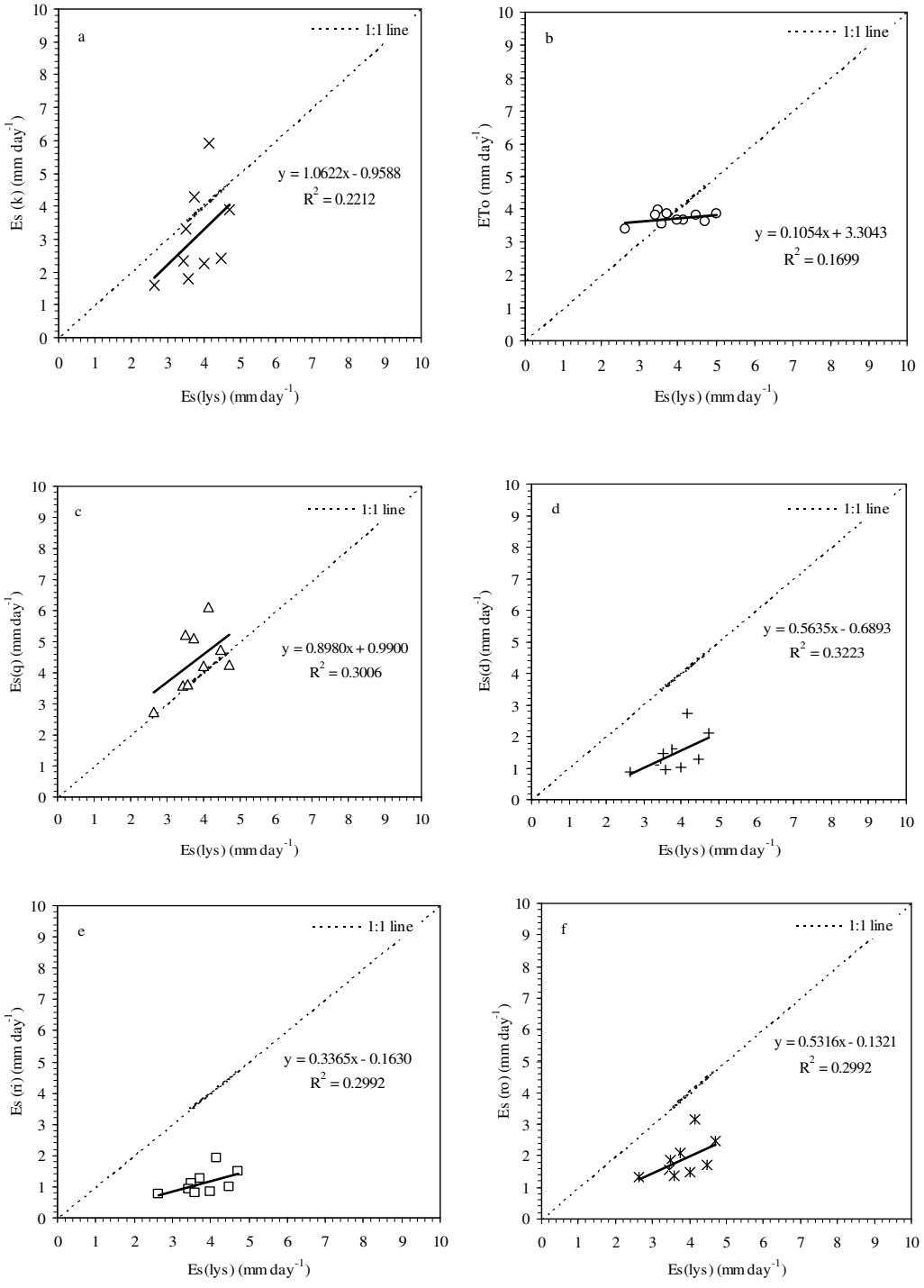

Figure 6.6 Simple linear regression and 1:1 lines showing the comparison between lysimeter measurements and those Es values obtained using five different methods for the second drying cycle namely: (a) Es(k); (b) ETo; (c) Es(q); (d) Es(d); (e) Es(ri) and (f) Es(ro)

6.3.4 Evaluation of Es calculation methods during the third drying cycle

All the five estimation methods during the third drying cycle underestimated Es close to each other by about 1.3 mm d^{-1} as illustrated in Figure 6.7 and had low indices of agreement, all with less than 0.5 and the R^2 values were more than 0.5 (Table 6.3). The FAO-56 Penman-Monteith method (Figure 6.8b) provided reference Es values shown to indicate the atmospheric evaporative demand and had an index of agreement of 0.3159.

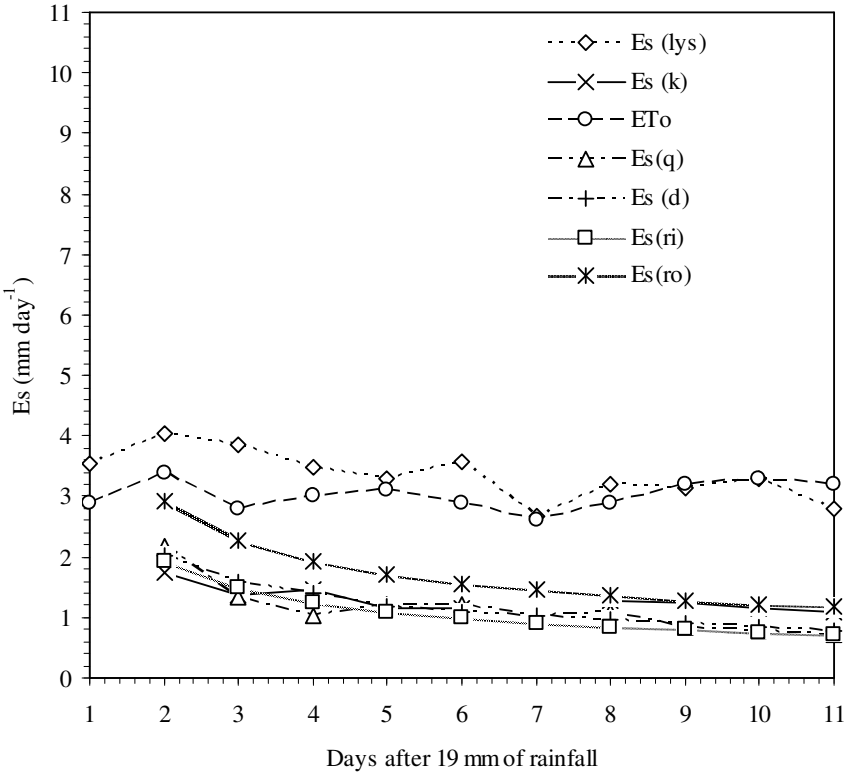

Figure 6.7 Lysimeter measurements Es(lys) and Es estimates from six methods plotted against time for the third drying cycle starting on DOY 199 in 2009

The RMSE and MAE for the Es(k) method were close with small difference between the errors at 0.0221 mm d^{-1} and an R^2 of 0.5639 slightly higher than that of Darcy at 0.5204 but not significantly different. The difference between the RMSE and MAE for the Es(q) method was 0.0200 mm d^{-1}. The Es(*d*) method estimated lysimeter measurements close to the Es(ri) method

during the third cycle and this is indicated by the R^2 of 0.6637 and 0.6775 for the Es(*d*) and Es(ri) methods. However, it was also interesting to note that the Es(ro) and Es(ri) methods had equal R^2 values at 0.6775 and the same trend of similar R^2 values was observed in the second cycle between these two methods. Urrea *et al*. (2006) and Wendroth *et al*. (1999) observed errors of between 10-40% when comparing lysimeter measurements with Es estimation methods using either soil or meteorological based methods of estimation.

Table 6.3 Evaluation of the five methods of calculating daily Es values during the third cycle

Method	Es (estimated) = a + b*[Es(lys)]			RMSE	MAE	D
	a	b	R^2			
Es(k)	-0.0942	0.4053	0.5639	2.1937	2.1749	0.3039
Es(q)	-1.3042	0.7343	0.5727	2.2073	2.1896	0.2427
Es(*d*)	-1.2891	0.7393	0.6637	2.1710	2.1579	0.2922
Es(ri)	-1.3729	0.7352	0.6775	2.2674	3.2555	0.2822
Es(ro)	-1.8669	1.0669	0.6775	1.6710	1.6440	0.3680

Willmot results of Es estimated by each method versus lysimeter measurements; a: ordinate at the origin (mm day^{-1}); b: slope; R^2: coefficient of determination; RMSE: root mean square error (mm day^{-1}); MAE: mean absolute error (mm day^{-1}); D*:* index of agreement; *: multiplication sign

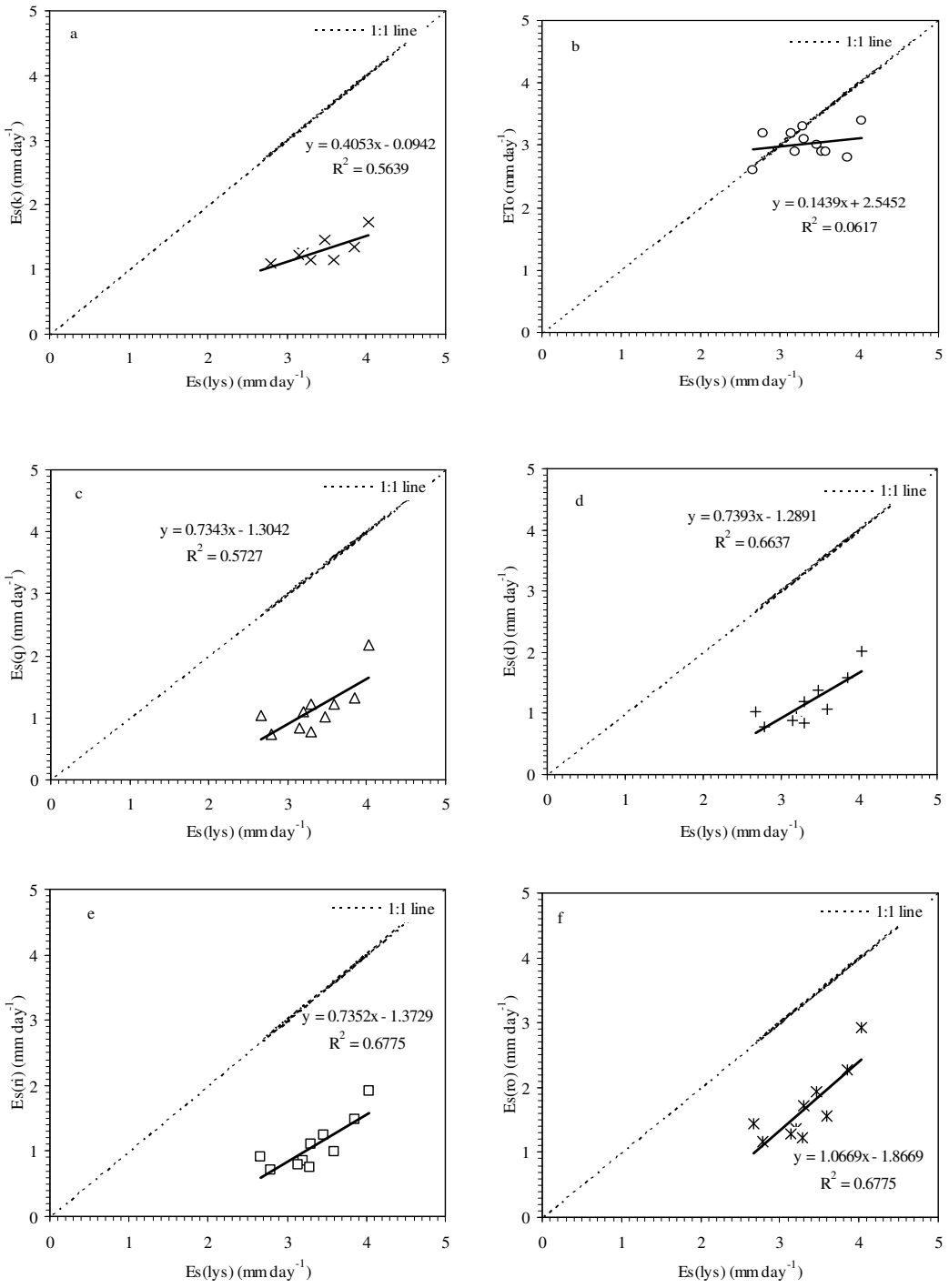

Figure 6.8 Simple linear regression and 1:1 lines showing the comparison between lysimeter measurements and those Es values obtained using five methods for the third cycle namely: (a) Es(k); (b) ETo; (c) Es(q); (d) Es(d); (e) Es(ri) and (f) Es(ro)

6.3.5 Estimation of soil coefficients for a bare Bo soil

The value of soil coefficient (Ks) is affected by the atmospheric demand, i.e., ETo. The higher the evaporation demand from the atmosphere, the quicker the soil will dry between wetting events and the smaller the time-averaged Ks will be for any particular period (Allen *et al.*, 1998). Figure 6.9 shows that after the fourth day during the first drying cycle the Ks values were smaller than those of the second and third drying cycles.

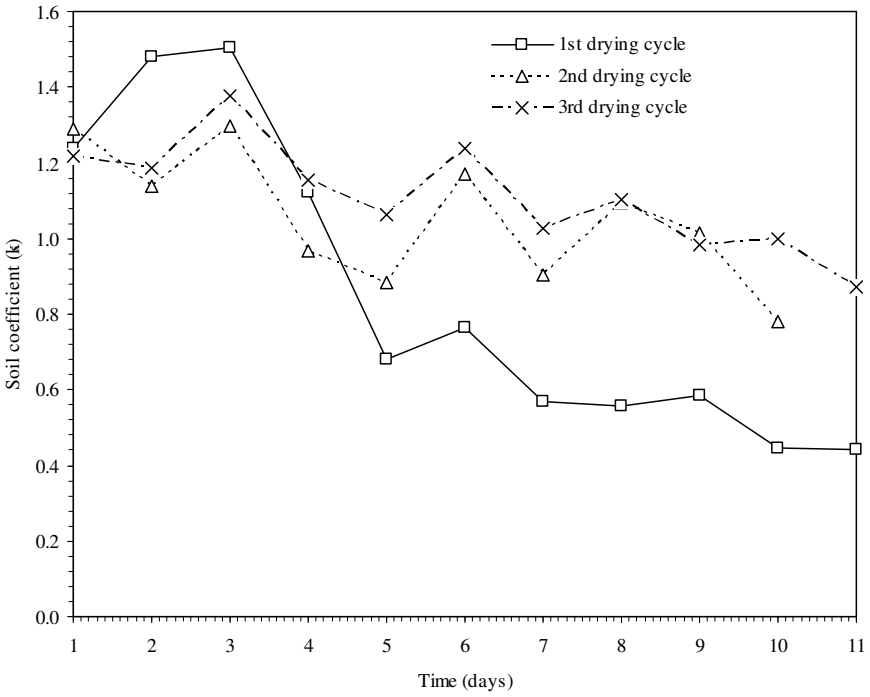

Figure 6.9 Daily soil coefficients (K_s) values during the three different drying cycles for the melanic A-horizon

The K_s values were smaller during the first drying cycle (Figure 6.9) due to the fact that K_s are a function of the magnitude of the initial wetting event and the evaporation potential of the atmosphere. The values were influenced by the amount of water available (88 mm per 350 mm) depth at the start of the cycle in the topsoil of the melanic A-horizon and the relatively high ETo values (Figure 6.3) compared to the other two drying cycles (Figures 6.5 and 6.7). K_s values for the first and second drying cycles and second drying cycles and second and third

drying cycles were not significantly different, with the only significantly difference being between the first and third cycles (Table 6.4) where the wetting situation was also not similar. Hence, it is concluded in this study that no-single distribution of K_s values distribution from the various drying cycles individually represent a standard for K_s values for a bare clay soil but average K_s values between the first and second cycles are recommended for use for clay soils; secondly, the Ks values calculated in this study can be extrapolated to other Bo soils only when the magnitude of the initial wetting and evaporative atmospheric conditions are known for a particular area.

Table 6.4 K-S paired comparisons of daily K_s values for the three drying cycles

Comparison of cycles	D-statistics	P-value
1^{st} vs 2^{nd}	0.5364^{ns}	0.0620
1^{st} vs 3^{rd}	0.6364*	0.0120
2^{nd} vs 3^{rd}	0.4091^{ns}	0.2650

*Significantly different at $\alpha = 0.05$; ^{ns} not significantly different at $\alpha = 0.05$

6.4 Conclusions

Results from this study, on the evaluation of five methods of estimating Es during three evaporation cycles namely the field hydraulic conductivity [Es(k)], Darcy-equation [Es(q)], Hydraulic diffusivity [Es(*d*)], Ritchie [Es(ri)] and Rose [Es(ro)] methods indicated that the Es(k) method performed better than the other four methods with a percentage error between 20-30%. It can be concluded that the Es(k) method is the best method that can be used to estimate Es under field conditions during soil profile-controlled stage, when the evaporation rate is limited by the rate at which the gradual drying soil profile can deliver water towards the evaporation zone. More importantly the Es(k) equation was derived from the melanic soil hydraulic properties that influence water movement and thus evaporation. The Es(k) method

requires only soil water content as an input vis-à-vis the other estimation methods which may require more parameters and relevant computer software to carryout Es estimations. It was also concluded that the K_s values obtained in this study can be used for Bo soils only when the initial soil water content is known.

CHAPTER 7

GENERAL DISCUSSION

In the semi-arid regions of sub-Saharan Africa, the major unproductive water loss in crop production systems is soil surface evaporation. Normally these areas are characterized by low and erratic rainfall, and thus if longer than normal drought spells are experienced crop failure becomes a threat to the livelihood of the human population in these regions. The ever increasing human population in the continent becomes more and more prone to drought and famine in the absence of sound water management practices due to the limited amounts of water either from rainfall or ground water sources. Therefore, an understanding of water flow through the soil-plant-atmosphere continuum is very important in dryland crop production agriculture for the sustainability of the human race. The soil, as a system provides a medium for plants to grow and therefore an in-depth knowledge of its thermal, physical and chemical properties and how these properties influence the rate of Es during the profile–controlled stage of evaporation.

This study was carried out in Free State Province of South Africa; on a melanic (clay) soil generally associated with gentle or low lying areas with annual precipitation between 550-800 mm. These soils cover 2% of the total land area of 122.8 million ha in South Africa. Generally, these soils have a high porosity and water holding capacity; and relatively high levels of organic matter and near-neutral pH making them very fertile. In the tribal areas of Thaba'Nchu, east and north-east of Bloemfontein, in spite of the favourable rainfall between 500-600 mm, the potential to grow crops was previously limited by these clay soils which have physical properties that render them unfavourable for crop production using conventional tillage practices (Eloff, 1984). Because of the dry soil water regime caused by excessive water losses

through Es and runoff; Bennie and Hensley (2001) reported that between 50-70% of the annual rainfall in these areas is lost through Es. Hensley *et al*. (2000) developed the IRWH crop production technique which over the years has been proved to be suitable and accepted by the subsistence of Thaba'Nchu to use for growing a number of field and vegetable crops. The IRWH has helped to improve maize yields by 50% (Kundhlande *et al*., 2004). Tribal authority land in Thaba'Nchu occupies about 10 500 ha, on which the IRWH technique can be applied to enhance crop production and help reduce the scourge of poverty and thus enable households to grow their own crops to enhance their livelihoods. However the high Es losses should be decreased by mulches.

Melanic soils are the predominant soils in the areas, east of Bloemfontein compared to other clay soil forms; hence the Bonheim soil was investigated. It was studied in terms of its thermal (Chapter 4) and hydraulic properties (Chapter 5) and as well as resulting evaporative characteristics (Chapter 6) under semi-arid conditions so as to fill a gap in knowledge and understanding of the IRWH system. Before these studies could be carried out, the ECH_20-TE probes needed to be calibrated to measure soil water content (θ) and soil temperature in the field. Therefore, the evaporative desorption procedure (EDP) was adapted (Chapter 2) so as to calibrate ECH_20-TE probes in a swelling clay (Bonheim) soil with probes installed in the soil horizon as they were placed in the field. Secondly, the ECH_20-TE probes were evaluated for their accuracy, repeatability and precision; they were found to give more accurate results if they are calibrated in two different soil temperature treatments (Chapter 3). Temperature compensated equations yielded more accurate results with precision and accuracies of with ranges between 93 and 99% and repeatability of 95%. Equations given by manufacturers for similar soils overestimated soil water content by as much as by 40% and therefore, it was concluded in this study that these probes must be calibrated for a specific soil to give meaningful and scientifically accepted results.

Another part of the study investigated the effect of mulch type and percentage coverage to temperature both above and below the soil surface for the Bonheim soil (Chapter 4).As the study provided a scientific background advising farmers on how much mulch to apply to minimise Es, which is directly linked to the amount of radiant energy available in the soil or atmosphere to initiate Es. The advice to give to farmers applying the IRWH system is that they must not keep soil bare even during fallow periods to avoid water loss through Es. The 100% reed mulch must be used to keep the soil cool in summer thus reducing Es; however in winter it lowers soil temperatures and may delay seed germination and slow down root growth. But, the 50% stone mulch can be used in winter so as to prevent frost damage and promote root development. The 50% reed mulch can be used on the IRWH both in winter or summer months as it does not greatly influence soil temperatures. For practical reasons it is recommended herein that the 100% reed mulch be used.

The characterization of the hydraulic properties (drainage patterns, soil water release characteristics (SWRC), soil water-matric suction [$\theta(h)$] and hydraulic conductivity [$K(\theta)$] relationships) for the Bonheim soil were carried out so as to help fill a gap in knowledge as they have never been done to such detail. A statistically sound procedure known as the *in situ* internal drainage (ISID) method was adopted and applied in this study on *in situ* drainage patterns of each master horizon to determine drained upper limit (DUL), separate pore domains into structural (macro pores), transitional (meso pores) and textural (micro pores). This study showed that the ISID method is practical and statistically sound and is therefore recommended for the determination of the DUL. The results indicated that the structural pores are associated with low suctions and allowed water to moderately flow between 8-15 mm hr^{-1} and drained within 12 hours for all horizons. The meso pores are associated with slightly slower water flows between 4-13 mm hr^{-1} and micro pores between 6.6-10.4 mm hr^{-1} in all horizons. The

pedocutanic layer micro pores stored and released 20% more water than the other soil horizons which is an important feature of this soil to crop production.

The last study evaluated five methods of estimating Es from the soil surface in the absence of a crop in a weighing lysimeter (Chapter 6) only for the melanic A-horizon. It was concluded in this study that the method using an equation describing Es as a function of soil water content determined in the field known as the Es(k) method was more accurate than the others overall in estimating Es, and therefore it should be applied and is recommended for use for melanic soils. Secondly, it is less tedious and requires only the soil water content as an input parameter to calculate Es.

Overall, the outputs from this study are important in making informed decisions in soil water management applications for the IRWH system in similar soils and thus contribute in the fight against poverty, unemployment and towards a sustainable crop production in semi-arid regions. For example, firstly by encouraging farmers to use 100% mulch coverage (during summer) and 50% stone mulch (during winter) on the system to reduce Es both during the growing season and the fallow period. Secondly, promote surface sealing of the surface soil of the runoff zone to reduce Es, this conclusion was drawn because whilst carrying out Chapter 6 on the weighing lysimeter there was a heavy hail storm that semi-sealed and compacted the top soil and resulted in lower Es values from the bare melanic soil surface.

REFERENCES

ALLEN, R., PEREIRA, L.S., RAES, D. & SMITH, M., 1998. Crop Evapotranspiration - Guidelines for computing crop water requirements. FAO Irrigation and Drainage Paper No. 56. Rome. Italy: pp 300.

ANDERSON, J.J., 2007. Rainfall-runoff relationships and yield responses of maize and dry beans on the Glen-Bonheim ecotope using conservational tillage and in-field rainwater harvesting. Ph.D. thesis, Department of Soil, Crop and Climate Sciences, University of the Free State, Bloemfontein. pp 317.

BACKEBERG, G.R., 2009. Improving livelihoods with rainwater and conservation on communal croplands in South Africa: Opportunities and obstacles. A paper presented at the International Seminar of the International Foundation for Sustainable Development in Africa and Asia, Gottingen, Germany, 14-16 July 2009.

BENNIE, A.T.P. & HENSLEY, M., 2001. Maximizing precipitation utilization in dryland agriculture in South Africa-a review. *J. Hydrol.* 241: 124-139.

BENNIE, A.T.P., HOFFMAN, J.E., COETZEE, M.J. & VREY, H.S., 1994. Storage and utilization of rainwater in soils for stabilizing crop production in semiarid areas [Afr]. Report No. 227/1/94, Water Research Commission, Pretoria, South Africa: pp 327.

BENNIE, A.T.P., STRYDOM, M.G. & VREY, H.S., 1998. The application of computer models or agricultural water management at ecotope level [Afr]. Report No. TT 102/98, Water Research Commission, Pretoria, South Africa: pp 235.

BLANCO-CANQUI, H., LAL, R., POST, W.M., IZAURRALDE, R.C. & SHIPITALO, M.J., 2007. Soil hydraulic properties influenced by corn in Ohio. *Soil Till. Res.* 92: 144-155.

BOGENA, H.R., HUISMAN, J.A., OBERDORSTER, C. & VEREECKEN, H., 2007. Evaluation of low-cost soil water content sensor for wireless network applications. *J. Hydrol.* 344: 32-42.

BOTHA, J.J., 2006. Evaluation of maize and sunflower production in a semi-arid area using in-field rainwater harvesting. Ph.D. thesis, Department of Soil, Crop and Climate Sciences, University of the Free State, Bloemfontein: pp 9.27.

BOTHA, J.J., ANDERSON, J.J., GROENEWALD, D.C., MDIBE, N., BAIPHETHI, M.N., NHLABATSI, N.N. & ZERE, T.B., 2007. On-farm application of In-field Rainwater Harvesting techniques on small plots in the Central region of South Africa. Report. TT313/07, Water Research Commission, Pretoria, South Africa: pp 147.

BOTHA, J.J. & VAN RENSBURG, L.D., 2004. Water harvesting to promote food security and employment. Landcare report to the Department of Agriculture, Pretoria, South Africa: p 1-20.

BOTHA, J.J., VAN RENSBURG, L.D., ANDERSON, J.J., HENSLEY, M., MACHELI, M.S., VAN STADEN, P.P., KUNDHLANDE, G., GROENEWALD, D.G. & BAIPHETHI, M.N., 2003. Water conservation techniques on small plots in semi-arid areas to enhance rainfall use efficiency, food security, and sustainable crop production. Report No. 1176/1/03, Water Research Commission, Pretoria, South Africa: pp 221.

BOTHMA, C.B., 2009. In-field runoff and soil water storage on duplex soils at Paradys experimental farm. M.Sc. dissertation, Department of Soil, Crop and Climate Sciences, University of the Free State, Bloemfontein. pp 113.

BRISTOW, K.L., 1988. The role mulch and its architecture in modifying soil temperature. *Aust. J. Soil Res.* 26: 269-280.

BRUCE, R.R, & KLUTE, A., 1956. The measurement of soil water diffusivity. *Soil Sci. Soc. Am. Proc*. 20: 458-462.

CAMPBELL, J.E., 1990. Dielectric-properties and influence of conductivity in soils at one to 50 MHz. *Soil Sci. Soc. Am. J.* 54 (2): 332-341.

CATE, R.B. & NELSON, L.A., 1971. A simple statistical procedure for partitioning soil test correlation data into two classes. *Soil Sci. Soc. Am. Proc.* 35: 658-660.

CHEN, Y. & OR, D., 2006. Geometric factors and interfacial processes affecting complex dielectric permittivity of partially saturated porous media. *Water Resour. Res.* 42: W06423.

CHENG, J.S. & ZHANG., X.X., 2000. Study on the ecological effects of plastic mulching on potato in cool and humid highland of Wei'nan county in Gansu province. *Chinese Potato* 14 (2): 83-84.

CHIMUNGU, J.G., 2009. Comparison of field and laboratory measured hydraulic properties of selected diagnostic soil horizons. M.Sc. dissertation, Department of Soil, Crop and Climate Sciences, University of the Free State, Bloemfontein: pp 113.

COBOS, D.R., 2009. Calibrating ECH_20 soil moisture sensors. Application note available at *http//www.Decagon.com/appnotes/echocal.pdf.* Viewed: 5th September 2009.

COBOS, D. & CAMPBELL, C.S., 2007. Correcting temperature sensitivity of ECH_20 soil moisture sensors. Decagon Devices Inc. Pullman, WA (available at *http//www.Decagon.com/appnotes/echo_analysis.pdf.*) Viewed: 5th September 2009.

CZARNOMSKI, N., MOORE, G., PYPKER, T., LICATA, J. & BOND, B., 2005. Precision and accuracy of three alternative instruments for measuring soil water content in two forest soils of the Pacific Northwest. *Can. J. For. Res*. 35 (38): 1867-1876.

DAHIYA, R., INGWERSEN, J. & STRECK, J., 2007. The effect of mulching and tillage on water and temperature regimes of a loess soil: Experimental findings and modeling. *Soil Till. Res*. 96: 52-63.

DECAGON DEVICES, 2007. ECH_2O-TE/EC-TM: Water Content, EC and Temperature sensors. Operator's manual. Decagon devices Inc. Pullman WA: 619-633.

DEPARTMENT OF AGRICULTURE-FREE STATE PROVINCE, 2006. Annual performance plan 2006-2009. Department of Agriculture-Free State, Glen, South Africa. pp 1-230.

DIRKSEN, C., 1999. Soil Physics Measurements. GeoEcology, *Catena Verlag*, Germany: 18-20.

DURAR, A.A., STEINER, J.L., EVETT, S.R. & SKIDMORE, E.L., 1995. Measured and simulated surface soil drying. *Agron. J*. 87: 235-244.

DU PLESSIS, M.C.F. & MOSTERT, J.W.C., 1965. Runoff and soil loss at the Agricultural Research Centre, Glen [Afr.] *S. Afri. J. Agric. Sci.* 8: 1051-1060.

ELOFF, J.F., 1984. The soil resources of the Free State Region. [Afr]. Ph.D. thesis, University of Stellenbosch, Cape Town, South Africa. pp 270.

FABRIZZI, K.P., GARCIA, F.O., COSTA, J.L. & PICONE, L.L., 2005. Soil water dynamics, physical properties and corn and wheat responses to minimum and no-tillage systems in southern Pampas of Argentina. *Soil Till. Res.* 81(1): 57-69.

FARES, A. & POLYAKOV, V., 2006. Advances in crop water management using capacitance water sensors. *Adv. Agron*. 90: 43-47.

FOX, D.G., 1981. Judging air quality model performance: A summary of the AMS workshop on dispersion model performance. *Bull. Am. Meteorol. Soc*. 62: 599-609.

FRAENKEL, C.H., 2008. Spatial variability of selected soil properties in and between map units. M.Sc. dissertation, Department of Soil, Crop and Climate Sciences, University of the Free State, Bloemfontein. pp 132.

FUJIMAKI, H. & INOUE, M., 2003. A transient evaporation method for determining soil hydraulic properties at low pressure. *Vadose Zone J.* 2: 400-408.

GARDNER, W.R. & MIKLICH, F.J., 1962. Unsaturated conductivity and diffusivity measurements by a constant flux method. *Soil Sci. J.* 93: 271-274.

GURNAH, A.M., 1987. Effect of mulches on soil temperature under Arabica coffee at Kabete, Kenya. *Agric. Meteorol*. 25: 234-244.

HAYLETT, D.G., 1960. Runoff and soil loss studies at Pretoria. *S. Afr. J. Agric. Sci.* 3: 379-394.

HENSLEY, M., BOTHA, J.J., ANDERSON, J.J., VAN STADEN, P.P. & DU TOIT, A., 2000. Optimising rainfall use efficiency for developing farmers with limited access to irrigation water. Report No. 878/1/00, Water Research Commission, Pretoria, South Africa: pp 213.

HENSLEY, M., LE ROUX, P.A.L., DU PREEZ, C.C., VAN HUYSSTEEN, C., KOTZE, E. & VAN RENSBURG, L.D., 2006. Soils: The Free State's agricultural base. *S. Afr. Geo. J.* 88 (1): 11-21.

HILHORST, M.A., DIRKSEN, C., KAMPERS, F.W.H. & FEDDES, R.A., 2001. Dielectric relaxation of bound water versus soil matric pressure. *Soil Sci. Soc. Am. J.* 65: 311-314.

HILLEL, D., 1998. Environmental Soil Physics. Academic Press Inc, New York. pp 129-241.

HILLEL, D., KRENTOS, V.D. & STYLIANOU, Y., 1972. Procedure and test of an internal drainage method for measuring soil hydraulic characteristics *in situ. Soil Sci.* 114: 395-400.

HORTON, R., BRISTOW, K.L., KLUITENBERG, G.J. & SAUER, T.J., 1996. Crop residue effects on surface radiation and energy balance–review. *Theor. Appl. Clim.* 54: 27-27.

HOU, X.Y., WANG, F.X., HAN, J.J., KANG, S.Z. & FENG, S.Y., 2010. Duration of plastic mulch for potato growth under drip irrigation in an arid region of northwest China. *Agric. For. Meteorol.* 150(1): 113-121.

JURY, W., GARDNER, W.R. & GARDNER, W.H., 1991. Soil Physics (5th Ed.). John Wiley & sons, New York: p 35-71.

KATAN, J., 1979. Solar heating of the soil by polyethylene mulching for the control of plant diseases and weeds. *Trans. ASAE*: 46-79.

KELLENERS, T.J., ROBINSON, D.A., SHOUSE, P.J., AYARS, J.E. & SKAGGS, T.H., 2005. Frequency dependence of the complex permittivity and its impact on dielectric sensor calibration in soils. *Soil Sci. Soc. Am. J.* 69 (1): 67-76.

KIZITO, F., CAMPBELL, C.G., COBOS, D.R., TEARE, B.L., CARTER, B. & HOPMANS, J.W., 2008. Frequency, electrical conductivity and temperature analysis of a low-cost capacitance soil moisture sensor. *J. Hydrol.* 352: 367-378.

KUNDHLANDE, G., GROENEWALD, D.G., BAIPHETHI, M.N., VILJOEN, G., BOTHA, J.J., VAN RENSBURG, L.D. & ANDERSON, J.J., 2004. Socio-economic study in Water Conservation Techniques in Semi-Arid Areas. Report No. 1267/1/04, Water Research Commission, Pretoria, South Africa: pp 241.

LANE, P.N.J. & MACKENZIE, D.H., 2001. Field and laboratory calibration and test of TDR and capacitance techniques for indirect measurement of soil water content. *Austr. J. Soil Res.* 39: 1371-1386.

LANGYINTUO, A.S, YIRIDOE, E.K, DOGBE, W. & LOWENBERG-DEBOER, J., 2002. Yield and income risk efficiency analysis of alternative fallow systems for rice production in the Savannah in the Guinea Savannah Ghana. Paper presented at the Northeastern Agricultural Resource Economics Association Annual Conference, Harrisburg, PA, in June 9-11, 2002.

LE ROUX, P.A.L., 2010. Personal communication. Department of Soil, Crop and Climate Sciences, University of the Free State, Bloemfontein.

LE ROUX, P.A.L., SCHOEMAN, J.L., SNYMAN, K., VERSTER, E., ELLIS, F., MERRYWEATHER, F. & VAN DEVENTER, P.W., 1997. Guidelines for mapping and interpretation of the soils of South Africa. Bloemfontein: p 106-140.

LUXMOORE, R., 1981. Micro, meso and macroporosity of soil. *Soil Sci. Soc. Am. J*. 45: 241-285.

MA, S.M. & LI, S.B., 1996. Effectiveness and technique of plastic mulching for potato. *Rain Fed Crops* 6: 30-32.

MARION, J., OR, D., ROLSTON, D., KAVVAS, M. & BIGGAR, J., 1994. Evaluation of methods for determining soil water retentivity and unsaturated hydraulic conductivity. *Soil Sci*. 158: 1-13.

MAURYA, P.R. & LAL, R., 1981. Effects of different mulch materials on soil properties and on the root growth and yield of maize and cowpea. *Field Crops Res*. 4: 33-45.

MCNEAL, B.L. & COLEMAN, N.T., 1966. Effect of solution composition on soil hydraulic conductivity. *Soil Sci. Soc. Am. Proc*. 30: 308-312.

MEIDEMA, R., KOULECHOVA, I.N. & GERASIMOVA, M.I., 1999. Soil formation in Greyzems in Moscow district: micromorphology, chemistry, clay mineralogy and particle size distribution. *Catena* 34: 315-347.

MOELETSI, M., 2010. Personal communication. Agricultural Research Council, Institute for Soil, Climate and Water. Pretoria.

MOHAMED, S.O., BERTUZZI, P., BRUAND, A., RAISON, L. & BRUCKLER, L., 1997. Field evaluation and error analysis of soil water content measurement using a capacitance probe method. *Soil Sci. Soc. Am. J.* 61(2): 394-403.

MORGAN, K.T., PARSONS, L.R., WHEATON, T.A., PITTS, D.J. & OBREZA, Y., 1999. Field calibration of a capacitance water content probe in fine sand soils. *Soil Sci. Soc. Am. J.* 63: 987-988.

NADLER, A. & LAPID, Y., 1996. An improved capacitance sensor for *in situ* monitoring of soil moisture. *Austr. J. Soil Sci. Res*. 34(3): 361-368.

NOVAK, M.D., CHEN, W., ORCHANSKY, A.L. & KETLER, R., 2000. Turbulent exchange processes within and above a straw mulch. Part 1: Mean wind speed and turbulent statistics. *Agric. For. Meteorol.* 102: 139–154.

OLASANTAN, F.O., 1999. Effect of time of mulching on soil temperature, growth and yield of white yam in western Nigeria. *Soil Till. Res.* 50(3-4): 215-221.

PEPIN, S., LIVINGSTON, N.J. & HOOK, W.R., 1995. Temperature-dependent measurement errors in time domain reflectometry determination of soil water. *Soil Sci. Soc. Am. J.* 59: 38-43.

RAES, D., 2009. The ETo calculator, reference manual, version 3.1. Land and Water Division, FAO. Rome, Italy: p 26.

RAMAKRISHNA, A., TAM, S.P. & LONG, T.D., 2006. Effect of mulch on soil temperature, moisture, weed infestation and yield of groundnut in Northern Vietnam. *Field Crops Res.* 95(2-3): 115-125.

RATLIFF, L.F., RITCHIE, J.T. & CASSEL, D.K., 1983. Field-measured limits of soil water availability as related to laboratory-measured properties. *Soil Sci. Soc. Am. J.* 47: 770-775.

RITCHIE, J.T., 1972. Model for predicting evaporation from a row crop with incomplete cover. *Water Resour. Res* 8: 1204-1213.

ROSE, C.W., 1966. Agriculture physics. Permagon Press, Oxford: pp 226.

SAITO, T., FUJIMAKI, H. & INOUE, M., 2008. Calibration and simultaneous monitoring of soil water content and salinity with capacitance and four-electrode probe. *Am. J. Environ. Sci*. 4(6): 683-692.

SARKAR, S., PARAMANICK, M. & GOSWAMI, S.B., 2007. Soil temperature, water use and yield of yellow sarson (*Brassica napus Lar. Glauca*) in relation to tillage intensity and mulch management under rainfed lowland ecosystem in eastern India. *Soil Till. Res*. 93: 911-916.

SEYFRIED, M.S. & MURDOCK, M.D., 2001. Response of a new soil water sensor to variable soil, water content, and temperature. *Soil Sci. Soc. Am. J.* 65: 28-34.

SEYFRIED, M.S. & MURDOCK, M.D., 2004. Measurement of soil water content with a 50 MHz soil dielectric sensor. *Soil Sci. Soc. Am. J.* 65(2): 394-403.

SHINNERS, K.J., NELSON, W.S. & WANG, R., 1993. Effects of residue-free band width on soil temperature and water content. *Trans. ASAE*. 37: 39-49.

SOIL CLASSIFICATION WORKING GROUP, 1991. Soil classification - A taxonomic system for South Africa. Memoirs on the Agricultural Natural Resources of South Africa Nr. 15. Department of Agricultural Development, Pretoria: pp 257.

STEEL, R.G.E., TORRIE, J.H. & DICKEY, D.A., 1997. Principles and procedures of statistics: A Biometrical Approach. 3rd Ed. McGraw-Hill, New York. pp 633.

STIGTER, C.J., OTENGI, S.B.B., OLUWASEMIRE, K.O., NASR AL-AMIN, N.K., KINAMA, J.M. & ONYEWOTU, L.O.Z., 2005. Recent answers to farmland degradation illustrated by case studies from African farming systems. *Ann. Arid Zone* 44 (3 & 4): 255-276.

SUI, H., ZENG, D. & CHEN, F., 1992. A numerical model for simulating the temperature and moisture regimes of soil under various mulches. *Agric. For. Meteorol.* 61: 281-299.

TEKLE, S.A., 2005. A soilscape survey to evaluate land for in-field rainwater harvesting in the Free State Province, South Africa. M.Sc. dissertation, Department of Soil, Crop and Climate Sciences, University of the Free State, Bloemfontein. pp 102.

TURNER, D.P., 2000. Soils of KwaZulu-Natal and Mpumalanga: Recognition of natural soil bodies. Ph.D. thesis, Department of Plant Production and Soil Science, University of Pretoria, Pretoria, South Africa: pp 278.

URREA-LOPEZ, R., OLALLA, F.M., FABEIRO, C. & MORATALLA, A., 2006. Testing evapotranspiration equations using lysimeter observations in a semi-arid climate. *Agric. Water Manage*. 85: 15-26.

VAN DER MERWE, G.M.E., LAKER, M.C. & BÜHMANN, C., 2002. Factors that govern the formation of melanic soils in South Africa. *Geordema. J.* 107: 165-176.

VAN DER WESTHUIZEN, R.J., 2009. Laboratory procedure to calibrate EC-10 and EC-20 capacitance sensors in coir. Ph.D. thesis, University of Stellenbosch, Stellenbosch, South Africa: pp 139.

VAN DOREN, D.M. & ALLMARAS, R.R., 1978. Effect of residue management practices on the soil physical environment, microclimate, and plant growth. In: W.R. Oschwald (Ed), Crop Residue Management Systems. Spec. Publ. 31 *Am. Soc Agron. J*. 49–83.

VAN RENSBURG, L.D., 2010. Advances in soil physics: Application in irrigation and dryland crop production. *S. Afr. J. Plant Soil* 27 (1): 9-18.

VAN RENSBURG, L.D., NHLABATSI, N.N., BOTHA, J.J., ANDERSON, J.J., VAN STADEN, P.P. & KUSCHKE, R., 2002. Modelling evaporation from the soil surface as affected by mulching and soil factors. Project No. GW 52/049, Optimising Soil water Use, Agricultural Research Council, Institute for soil climate and Water, Pretoria, South Africa: pp 61.

WANG, J., LI, F.M. & SONG, Q.H., 2003. Effects of plastic film mulching on soil temperature and moisture and on yield formation of spring wheat. *Chin. J. Ecol.* 14 (2): 205-210.

WEISS, A. & HAYS, J.C., 2005. Calculating daily mean air temperature by different methods: Implications from a non-linear algorithm. *Agric. For. Meteorol*. 128: 57-65.

WELDERUFAEL, W.A., 2006. Quantifying rainfall-runoff relationships on selected benchmark ecotopes in Ethopia: A primary step in water harvesting research. Ph.D. thesis, Department of Soil, Crop and Climate Sciences, University of the Free State, Bloemfontein, South Africa. pp 204.

WENDROTH, O., ROGASIK, S., KOSZINSKI, S., RITSEMA, C.J., DEKKER, L.W. & NIELSEN, D.R., 1999. State-space distribution of field-scale soil water content time series in a sandy loam. *Soil Till. Res*. 50: 85-93.

WILLMOTT, C.J., 1981. On the validation of models. *Phys. Geogr.* 2: 184-194.

WILLMOTT, C.J., 1982. Some comments on the evaluation of model performance. *Bull. Am. Meteorol. Soc*. 63: 1309-1313.

WILLMOTT, C.J., ACKLESON, S.G., DAVIS, R.E., FEDDEMA, J.J., KLINK, K.M., LEGATES, D.R., O'DONNELL, J. & ROWE, C.M., 1985. Statistics for the evaluation and comparison of models. *J. Geophys. Res.* 90: 8995-9005.

WILLMOTT, C.J. & WICKS, D.E., 1980. An empirical method for the spatial interpolation of monthly precipitation within California. *Phys. Geogr* 1: 59-73.

WORLD REFERENCE BASE FOR SOIL RESOURCES (WRB), 1998. World soil resources report No. 84. ISSS/ISRIC, FAO, Rome, Italy: pp 88.

WRAITH, J.M. & OR, D., 1999. Temperature effects on soil bulk dielectric permittivity measured by time domain reflectometry: experimental evidence and hypothesis development. *Water Resour. Res*. 35(2): 361-369.

WRAITH, J.M. & OR, D., 2001. Soil water characteristics determination from concurrent water content measurements in reference porous media. *Soil Sci. Soc. Am. J.* 65: 1659-1666.

WU, Y., PERRY, K.B. & RISTAINO, J.B., 1996. Estimating temperature of mulched and bare soil from meteorological data. *Agric. For. Meteorol*. 81: 299–323.

ZEKELE. T.B., GREVERS, M.C., MERMUT, A.R. & BEYENE, S., 2004. Effect of residue on physical properties of the soil in the south central rift valley of Ethopia. *Soil Till. Res*. 77: 36-46.

ZHANG, S., LOVDAHL, L., GRIP, H. & TONG, Y., 2007. Soil hydraulic properties of two loess soils in China measured by various field scale and laboratory methods. *Catena* 69: 264-273.

ZHANG, S., LOVDAHL, L., GRIP, H., TONG, Y., YANG, X. & WANG, Q., 2009. Effects of mulching and catch cropping on soil temperature, soil moisture and wheat yield on the loess plateau of China. *Soil Till. Res.* 102: 78-86.

ZHOU, L.M., LI, F.M., JIN, S.L. & SONG, Y., 2009. How two ridges and the furrow mulched with plastic film affect soil water, soil temperature and yield of maize on the semi-arid Loess Plateau of China. *Field Crops Res*. 113: 41-47.

APPENDIX 1

Photo showing the swelling properties of the melanic A-horizon (Section 2.2.1)

Figure A1.1 Photo showing the swelling properties of the melanic A-horizon (Section 2.2.1)

APPENDIX 2

The ECH_2O-TE and Watermark-200 probes (Section 2.3.1.2)

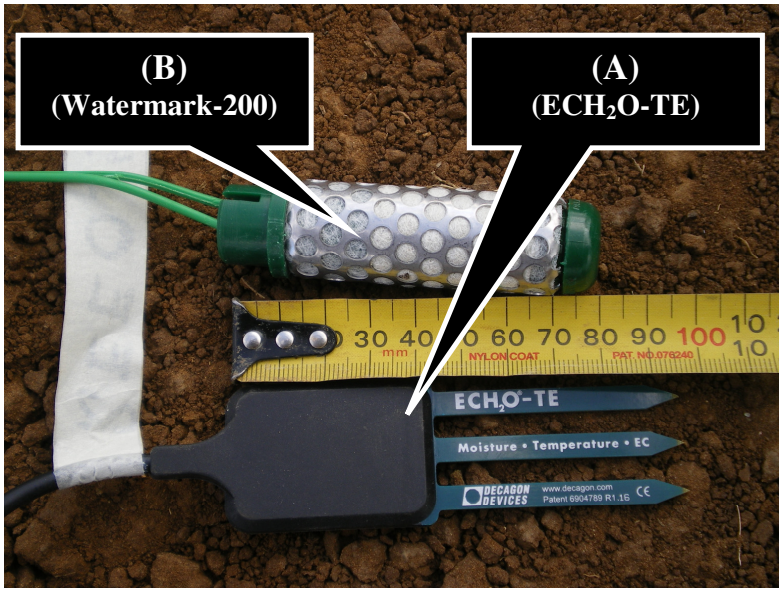

Figure A2.1 Photo showing ECH_2O- TE and Watermark-200 probes

APPENDIX 3

Photo showing the 8 m by 8 m experimental layout before the reeds and stone mulch were laid (Section 4.2.1)

Figure A3.1 Photo showing ECH_20-TE and Vaisala probes cabling, CR1000 & multiplexer box and modem box holder

APPENDIX 4

Table A4.1 Soil water flux at different depths versus time during redistribution during internal drainage

t (hrs)	z (cm)	$\Delta\theta/\Delta t$ (hr^{-1})	dz ($\Delta\theta/\Delta z$) (cm hr^{-1})	q =$\sum dz$ ($\Delta\theta/\Delta t$) (cm hr^{-1})
6	0-25	0.02350	0.059	0.059
	25-75	0.01525	0.076	0.135
	75-150	0.01280	0.096	0.231
	150-450	0.01294	0.388	0.619
	450-750	0.01934	0.580	1.199
	750-1050	0.03286	0.986	2.185
24	0-25	0.00409	0.010	0.010
	25-75	0.00281	0.014	0.024
	75-150	0.00241	0.018	0.042
	150-450	0.00244	0.073	0.115
	450-750	0.00353	0.106	0.221
	750-1050	0.00568	0.170	0.392
50	0-25	0.00130	0.003	0.003
	25-75	0.00093	0.005	0.008
	75-150	0.00081	0.006	0.014
	150-450	0.00082	0.025	0.039
	450-750	0.00116	0.035	0.073
	750-1050	0.00180	0.054	0.127
72	0-25	0.00071	0.002	0.002
	25-75	0.00052	0.003	0.004
	75-150	0.00045	0.003	0.008
	150-450	0.00046	0.014	0.022
	450-750	0.00064	0.019	0.041
	750-1050	0.00098	0.029	0.070
120	0-25	0.00043	0.001	0.001
	25-75	0.00032	0.002	0.003
	75-150	0.00028	0.002	0.005
	150-450	0.00062	0.019	0.023
	450-750	0.00086	0.026	0.049
	750-1050	0.00129	0.039	0.088
240	0-25	0.00022	0.001	0.001
	25-75	0.00016	0.001	0.001
	75-150	0.00014	0.001	0.002
	150-450	0.00015	0.004	0.007
	450-750	0.00020	0.006	0.013
	750-1050	0.00030	0.009	0.022
288	0-25	0.00013	0.000	0.000
	25-75	0.00010	0.001	0.001
	75-150	0.00009	0.001	0.002
	150-450	0.00004	0.001	0.003
	450-750	0.00005	0.002	0.004
	750-1050	0.00007	0.002	0.006
480	0-25	0.00009	0.000	0.000
	25-75	0.00007	0.000	0.001

	75-150	0.00006	0.000	0.001
	150-450	0.00010	0.003	0.004
	450-750	0.00014	0.004	0.008
	750-1050	0.00020	0.006	0.014
720	0-25	0.00005	0.000	0.000
	25-75	0.00004	0.000	0.000
	75-150	0.00004	0.000	0.001
	150-450	0.00004	0.001	0.002
	450-750	0.00005	0.002	0.003
	750-1050	0.00007	0.002	0.006

Calculations of soil water flux at different depths versus time during redistribution during the internal drainage method (section 5.2.5)

APPENDIX 5

Table A5.1 Hydraulic conductivity, from soil water flux and changing hydraulic head during redistribution

z (cm)	t (hrs)	$q=\sum dz(\Delta\theta/\Delta t)$ (cm hr^{-1})	$\Delta\theta$ (cm^3 cm^{-3})	$\Delta H/\Delta z$	$K(\theta)$ (cm/day)	$\Delta\theta$ (cm^3 cm^{-3})
	6.00	0.059	0.440	1.240	0.047	0.440
	24.00	0.010	0.367	1.580	0.006	0.367
	50.00	0.003	0.333	1.872	0.002	0.333
	72.00	0.002	0.317	1.774	0.001	0.317
2.5	120.00	0.001	0.297	1.522	0.001	0.297
	240.00	0.001	0.271	0.719	0.001	0.271
	288.00	0.000	0.264	0.604	0.001	0.264
	480.00	0.000	0.247	0.358	0.001	0.247
	720.00	0.000	0.234	0.600	0.000	0.234
	6.00	0.135	0.399	1.240	0.109	0.399
	24.00	0.024	0.349	1.580	0.015	0.349
	50.00	0.008	0.325	1.872	0.004	0.325
	72.00	0.004	0.313	1.774	0.002	0.313
7.5	120.00	0.003	0.298	1.522	0.002	0.298
	240.00	0.001	0.278	0.719	0.002	0.278
	288.00	0.001	0.274	0.604	0.001	0.274
	480.00	0.001	0.260	0.358	0.002	0.260
	720.00	0.000	0.250	0.600	0.001	0.250
	6.00	0.231	0.395	1.063	0.217	0.395
	24.00	0.042	0.352	1.052	0.040	0.352
	50.00	0.014	0.331	0.870	0.016	0.331
	72.00	0.008	0.321	0.584	0.013	0.321
15	120.00	0.005	0.308	0.348	0.014	0.308
	240.00	0.002	0.290	0.407	0.006	0.290
	288.00	0.002	0.286	0.580	0.003	0.286
	480.00	0.001	0.274	0.200	0.005	0.274
	720.00	0.001	0.265	0.067	0.009	0.265
	6.00	0.619	0.408	0.954	0.649	0.408
	24.00	0.115	0.364	0.879	0.131	0.364
	50.00	0.039	0.343	0.747	0.052	0.343
	72.00	0.022	0.332	0.627	0.034	0.332
45	120.00	0.023	0.319	0.548	0.043	0.319
	240.00	0.007	0.301	0.270	0.025	0.301
	288.00	0.003	0.297	0.151	0.018	0.297
	480.00	0.004	0.284	0.018	0.226	0.284
	720.00	0.002	0.275	0.083	0.022	0.275
	6.00	1.199	0.483	0.977	1.228	0.483
	24.00	0.221	0.419	0.935	0.237	0.419
	50.00	0.073	0.389	0.861	0.085	0.389
	72.00	0.041	0.375	0.795	0.051	0.375
75	120.00	0.049	0.356	0.752	0.066	0.356
	240.00	0.013	0.331	0.678	0.019	0.331
	288.00	0.004	0.325	0.547	0.008	0.325
	480.00	0.008	0.309	0.507	0.016	0.309
	720.00	0.003	0.296	0.376	0.009	0.296

	6.00	2.185	0.592	0.994	2.197	0.592
	24.00	0.392	0.490	0.980	0.400	0.490
	50.00	0.127	0.443	0.950	0.134	0.443
	72.00	0.070	0.421	0.920	0.076	0.421
105	120.00	0.088	0.393	0.901	0.098	0.393
	240.00	0.022	0.358	0.868	0.025	0.358
	288.00	0.006	0.349	0.815	0.008	0.349
	480.00	0.014	0.325	0.801	0.018	0.325
	720.00	0.006	0.308	0.766	0.007	0.308

Calculation of hydraulic conductivity, from soil water flux and changing hydraulic head during redistribution (section 5.2.5)

APPENDIX 6

Figure showing measured changes in hydraulic head with depth over time during redistribution (section 5.2.5)

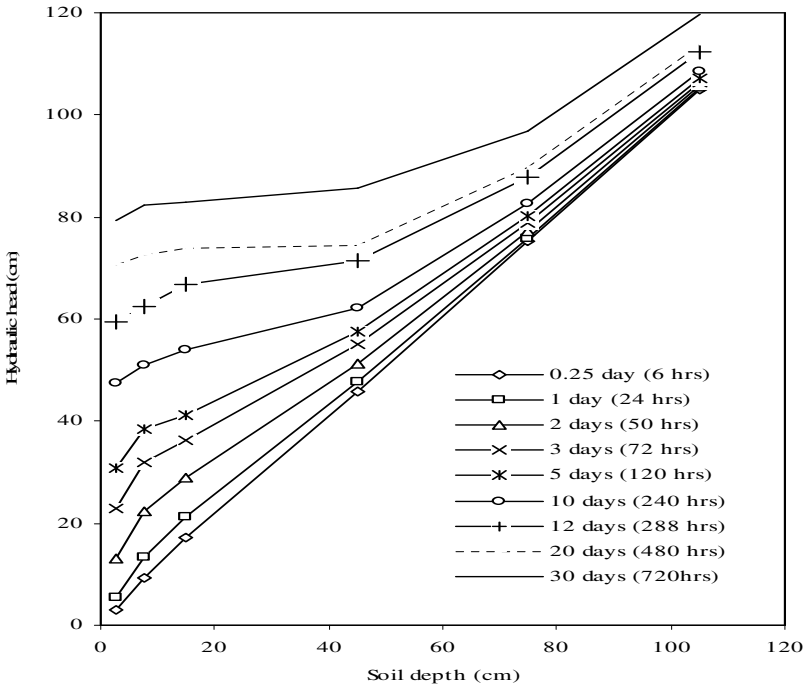

Figure A6.1 Graph showing measured changes in hydraulic head with depth over time during redistribution

APPENDIX 7

Table A7.1 Showing readings during addition and removal of bottles from the lysimeter.

		Millivolt reading	
Bottle No.	Mass (kg)	Adding bottles	Removing bottles
	0	23484	23482
1	2.0243	23500	23501
2	4.1198	23514	23521
3	6.2189	23524	23530
4	8.3181	23533	23540
5	10.4192	23552	23558
6	12.5134	23572	23578
7	14.6068	23592	23587
8	16.7118	23601	23597
9	18.8014	23611	23616
10	20.8876	23620	23626
11	23.0022	23640	23646
12	25.0897	23650	23655
13	27.1944	23670	23675
14	29.292	23679	23684
15	31.3883	23689	23694
16	33.4879	23699	23714
17	35.6323	23718	23722
18	37.725	23728	23732
19	39.8226	23738	23752
20	41.9132	23758	23772
21	44.012	23778	23782
22	46.0484	23787	23791
23	48.1483	23797	23811
24	50.2252	23817	23831
25	52.351	23836	23841
26	54.4468	23846	23861
27	56.5503	23856	23870
28	58.6736	23877	23890
29	60.7691	23888	23909
30	62.877	23908	23919
31	64.983	23918	23938
32	67.0854	23938	23948
33	69.1985	23949	23958
34	71.2974	23959	23977
35	73.4006	23979	23987
36	75.4925	23999	24006
37	77.5983	24019	24016
38	79.6872	24029	24035
39	81.7907	24039	24044
40	83.8864	24060	24062
41	85.9559	24079	24082
42	88.0408	24089	24091
43	90.1236	24099	24100
44	92.2731	24119	24119

Cumulative bottle masses versus millivolt readings (section 6.2.3)

APPENDIX 8

Photo showing weighing lysimeter on it, some of the two-liter bottles used for calibration (section 6.2.3)

Figure A8.1 Photo showing weighing lysimeter on it, some of the two-liter bottles used for calibration

APPENDIX 9

Table A9.1 Soil hydraulic diffusivity values for the melanic layer

θ (mm mm^{-1})	D (mm^2 d^{-1})
0.349	387
0.338	293
0.327	223
0.316	171
0.305	132
0.294	103
0.283	80
0.272	64
0.261	51
0.250	41
0.239	34
0.228	28
0.217	23
0.206	20
0.195	17
0.184	15
0.173	14
0.162	13
0.151	12
0.140	12

Table showing soil hydraulic diffusivity values for the melanic layer (section 6.2.8)

APPENDIX 10

Plot of volumetric soil water content versus soil hydraulic diffusivity (*D*) (section 6.2.8)*

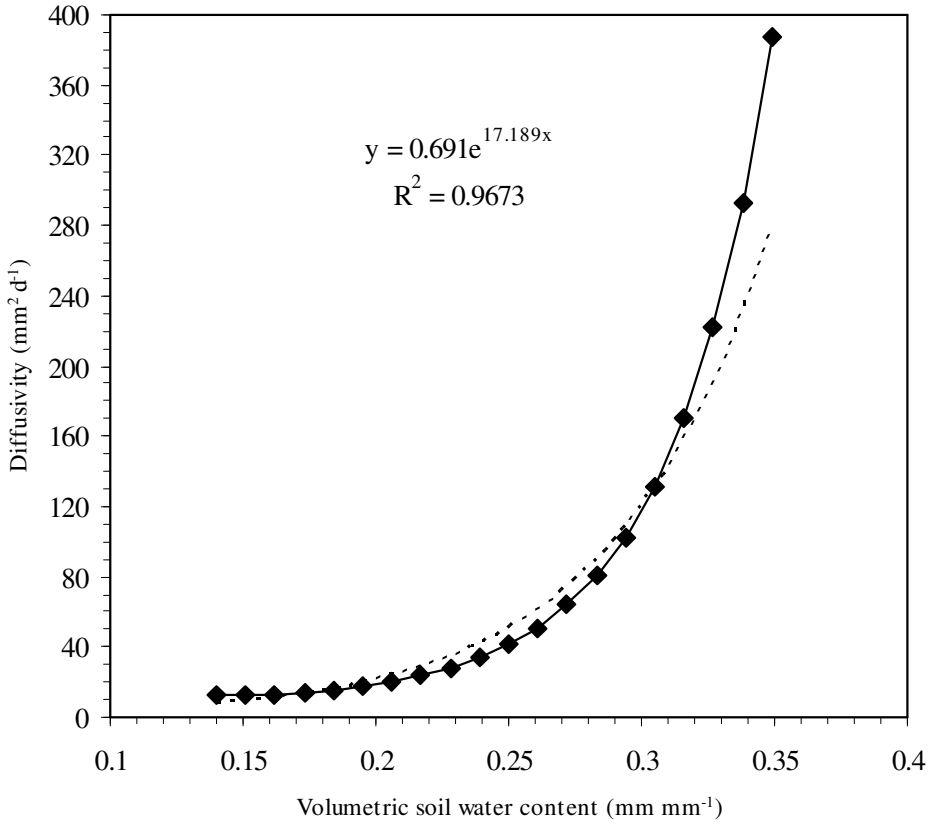

Figure A10.1 Plot of volumetric soil water content versus soil hydraulic diffusivity (The *D* values were determined by dividing K(θ) value with a corresponding specific water capacity (C_0) value at a specific soil water content for the melanic A-horizon. The dotted line on the graph represents an exponential function used to obtain *D* from a given θ values)

APPENDIX 11

Photo showing the surface of the weighing lysimeter after a heavy hail (section 6.3.3)

Figure A11.1 Photo showing the surface of the weighing lysimeter after a heavy